Skin Innervation Patterns and Neurotrophic Factor Expression in Neuropathic Pain Models

Jennifer Peleshok

Department of Pharmacology and Therapeutics

McGill University, Montreal

August 2011

A thesis submitted to the Faculty of Graduate Studies and Research in partial fulfillment of the requirements for the degree of Doctor of Philosophy

Dedication

To my parents; this is the culmination of more years of advanced education than I'm sure any of us would like to fully acknowledge and this achievement could not have been possible without your understanding, patience and support.

Abstract

Neuropathic pain presents itself with many faces. It can be devastatingly painful leading to a person's inability to lead a productive life or it can be mild, manageable with life style choices and mild analgesics. In this thesis I am discussing one of the countless possible mechanisms which could underlie the development and maintenance of this disorder; namely the involvement of peripheral changes in innervation. The approach taken in this thesis was mainly based on protein analyses, based on the assumption that protein expression (or lack thereof) is indicative of changes in the physiological properties of structures that either express or secrete proteins. I also address the models which are commonly used by researchers to elucidate the mechanisms underlying chronic neuropathic pain in hopes of developing viable treatments.

The focus of this work is on the periphery, more specifically involving the glabrous skin of the rat hind paw. This skin is innervated by branches of the sciatic nerve which are comprised of, in part, sensory fibres. These are further sub-classified into the thickly and thinly myelinated A-beta and A-delta afferents, respectively, as well as unmyelinated C-fibres. The latter population can be divided into two subgroups based on their peptide content where the peptide rich are termed peptidergic and the peptide-poor, non-peptidergic. This area also receives innervation from post-ganglionic sympathetic efferents.

This thesis comprises three experimental chapters of my independent work into further exploring the models and mechanisms underlying the maintenance and generation of neuropathic pain.

The first experimental chapter addresses the long term changes of skin innervation which occur following the application of a commonly used model of neuropathic pain, namely the chronic constriction injury (CCI) of the sciatic nerve model. I examined the myelinated afferent population as a whole, the unmyelinated peptidergic afferents as well as the non-peptidergic C-fibres from three days through 1.5 years following the application of the nerve injury. There was a persistent loss of myelinated afferents, loss and delayed sprouting of non-peptidergic C-fibres as well as a brief loss and permanent sprouting of peptidergic afferents within the upper dermis.

The second study is a comparative examination of the morphological and behavioural changes following application of two very similar models of neuropathic pain. The CCI model is based on the application of loose chromic gut ligatures and the variation of this is the cuff model in which the chromic gut ligatures are replaced by a fixed diameter polyethylene cuff. The application of the cuff model resulted in a persistent mechanical hypersensitivity in contrast to the CCI in which the mechanical hypersensitivity resolved within about a month. However, the application of either model resulted in a transient thermal hypersensitivity. Innervation changes following application of the cuff model included a reduction in myelinated afferent density within the upper dermis in both models, the unmyelinated, non-peptidergic afferents declined in fibre density followed by a delayed recovery in the cuff model and the peptidergic afferents gradually declined and remained so following application of the cuff in contrast to the application of the CCI.

The third chapter addresses the changes in the expression of nerve growth factor (NGF) and its receptors following CCI. The precursor form

of NGF, proNGF was localized to mast cells, vascular endothelium and keratinocytes in the epidermis in naïve skin. Following injury, proNGF increased. After lesion, Schwann cells expressed high levels of the NGF receptor p75. The two receptors for NGF, TrkA and p75, were differentially regulated during the progression of the nerve injury.

The work of this thesis has provided new findings documenting the morphological changes underlying the generation and maintenance of neuropathic pain as well as the molecular generators of these changes.

Résumé

La douleur neuropathique peut se présenter sous plusieurs formes. Elle peut être terriblement douloureuse conduisant à l'incapacité d'une personne à mener une vie productive ou elle peut être subtile, gérable avec des choix de style de vie et analgésiques légers. Dans cette thèse, j'analyse les mécanismes périphériques pouvant déclencher et maintenir la douleur neuropathique. L'approche adoptée dans cette thèse est surtout basée sur une analyse de la concentration et distribution anatomique de protéines, avec l'idée sous-jacente que son niveau d'expression (ou absence d'expression) est révélatrice de changements physiologiques dans les structures qui produisent ou sécrètent ces protéines. Je vais également aborder les modèles qui sont couramment utilisés par les chercheurs pour élucider les mécanismes sous-jacents à la douleur neuropathique chronique dans l'espoir de développer des traitements viables.

Le focus de ce travail se déroule dans la périphérie, en particulier la peau non couverte de poils de la surface plantaire du membre postérieur du rat. Cette peau est innervée par des fibres nerveuses sensorielles provenant du nerf sciatique. Ces fibres sont normalement classées comme afférences myélinisées épaisses et finement myélinisées (A-bêta et A-delta respectivement), ainsi que comme fibres amyéliniques (C). La dernière population peut être divisée en deux sous-groupes en fonction de présence ou absence de neuropeptides en peptidergiques et non-peptidergiques. Cette région reçoit également une innervation par des fibres post-ganglionnaires sympathiques.

Cette thèse est composée de trois chapitres expérimentaux.

Le premier chapitre se penche sur les changements à long terme de l'innervation cutanée qui se produisent après l'application d'un modèle de douleur neuropathique couramment utilisé, à savoir la blessure par constriction chronique du nerf sciatique (CCI). J'ai examiné les

changements des fibres myélinisées dans son ensemble, des fibres amyéliniques peptidergiques, ainsi que des fibres non-peptidergiques dès trois jours après l'application de la lésion nerveuse jusqu'à un an et demi après la lésion. Il y avait une perte persistante des afférences myélinisées, une perte suivie d'une récupération tardive des fibres C non-peptidergiques ainsi qu'une brève perte suivie de récupération permanente des afférences peptidergiques dans la partie supérieure du derme.

Le second chapitre expérimental est un examen comparatif des changements morphologiques après l'application de deux modèles très similaires de douleur neuropathique. Le premier est la constriction chronique du nerf sciatique (CCI) suivant l'application de 4 ligatures lâches de catgut chromique; dans le deuxième la constriction du nerf sciatique est obtenue par l'application autour du nerf d'un segment de tube polyéthylène de diamètre fixe (« cuff »). L'application du « cuff » résultait en une hypersensibilité mécanique persistante, contrairement au CCI dans lequel l'hypersensibilité mécanique disparaissait dans un mois environ. Toutefois, les résultats de l'application des deux modèles sur la sensibilité thermique étaient similaires, avec une hyper-sensitivité à la chaleur qui durait environ un mois. Les afférences myélinisées étaient réduites en densité dans la partie supérieure du derme dans les deux modèles et cette baisse était permanente. Cependant, les afférences non-peptidergiques ont souffert une baisse de densité suivie d'un retour retardé à des valeurs des contrôles dans le modèle « cuff ». Dans ce dernier modèle, les afférences peptidergiques ont diminué progressivement en densité et n'ont pas récupéré, à la différence de l'application de la CCI.

Le troisième chapitre expérimental concerne les changements dans l'expression du facteur de croissance nerveuse (NGF) et de ses récepteurs dans des animaux avec une lésion CCI. Le précurseur du

NGF, proNGF a été localisé aux mastocytes, l'endothélium vasculaire et les kératinocytes dans l'épiderme de la peau naïve. À la suite de la lésion CCI, nous avons détecté une augmentation du proNGF. Après la lésion, les cellules de Schwann avaient une expression très augmentée du récepteur du NGF p75 et quelques unes se distribuaient autour de fibres nerveuses régénérés. Les récepteurs au NGF, TrkA et p75 sont différentiellement régulés dans la période après la lésion du nerf. Le travail de cette thèse a eu comme objectif de clarifier les changements morphologiques contribuant au déclanchement et la manutention de la douleur neuropathique, ainsi que les mécanismes moléculaires de ces changements.

Table of Contents

Index of Figures

Chapter 4:

Appendices:

Acknowledgments

I would like to thank my supervisor, **Dr. Alfredo Ribeiro-da-Silva** who saw in me the potential as a researcher and professional. He brought me into his lab and provided me the opportunity to realize these qualities through the completion of my doctoral work. This would not have been possible without his realization that a doctoral student should not only be educated at the bench and in theory, but socially through professional interactions and administrative exposures, to fully realize their true potential. Thank you Alfredo for all of the many opportunities you have given me.

I would also like to thank the people within the department who have helped make this possible. My advisor, **Dr. Brian Collier** whose sense of humour, critical analysis of my strengths and all my weaknesses as well as his support and presence when it was needed is greatly appreciated. Thanks to my thesis committee, **Dr. Dusica Maysinger, Dr. Claudio Cuello** and **Dr. Laura Stone** for guiding me through this process. **Dr. Gary J. Bennett** who has graciously allowed use of his animal behaviour testing room as well as his wisdom to help in developing ideas. **Dr. Zingg** for your help from the beginning, I feel as though you really had watched over me through my development during these years and knowing this has made all the difference. **Dr. Uri Saragovi**, my first doctoral supervisor, provided me the opportunity to learn about the world of trophic factors as well as a variety of valuable molecular biology techniques. As well, I would like to thank the ladies in the office especially **Hélène Duplessis** – you have been a model for me in your organizational abilities and your patience.

This work would not have been possible if not for my lab mates; past and present. Firstly thank you **Manon St. Louis** for your amazing ability in keeping us all organized and grounded. **Anna Taylor** for your fantastic

partnership from the start, learning about the skin and exactly what is the peripheral nervous system, through to the end. **Simon Allard**, your scientific abilities and rationale were immensely helpful. **Abeer Saeed** and **Lina Almarestani** for your scientific and 'softer' contributions. **Louis-Etienne Lorenzo**, thank you for your daily contributions to my quality lab experiences. As well, thanks to **Maria Osikowicz**, **Geraldine Longo** and **Claire Magnussen**; thank you for adding to my lab experience these past few years. As well as the original ladies, **Carlis Rejon, Ljubica Ivanisevic** and **Pooja Jain**: your support through my transition to this point allowed this project to be possible.

Thank you to my dad, **Steven Peleshok**, for helping to edit this manuscript.

Finally I would like to thank my husband, **Gary Mo**. You've provided me with the motivation to write this. You've also provided me with invaluable advice and assistance not only for experiments, papers, presentations and grants.

Contribution of Authors

This thesis is based on data obtained for the generation of the following three manuscripts which are found in chapters two through four:

Chapter 2: Delayed reinnervation by non-peptidergic nociceptive afferents of the glabrous skin of the rat hindpaw in a neuropathic pain model

J.C. Peleshok and A. Ribeiro-da-Silva

Journal of Comparative Neurology (2011) 519; 49-63

Chapter 3: Comparative study of two chronic constriction injury neuropathic pain models

J.C. Peleshok, A.W. Saeed and A. Ribeiro-da-Silva

(Submitted to Journal of Comparative Neurology)

Chapter 4: Changes in neurotrophic factors in the rat thick skin following chronic constriction injury of the sciatic nerve

J.C. Peleshok and A. Ribeiro-da-Silva

(Molecular Pain, under revision)

Responsibilities of authors and co-authors:

The following statements describe the responsibilities of all the authors of the above co-authored manuscripts:

Dr. Alfredo Ribeiro-da-Silva: Principal investigator and primary genesis of all intellectual content for all manuscripts submitted.

Jennifer C. Peleshok: Carried out the majority of all experimental work leading to the generation of data for the manuscripts. Wrote the first version of all manuscripts.

Abeer W. Saeed: Performed the animal surgeries for the application of the polyethylene cuff for the second experimental chapter as well as assisted in the performance of the behavioural tests for the first and second experimental chapters. She has also helped in the revision of the manuscript.

Chapter One

General Introduction

1.1. Neuropathic Pain

Neuropathic pain is defined by the International Association for the Study of Pain as "pain initiated or caused by a primary lesion or dysfunction of the nervous system that, under normal conditions, transmits noxious information" (Merskey and Bogduk, 1994). In this case, pain has ceased to function in its normal role to alert the body of potential damage and becomes harmful in its own right. Peripheral neuropathic pain may result from injury, trauma or disease to the peripheral nervous system or may also be idiopathic when no obvious cause for its genesis can be found. Peripheral neuropathic pain is exceedingly difficult to treat and manage because of the lack of correlation between pain severity and objective evidence of injury and poor response to analgesics. Neuropathic pain can be further defined with respect to its chronicity. Indeed, acute neuropathic pain spontaneously disappears, but when it lasts for more than 3-6 months in humans, it becomes chronic neuropathic pain.

1.1.1 Epidemiology

Chronic pain affects between 16-29% of the working Canadian population aged 12 to 65 based on current data (Moulin et al., 2002; Ramage-Morin, 2008; Ramage-Morin and Gilmour, 2010). The incidence of chronic pain of neuropathic origin ranges from 8.2% of the UK population of people aged 18 and over (Torrance et al., 2006) to 17.9% of the Canadian population, however this includes such conditions as migraine, fibromyalgia and vulvodynia which may or may not commonly be considered part of the neuropathic pain spectrum of disorders (Toth et al., 2009). The socioeconomic burden of a person suffering from neuropathic pain was found to be $17,555 in health-care costs during the 2000 calendar year compared to $5,715 for aged-matched control (Berger et al., 2004). When one considers that 10% of the general population suffer from neuropathic pain and will endure this condition for approximately ten years (Meyer-Rosberg et al., 2001) and incur health care costs at three times that of the normal population, this is a very significant burden on our health-care system, validating the need for further research to find an adequate treatment.

1.1.2. Types of Neuropathic Pain

As alluded to in the previous section, neuropathic pain is made up of a spectrum of disorders. For the purposes of this thesis, I will focus on neuropathic pain involving the peripheral nervous system. Common types of peripheral neuropathic pain include chemotherapy-induced polyneuropathy, complex regional pain syndrome, entrapment neuropathies, painful diabetic neuropathy, post herpetic neuralgia, and posttraumatic neuralgias (Dworkin et al., 2003). A diagnosis of peripheral neuropathic pain is reached based on neurological assessments including both positive and negative sensory symptoms and signs. Common perceptions from patients afflicted with neuropathic pain include spontaneous stimuli-independent "burning" or "shock-like paroxysms". There can also be evoked sensations such as from gentle touch and pressure of clothing, wind, riding in a car and hot and cold temperatures (Dworkin et al., 2003).

Chemotherapy-evoked neuropathy is a side effect of the commonly used chemotherapeutics used to treat cancer. This is a consequence to the chemotherapy which can restrict the dose prescribed to patients and affects 20% of patients receiving standard doses and affects the longest peripheral axons first. Patients complain of a symmetrical burning sensation affecting their feet first progressing to hands which can, in part, be attributed to a loss of intraepidermal sensory afferents as well as generation of spontaneous discharges from A- and C-fibres (Bennett, 2010).

Complex Regional Pain Syndrome (CRPS) can be divided into two categories depending on the presence of nerve injury. CRPS type I is a chronic pain syndrome that occurs following traumatic injuries and there is no obvious nerve injury. CRPS type II, previously known as causalgia, presents with an identifiable injury to the peripheral nerve which accounts for the symptoms. The typical symptoms associated with CRPS are spontaneous pain (characterized by a burning or aching sensation) and sensitivity to thermal and mechanical stimulation. Currently it is hypothesized that a progression of events underlies CRPS-I. These include an initial deep tissue injury resulting in inflammation with oedema. The pathological component involves injury to microvasculature and

subsequent alterations in blood-flow. There is then a progression to chronic inflammation resulting in peripheral and subsequent central sensitization which are hallmarks of neuropathic pain (Coderre and Bennett, 2010).

Entrapment neuropathies usually occur to nerves passing through a joint or boney tunnel. Such neuropathies result from any sort of chronic compression to the nerve leading to a loss of sensation, pain and motor deficits. Examples of entrapment neuropathies include carpal tunnel syndrome and sciatica, the latter resulting from a narrowing of the foramina as a result of degenerative vertebral disorders. These conditions are usually corrected with decompression surgeries and physical therapy (Rempel and Diao, 2004).

Painful peripheral diabetic neuropathies accompany patients with long-standing diabetes and are thought to arise due to metabolic and microvasculature alterations resulting from chronic hyperglycaemia. The symptoms usually present in a symmetrical fashion affecting the longest axons first (i.e. in hands and feet).

Post-herpetic painful neuralgia usually affects adults later in life. The herpes zoster virus (latent after childhood infection) becomes reactivated due to opportunistic circumstances in which normal immuno-surveillance fails. The virus residing within the sensory dorsal root ganglion travels antidromically to the sensory terminals within the skin, bursting and damaging the nerve. The exact mechanisms underlying this have not been clearly delineated as some patients see this pain resolve with the cessation of viral replication whereas others do not (Bennett and Watson, 2009).

Post-traumatic neuralgia usually arises after direct injury (such as brachial plexus avulsions) or as an unfortunate consequence of surgical intervention (such as mastectomies). The neuropathy develops as a result of direct nerve damage and may include pain associated with the formation of a terminal end bulb in which the severed nerve terminals develop into a tangled mass of disconnected sprouted nerves (also known as neuroma) (Devor and Wall, 1976).

1.1.3. Current Pharmacological Treatments

First line medications for the treatment of chronic neuropathic pain in man are typically based on inhibitory mechanisms and include the following:

gabapentin, pregabalin, 5% lidocaine patch, opioid analgesics, tricyclic antidepressants for generalized neuropathic pain, and carbamazepine for the treatment of trigeminal neuralgia. Gabapentin and pregabalin share structural similarities and were developed to mimic the inhibitory effects of γ-aminobutyric acid (GABA). Gabapentin was initially used as an antiepileptic prior to its demonstrated efficacy in treating neuropathic pain (Mellick and Mellick, 1995). Controversy surrounds the mechanism of action of these two drugs. It is currently thought that instead of targeting GABAergic receptors as originally hoped, they inhibit the activity dependent release of neurotransmitters by binding a high-affinity binding site within a subunit of a voltage-gated calcium channel ($Ca_v\alpha_2$-δ) (Taylor, 2009; Taylor et al., 2007). The 5% lidocaine patch blocks peripheral voltage-gated sodium channels and as such broadly prevents the ectopic discharge of sensory afferents (Devers and Galer, 2000; Gammaitoni et al., 2003; Puig and Sorkin, 1996). Opioid analgesics such as morphine act presynaptically, decreasing calcium currents in primary afferents, resulting in inhibition of release of pro-nociceptive mediators such as substance P (sP) and glutamate, and postsynaptically, by increasing potassium currents in dorsal horn and supraspinal neurons, which are hyperpolarized. Tricyclic antidepressants were found to be efficacious in the treatment of neuropathic pain and act by inhibiting monoaminergic reuptake (serotonin and noradrenaline) from presynaptic terminals (Jensen et al., 2009; Verdu et al., 2008). Carbamazepine, an antiepileptic medication traditionally used for the treatment of trigeminal neuralgia, acts by blocking voltage-gated sodium channels, thus inhibiting ectopic discharge of sensory afferents (Eisenberg et al., 2007).

1.2. The Sciatic Nerve

The longest nerve of the human body is the sciatic nerve. Just above the human knee it branches into its principal two components: the common peroneal and tibial nerves. The sciatic nerve grossly innervates all lower limb regions joint, deep muscle as well as skin. The sciatic nerve arises from the lumbrosacral plexus which in the human is L4, L5, S1, S2 and S3. The tibial nerve branches further into the medial sural nerve which innervates the skin of lateral side of the foot whereas the superficial peroneal nerve innervates nearly all the dorsum of the foot and most of the digits. In the rat, the sciatic nerve combines the L4 and L5 and to some extent the L6 spinal nerves, and trifurcates into the sural, common peroneal and tibial nerves. The plantar surface of the hind paw is innervated by the sural at the most lateral aspect and tibial in the center and saphenous towards the more medial part. The sciatic nerve is a mixed nerve which contains both motor (efferent) and sensory (afferent) fibres. Motor fibres conduct impulses from the central nervous system to target tissues. The sensory neurons receive information from skin, muscle and joints and transmit to the central nervous system for processing. The basic classification of the neuron is based on its axo-dendritic composition in which the neuron has one axon which transmits information and one dendrite

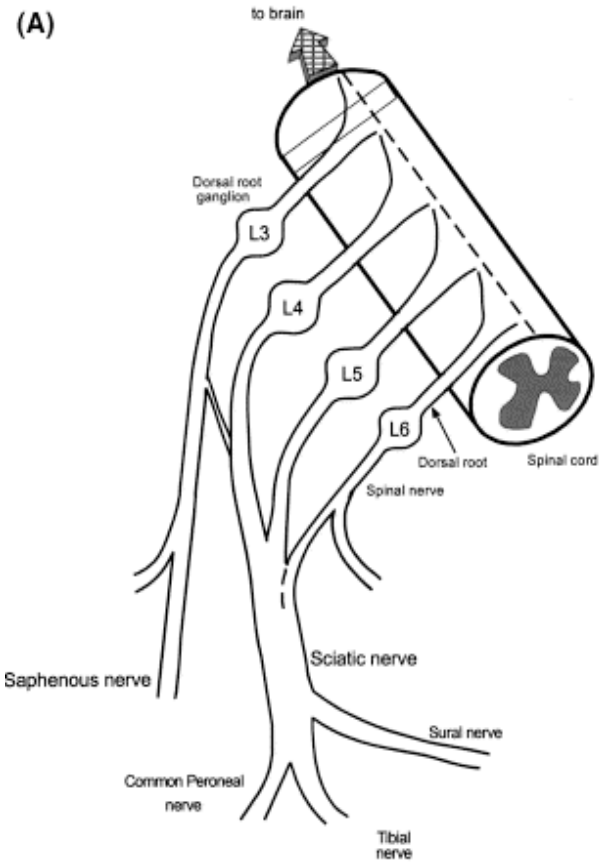

Figure 1: Rat sciatic nerve including terminal branches, dorsal root ganglia and spinal insertions. The sciatic nerve contributes the majority of the spinal input through L4 and L5, with a partial contribution through the L6 spinal nerve. (From Decosterd and Woolf, 2000).

which receives (bipolar). Sensory neurons receive a unique classification as pseudounipolar in which a single process branches in two, one axon branch terminating in the spinal cord and the other in the periphery. The peripheral terminations are able to relay sensory information back to the cell body and in turn respond to these cues in an efferent capacity by releasing neuropeptides such as calcitonin gene related peptide (CGRP) and sP in the periphery (Basbaum and Bushnell, 2009; Tandrup, 1995).

1.2.1. Microanatomy

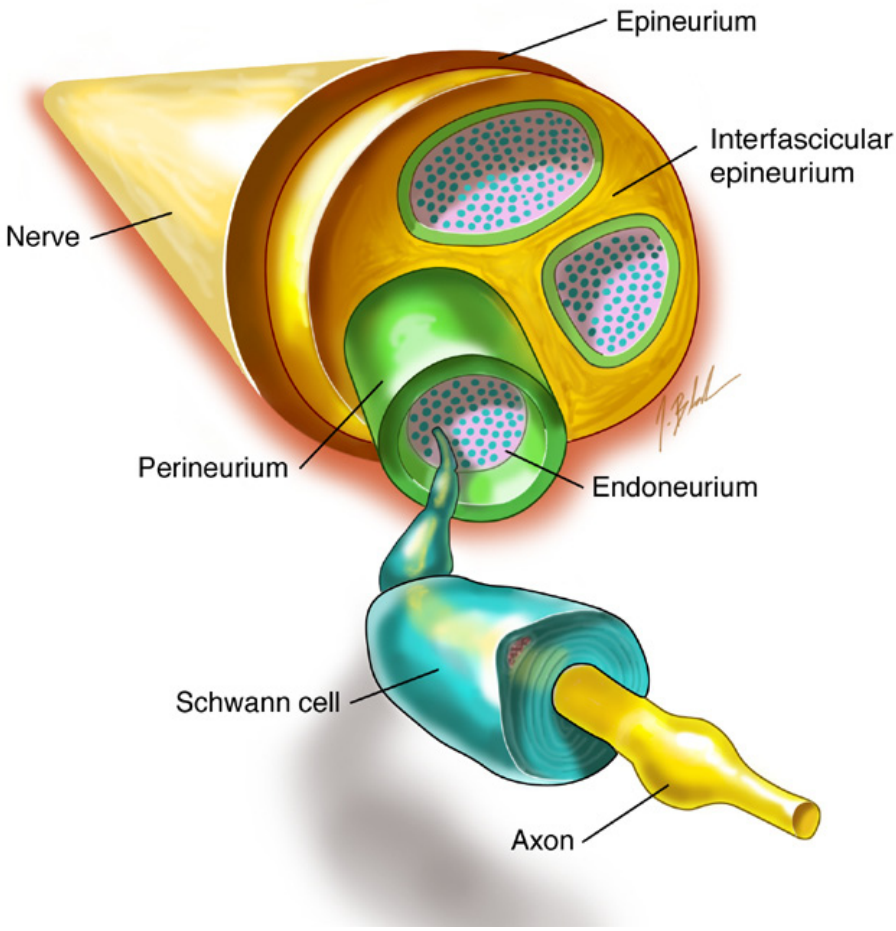

Figure 2: Diagramatic representation of a nerve. The outermost layer of connective tissue is the epineurium which surrounds nerve bundles and their perineurium. Individual myelinated fibers and unmyelinated fiber groups in Schwann cells are surrounded by the endoneurium. (From www.backpain-guide.com)

Peripheral nerves are broadly enclosed by the epineurium and comprise groups of many nerve fibres called fascicles (or bundles). Nerve fascicles are surrounded by the perineurium which is made up of flattened epithelial cells joined together by tight junctions which form a barrier to the passage of large molecules. Individual fibres and their surrounding Schwann cells are in turn surrounded by the endoneurium which represents loose connective tissue (see Figure 2). The sciatic nerve is comprised of myelinated motor and sensory axons which are surrounded by myelinating Schwann cells in a 1:1 of medium to large diameter myelinated axons as well as unmyelinated sensory afferents which are in turn grouped and surrounded by non-myelinating Schwann cells (see Figure 3). Schwann cells act to protect the ensheathed axon as well as to provide insulation (in the case of myelinated afferents). The nerve contains a small number of blood vessels (vasa nervorum), which penetrate the epineurium and perineurium and terminate in a loose capillary plexus at the level of the endoneurium (Gartner and Hiatt, 2001).

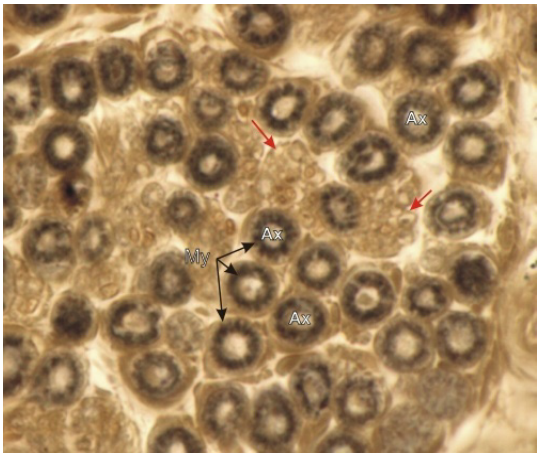

Figure 3: A transverse section of a nerve. Myelin sheath (My, black arrows) can be seen around individual axons (Ax) and groups of unmyelinated axons or poorly myelinated axons (red arrows) can also be seen. (From Clermont Y., http://audilab.bmed.mcgill.ca/HA)

1.2.2. Central Nervous System

The sciatic nerve possesses central projections terminating in the dorsal and ventral regions of the spinal cord. The spinal cord has been divided into horizontal layers named laminae based on the morphological properties of the cells they contain as observed with the Nissl method (Rexed, 1952; 1954). The most superficial layers of the dorsal horn (laminae I and II) are particularly important in the processing of noxious information. Lamina II can be further

subdivided into inner and outer regions. Laminae I and II receive input from sensory afferents in which the majority (but not all) respond to polymodal nociceptive stimuli such as heat, cold and pinch. The deeper laminae, specifically lamina V, receive input from neurons responsive to both noxious and innocuous stimuli. The spinal cord not only receives the central terminations from neurons whose cell bodies reside in the dorsal root ganglia but also possesses neurons which project to the brain, as well as excitatory and inhibitory interneurons (or local circuit neurons). Interneurons receive synapses from primary afferents and also establish pre-synaptic contacts on them. Interneurons are also pre-synaptic to projection neurons or other interneurons. This complex dorsal horn circuitry is still far from being well clarified and plays a major role in the modulation of pain-related information from the periphery before it is forwarded to higher centers (Ribeiro-da-Silva and De Koninck, 2009; Todd, 2010). Much of this research has been done in rats. Besides neurons, the spinal cord consists of neuroglial cells such as astrocytes and microglia. These cells normally protect the spinal cord by quickly responding to trauma through the release of inflammatory mediators and phagocytosing cellular debris. The spinal cord also possesses another cell of the neuroglia, the oligodendrocyte, which produces myelin in the central nervous system (CNS). The spinal cord is vascularised; blood vessels are separated from the spinal cord parenchyma by the blood-spinal cord-barrier.

1.3. Glabrous skin

Glabrous and hairy skin differs in that hairy skin is thinner, possess hair follicles and sebaceous glands whereas glabrous skin does not and is much thicker. For the purposes of this thesis, we will focus on glabrous skin. Skin contains two principal layers: the epidermis and dermis.

1.3.1. Epidermis

The epidermis forms the outermost, protective layer of skin. Keratinocytes, the principal cell type of the epidermis, are arranged to form five distinct layers which protect the skin against dehydration and is the first protective barrier against infection or insult.

1.3.1.1. Anatomy

The *stratum basale* is a single layer of cuboidal-to-columnar cells above the basement membrane in which the cells are almost continuously undergoing mitosis. As these cells divide, they push up the other layers to the most superficial regions where these cells become increasingly flattened so the keratin content of the superficial layer dominates. The *stratum spinosum* also contains mitotic activity. The *stratum granulosum* possesses more flattened cells which progress upwards to the *stratum lucidum,* a thin translucent layer, terminating at the *stratum corneum* made up of flattened keratinised cells.

1.3.1.1.1. Cellular Makeup

The epidermis contains four separate cell types: keratinocytes, melanocytes, Langerhans and Merkel cells. Keratinocytes are those described above and produce keratin, a fibrous protein which confers to the skin its protective abilities. The formation of keratin leads to the death of the cells that produce it. Keratinocytes have recently been implicated as functional mediators between the innervating sensory afferents and changes in the external environment by responding directly to cues through the release of agents which act on the innervating nerve terminals. Receptors which have been implicated in mediating this interaction include the thermoreceptive TRP channels, TRPV3 and TRPV1. TRPV3 is sensitive to temperatures ranging from 22-40^{o}C (Peier et al., 2002) and the TRPV1 channel is sensitive to temperatures >42^{o}C and upon its activation, results in the increase of intracellular calcium (Inoue et al., 2002). Cultured rat keratinocytes have also been shown to express the purinergic ligand-gated cation channels P2X1, P2X2, P2X3, and P2X7 (Inoue et al., 2005). Keratinocytes also express the cannabinoid receptor CB2 which, when bound by an agonist (such as the endocannabinoids), causes the release of the endogenous opioid β-endorphin which has anti-nociceptive actions (Ibrahim et al., 2005). It has also been demonstrated that keratinocytes also express low levels of the sodium channels Nav 1.5-1.7, an observation that is significant in that membrane depolarization causes the channel to open further depolarizing the membrane ultimately leading to the release of ATP (Zhao et al., 2008). Keratinocytes

contain and respond to a number of trophic factors and proinflammatory cytokines which will be addressed within the section on neurotrophins. Melanocytes synthesize the pigment melanin which confers the skins' color. Langerhans cells, a class of dendritic cell, are restricted to the epidermis and are the superficial immune cells responsible for the initial cell-mediated immune response to injury or infection. This initial immune response is mediated by antigen presentation via expression of high levels of class II major histocompatability complex molecules to local T-helper cells. Merkel cells are immediately distal to mechanosensitive sensory nerve endings. The epidermis is also innervated by free nerve endings which respond to nociceptive stimuli (Gartner and Hiatt, 2001).

1.3.2. Dermis

The dermis comprises the bulk of the skin. It lies between the epidermis and the hypodermis (which is not part of the skin) which is composed mostly of loose connective tissue and adipose tissue and functions as an anchor between the skin and underlying structures. The dermis has an important role in maintaining homeostasis.

1.3.2.1. Anatomy

The dermis consists of a large variety of cell types including fibroblasts, macrophages, mast cells, and vascular smooth muscle and endothelium. The dermis is the most superficial layer which is vascularised and contains continuous capillaries. The dermis is described by histology textbooks as being divided into two layers, the papillary and reticular. The papillary layer is made up of connective tissue between the epidermis and the dermis. It sends its dermal papillae into the epidermis, which is usually infiltrated by Meissner's corpuscles or, in the rat, Meissner's-like lamellar structures and capillary loops. The reticular layer mainly consists of dense, irregular connective tissue and collagen which confers to the skin its elasticity and hydration properties. Sweat glands are found predominantly in glabrous skin. In rat, they are exclusively found in the glabrous skin and are relatively rare compared to primates. Sweating is regulated by the sympathetic nervous system through cholinergic fibres. Glabrous skin is unique

in its rich capacity of venous plexuses which can change its blood flow velocity dramatically based on neural input from sympathetic and to a lesser extent, peptidergic nerve fibres (Ruocco et al., 2002). This is significant in the role of neurogenic inflammation and plasma extravasation which will be discussed below. In rat, the papillary and reticular layers are difficult to distinguish. Therefore, based on previous work from our laboratory, we divide the dermis into two regions. The upper dermis of the rat, which corresponds to the tissue which ends at the level of the opening of the sebaceous glands in hairy skin and roughly corresponds with an approximate distance of 150 μm from the dermo-epidermis junction in glabrous skin and is virtually devoid of sympathetic fibres, and the lower dermis, which is the remaining dermis ending at the level of the hypodermis (Ruocco et al., 2000; Yen et al., 2006).

1.3.2.1.1. Immune Roles

The dermis is populated by a number of resident immune cell types such as mast cells. Cell types normally found in circulation include neutrophils, T and B lymphocytes, eosinophils and monocytes. In inflammation, these cell types migrate to the skin. Mast cells differentiate once they enter tissue from blood and possess histamine and heparin within their cytoplasmic granules. This acidic heparin content allows for their identification using the histological dye toluidine blue via the formation of a metachromatic precipitate (Blumenkrantz and Asboe-Hansen, 1975). It has been demonstrated that mast cells infiltrate the sciatic nerve at the lesion site (Scholz and Woolf, 2007). Upon activation and degranulation, mast cells release potent pro-inflammatory mediators such as histamine, serotonin, cytokines, and trophic factors (Thacker et al., 2007). Mast cell tissue content can be increased through the expression of local trophic factors follow injury which mediate chemotaxis of mast cells towards site of injury (Aloe et al., 1995). Macrophages respond within the first 2-3 days following nerve injury (Perry et al., 1987). Macrophages are involved in the clearance of myelin and cellular debris following nerve injury and attenuation of macrophage infiltration reduces the ability of the organism to mount a successful Wallerian degeneration response (Thomson et al., 1991). Wallerian degeneration will be more thoroughly

described later in this introduction. Schwann cells, although they are not classified as immune cells, possess cellular capabilities in line with those cell types described above. Schwann cells surround myelinated and non-myelinated peripheral axons as well as post-ganglionic sympathetic efferents. Schwann cells are identified based on their expression of the S100 protein, a member of a large family of calcium binding proteins. S100 has two isoforms, α and β. The α isomer is found in less than 5% of neurons whereas the β is found predominantly in glia within the PNS. S100-β expression is directly proportional to the degree of myelination where a high degree of expression is associated with myelinating Schwann cells and low levels associated with non-myelinating Schwann cells. S100-β is also found in low levels within Schwann cells of post-ganglionic sympathetic efferents (Gonzalez-Martinez et al., 2003). Schwann cells provide trophic support to the surrounded axons and are able to produce a number of pro-inflammatory mediators, cytokines as well as proteases.

1.4. Sensory Innervation

The dermis and epidermis are innervated by sensory afferents terminating in the dorsal horn. Sensory afferents can be divided according to their anatomy, cable properties and neurochemistry. Sensory afferents can be broadly classified as Aβ, Aδ and C fibers and can be further classified according to their neurofilament content. Initial descriptions were based on the observation of trigeminal ganglion neurons using polarization light microscopy and it was shown that large soma appeared light and small soma appeared dark (Koneff, 1886). This observation was later found to be due to the relative content of the intermediate neurofilament of molecular weight 200 kDa (also known as NF200) where the large-light neurons posses this neurofilament in relative abundance and the small-dark are neurofilament poor (Anderton et al., 1982; Lawson et al., 1984; Wood, 1981).

1.4.1. Sensory Afferent Neurochemistry

Sensory afferents are able to respond to environmental cues and conduct this information to higher order structures due to the presence of dedicated

receptors, channels, neurotransmitters and neuropeptides. Sensory fibers in general (i.e. Aβ, Aδ & C-fibers) can be indiscriminately labeled based on their expression of the pan-neuronal marker, protein gene product 9.5 (PGP-9.5) which also labels motor and autonomic fibers. PGP-9.5 is a ubiquitin carboxyl-terminal hydrolase which is ubiquitously expressed in all neuronal cell types (Wilkinson et al., 1989). On myelinated sensory afferents, voltage dependant sodium channels are present in high density within the node of Ranvier, in lower densities under the myelin sheath and are also found on unmyelinated afferents (Black et al., 1990) and are responsible for action potential generation (Catterall et al., 2005). Sodium channels are formed of a single α-subunit of which nine members have been identified (for channels Nav 1.1-1.9) and fold into four domains with each domain made up of six transmembrane regions and can be associated with a β-subunit (Dib-Hajj et al., 2010). Nav 1.1 & 1.3, 1.6-1.9 are principally distributed within the DRG on small through large diameter afferents, however Nav 1.3 is normally expressed only during embryogenesis (Black et al., 1990; Catterall et al., 2005; Dib-Hajj et al., 2010). The expression of sodium channels can be unevenly distributed between small and large diameter afferents. For example, Nav 1.8 expression is negatively correlated with conduction velocity, meaning it is expressed preferentially by unmyelinated small diameter afferents (Djouhri et al., 2003). This observation also holds true for the Nav 1.9 sodium channel where its expression is restricted to ~31% of sampled small diameter nociceptive afferents (Djouhri and Lawson, 2004; Fang et al., 2002). Calcium channels are a group of voltage-gated ion channels (VGCC) made up of low-threshold T-type channels as well as the high-threshold L-, N, P/Q and R-type channels (Snutch, 2005). For example, N-type VGCC are highly expressed on DRG neurons and its blockage prevents the release of neuropeptides and glutamate (Perret and Luo, 2009). The receptors which confer heat or cold sensitivity to sensory afferents are members of the TRP family. TRPV1, a ligand gated cation channel exhibiting a high degree of permeability to calcium, is responsive to temperatures greater than 43^{o}C and is activated by the primary component of chilli peppers, capsaicin (Caterina et al., 1997). Activation of those primary afferents containing neuropeptides, in

part through TRPV1 activation, results in their release. Pro-nociceptive neuropeptides found in both myelinated and non-myelinated sensory afferents (i.e. peptidergic afferents) include calcitonin-gene related peptide (CGRP) which exerts its effects peripherally as a potent vasodilator through its receptor, a heteromeric receptor comprising of the GPCR calcitonin receptor-like receptor (CRLR) and RAMP1. CRLR signals through a Gα mediated pathway meaning upon agonist binding, it subsequently activates adenylyl cyclase to generate intracellular cyclic adenosine monophosphate. Substance P (sP) another pro-nociceptive neuropeptide, is ~98% colocalized to CGRP immunoreactive primary afferents and exerts its effects peripherally to elicit plasma extravasation and centrally via its receptor neurokinin-1 (NK-1R) inducing its internalization on projection neurons (Burnstock, 1990; Ribeiro-da-Silva, 1995). CGRP and sP possess potent pro-inflammatory and pro-nociceptive effects when released peripherally via their actions on their cognate receptors namely CRLR and NK-1R respectively. It is the antidromic effects of sP and CGRP release in the periphery that contribute to the hallmark signs of neurogenic inflammation. These are arteriolar vasodilatation, enhancement of vascular permeability and protein exudation.

1.4.2. A-Beta Fibres

The Aβ-fibres are predominantly responsive to low threshold mechanostimulation, are thickly myelinated and are of large diameter and rapidly conducting.

1.4.2.1. Anatomy

Aβ sensory afferents terminate in the deeper laminae of the dorsal horn as well as in the dermis of the skin.

1.4.2.1.1. Central Terminations

Aβ-afferents innervate cutaneous low-threshold mechanoreceptors, terminate in laminae III-IV (also known as the nucleus proprius) and are thought to occupy a territory receiving non-nociceptive input within the spinal cord

(Ribeiro-da-Silva and De Koninck, 2009). The initial descriptions of the low threshold sensory afferents were done as part of a series of publications in which horseradish peroxidase was used to trace individual axons from cats and monkeys and these traced axons were further classified according to their physiological properties (Light and Perl, 1979a). The nucleus proprius also houses wide dynamic range cells, interneurons as well as projection neurons forming part of the major ascending pathways, namely the spinothalamic, spinocervical and dorsal column postsynaptic pathways. The Aβ afferents form axodendritic connections onto glutamatergic (excitatory) and GABAergic (inhibitory) neurons and are postsynaptic at axoaxonic connections to GABAergic (inhibitory) interneurons (Ribeiro-da-Silva and De Koninck, 2009).

1.4.2.1.2. Peripheral Terminations

Aβ primary afferents terminate within the dermis of higher order species as a number of specialized nerve formations, namely Meissner's and Pacinian corpuscles, Merkel disks, Ruffini endings and hair follicle receptors. Aβ-fibers travel in cutaneous nerves in the dermis where they later branch to form (in part) these anatomical structures. Aβ-fibers in rats can usually be discriminated based on axon diameters of approximately 6-12μm and a soma size of >800μm^2 (Djouhri et al., 2003). There is a minority of Aβ-fibers that form non-specific terminations within the dermo-epidermal junction and these may be considered the mechanical nociceptors (Kruger et al., 1981).

1.4.2.2. Physiological Properties

Sensory afferents were given their names based on a proposed sequence of compound action potentials evoked by a single brief electrical stimulus namely A, B and C. But, from the cutaneous nerves measured, there was only a prominent A and C wave and within the A wave three separate and distinct components namely the α, β and δ (Birder and Perl, 1994). The Aβ afferents (or nociceptive insensitive fibers as they were initially classified) were initially described as in conducting upwards of 51 m/sec (Burgess and Perl, 1967) and are now classified as conducting between 25-72m/s depending on the species from which they are

sampled (Djouhri and Lawson, 2004; Kandel et al., 2000). Aβ-fibers can be either rapidly adapting and responsive to light touch such as stroking or fluttering, or slowly adapting and responsive to stretch, pressure or texture. Rapid adaptation refers to the cells' ability to generate rapid action potential discharges once given an adequate continuous stimulus, and in this case, quickly ceases during the initial stimulus application (Kandel et al., 2000). The term slowly adapting afferents refers to the ability of such afferents to generate action potentials for a prolonged period of time during the sustained application of stimulus and gradually resume a normal action potential discharge in contrast to the rapidly adapting afferents (Kandel et al., 2000).

1.4.2.3. Sensory Transmission

Aβ-fibers are generally described as providing non-nociceptive input such as mechanical information. Aβ–fibers are mostly low-threshold mechanosensitive (LTM) afferents sensitive to touch, vibration, brush and texture and are heat insensitive (Julius and Basbaum, 2001). There is literature on the presence of high-threshold mechanoreceptors (HTM) conducting within the Aβ range (i.e. 30-55m/s), and that approximately 20% of these sensory afferents respond to noxious heat in monkeys, rats and guinea pigs (i.e. 40-50^{o}C) (Campbell et al., 1979; Djouhri and Lawson, 2004). However, this is still controversial and mostly based on the arbitrarily-set cut-off of conduction velocities of Aδ and Aβ-afferents (Julius and Basbaum, 2001).

1.4.2.4. Neurochemistry

The current method for identifying A-fibers using immunocytochemical methods has been largely based on the initial observation of relative neurofilament content. As such, antibodies have been raised against the NF200 protein predominantly found in these myelinated afferents. The most common of these is the RT97 monoclonal antibody however the N52 monoclonal antibody has also been used (Anderton et al., 1982; Lawson et al., 1984; Wood, 1981). For the remainder of this section, the description of cytochemical markers relevant to

the Aβ-fiber population will be restricted to those observed in rats as there is interspecies variation.

A minority (~21%) of large diameter myelinated DRG neurons were immunoreactive for the sodium channel Nav 1.8 (Djouhri et al., 2003). Nav 1.7 is expressed on some large diameter neurons and Nav 1.6 expressed on all DRG neurons (Dib-Hajj et al., 2010). The Aβ population is also characterized by the expression of trophic factor receptors such as TrkA, TrkB and TrkC. The tyrosine kinase receptor TrkA is seldom found on myelinated afferents; although 18% of all TrkA immunoreactive DRG neurons also label with the NF200, these are usually within the Aδ size range (Averill et al., 1995). In contrast, the majority of TrkB and TrkC expression was found on DRG afferents with large soma diameters. The TrkB expressing afferents overlapped the medium and large diameter DRG, whereas TrkC expression was restricted to large diameter afferents (McMahon et al., 1994). It has also been shown that a large proportion of large diameter Aβ primary afferents possess the vesicular glutamate transporter 1 (VGLUT1) and are negative for markers normally associated with nociceptive primary afferents such as CGRP and sP (Oliveira et al., 2003; Todd, 2003).

1.4.3. A–Delta Fibres

Aδ primary afferents are generally characterized as being receptive to nociceptive sensory input and having peripheral terminations within the dermis and epidermis. These afferents terminate in the superficial dorsal horn of the spinal cord. They are thinly myelinated and possess a moderate conduction velocity.

1.4.3.1. Anatomy

1.4.3.1.1. Central Terminations

The Aδ primary afferents terminate in deeper lamina II and lamina III in the case of non-nociceptive afferents innervating down hairs. Those Aδ afferents receiving nociceptive input terminate in laminae I and V (Light and Perl, 1979b). The nociceptive Aδ afferents terminating in lamina I provide monosynaptic input directly onto neurons which project directly to those centers in the brain

responsible for nociception such as the spinothalamic tract (Craig, 2003). Lamina V contains primarily wide dynamic range (WDR) cells (Eckert Iii et al., 2006). WDR are a cell type activated by both noxious and innocuous input and include interneurons as well as projection neurons and can receive input from all three fibre types (Aβ, Aδ and C-fibres).

1.4.3.1.2. Peripheral Terminations

In contrast to the Aβ afferents (with the exception of the D-hair fibres found in hairy skin), the Aδ afferents are not associated with specific dermal structures but rather terminate as free nerve ending in the same manner as the C-fibres. There is very little known about the anatomical organization of these fibres as we lack a specific marker for them, although it is known that some of them terminate in the epidermis as free nerve endings. The average diameter of the Aδ axons in rat is ~1-6μm and the soma size is between 400 to 700 μm^2 (Harper and Lawson, 1985). By electron microscopy, it has been shown that Aδ fibres are thinly myelinated and lose their myelin sheath at a certain distance from the site of termination in the epidermis.

1.4.3.2. Physiological Properties

The Aδ afferents conduct signals at about 5-30m/s which, in comparison to the Aβ and C-fibres, is mid-range (Kandel et al., 2000).

1.4.3.3. Sensory Transmission

The thinly myelinated afferents are responsible for the first or sharp pain initially felt after insult and this is attributed to its fast conduction velocity. They are responsive to temperatures either above 45^{o}C or below 5^{o}C and also consist of afferents possessing high threshold mechanoreceptors, which can also be named A-fibre mechano-heat-sensitive units (AMH) or A-fibre mechano-cool-sensitive units (AMC) depending on their properties (Djouhri and Lawson, 2004; Birder and Perl, 1994).

1.4.3.4. Neurochemistry

The medium diameter myelinated primary afferents, like the large diameter, express the intermediate neurofilament NF200 and can be differentiated from C-fibres based on their immunoreactivity toward NF200. There is much overlap of receptor or neuropeptide expression between the Aδ- and C-fibre afferents. N-type calcium channels are restricted to the Aδ- and C-fibres (Snutch, 2005). TRPM8 is activated by temperatures between 8-26^{o}C and are found on small diameter C-fibres as well as medium diameter Aδ-fibres (McKemy et al., 2002). Approximately 27% of Aδ afferents were also shown to possess the kainite receptors (made up of GluR5-7 subunits), a type of ionotropic glutamate receptor that is permeable to either K^+ or Na^+ (Carlton and Coggeshall, 1999). Those afferents which posses the kainate receptor also possess the TRPV1 channel. Finally, the sodium channel expression of nociceptive-specific Aδ afferents includes Nav 1.8, 1.9 and to a very limited extent, Nav 1.7 (Cummins et al., 2007; Dib-Hajj et al., 2010; Fang et al., 2002). Some Aδ-fibres can be identified based on their expression of both NF200 and CGRP. It has been demonstrated that 18% of TrkA expressing afferents also express NF200 and all those cells which express TrkA also express CGRP (Averill et al., 1995).

1.4.4. C-Fibres

The third and final class of primary sensory afferents are the C-fibres. C-fibres can be divided into two categories based on relative peptide content in which those that are peptide rich are considered peptidergic and those that are peptide poor are considered non-peptidergic. C-fibres are unmyelinated and associate with non-myelinating Schwann cells.

1.4.4.1. Physiological Properties

C-fibres are unmyelinated and conduct nerve impulses slowly (~0.4-2.0m/s) making these sensory afferents the slowest of the three afferent types.

1.4.4.2. Peripheral Morphology

C-fibres terminate within the epidermis as free nerve endings. They travel within the upper dermis in small cutaneous nerves, some of them along the

dermo-epidermal junction where they form a dense plexus; they also terminate as free nerve endings in the dermis (Grelik et al., 2005a; Grelik et al., 2005b; Taylor et al., 2009a; Yen et al., 2006). C-fibres in general are most dense along the dermo-epidermal junction. Those free nerve endings which terminate within the epidermis are mostly not NF200 immunoreactive indicating that most of the free nerve endings in the epidermis are not Aδ- or Aβ- sensory afferents and rather are of the C-fibre subtype (Oaklander and Siegel, 2005). C-fibres have an average axon diameter of ~0.2-1.5μm and a soma area of <400μm^2 (Fang et al., 2006). These afferents, in contrast to the myelinated axons, are associated with non-myelinating Schwann cells. This class of Schwann cell also posses the S100-β protein, albeit in lower levels than the myelinating sub-type (Gonzalez-Martinez et al., 2003). Recently our lab has confirmed that it is the non-peptidergic subtype of C-fibres which comprise the majority of the epidermal innervation (Taylor et al., 2009).

1.4.4.3. Sensory Transmission

C-fibres are generally known as nociceptive afferents, meaning that the majority of these afferents play a role in the perception of noxious stimuli. These afferents are polymodal in that they respond to noxious heat, cold and pinch. Because of their relatively slow conduction velocity, C-fibres have been associated with the transmission of 'second' pain sensation, or the dull aching sensation proceeded by the initial sharp 'first' pricking pain conducted by the Aδ nociceptive afferents. C-fibres not only respond to purely external stimuli (such as pinch) as they also respond to tissue damage following the release of proinflammatory mediators or decrease in local pH. There is a subpopulation of C-fibres which are non-nociceptive and respond to low-threshold mechanostimulation, and exist principally in hairy skin (Lawson, 2002; Olausson et al., 2002). In addition to being either nociceptive or innocuous responders, C-fibres may include a group of silent glutamatergic nociceptors which terminate within the superficial dorsal horn pre-synaptically to neurons expressing NMDA receptors (Zhuo, 2000).

1.4.4.4. Subclassification

The C-fibre population of primary afferents can be divided into either those which are peptide rich (peptidergic) or those which are peptide poor (non-peptidergic). Each of these two populations have their own specific cytochemical correlates, however both are neurofilament poor or known as the 'small dark' group of DRG neurons (Lawson et al., 1984).

1.4.4.4.1. Non-peptidergic

1.4.4.4.1.1. Central Terminations

The non-peptidergic afferents terminate in the spinal cord dorsal horn in inner lamina II (lamina IIi) also known as the ventral part of the *substantia gelatinosa* or lamina II (Bailey and Ribeiro-da-Silva, 2006; Vulchanova et al., 1997; Vulchanova et al., 1998).

1.4.4.4.1.2. Peptide Content

The non-peptidergic afferents do not contain neuropeptides. These afferents (in addition to the peptidergic) excite post-synaptic cells via the excitatory amino acid glutamate and can be identified immunohistochemically based on the expression of the vesicular glutamate transporter 2 (VGLUT2). C-fibers express relatively low levels of this transporter, whereas VGLUT1 is expressed by myelinated afferents (Alvarez et al., 1996; Alvarez et al., 2004; Todd, 2003).

1.4.4.4.1.3. Receptor Content

It has been shown that the non-peptidergic afferents express the sodium channel Nav 1.9 at higher levels than the peptidergic afferents (Fang et al., 2006). The non-peptidergic afferents, as with the nociceptive Aδ and peptidergic C-fibres, express TRPV1 (Guo et al., 1999). Non-peptidergic C-fibres express an α-D-galactopyranosyl group within a population of cell surface oligosaccharides and are selectively recognized by the plant isolectin B4 (IB4) from *Griffonia simplicifolia* (Bogen et al., 2005; Silverman and Kruger, 1990; Streit et al., 1986). The non-peptidergic afferents are responsive to the glial cell line derived neurotrophic factor (GDNF) family of neurotrophins. This responsiveness is

mediated through the dual expression of the receptor tyrosine kinase, Ret acting as the signal transduction domain and any one of the four GDNF family receptor alpha family of glycosylphosphatidylinositol (GPI)-linked receptors (GFRαs) as the ligand binding domain (Bennett et al., 2006; Durbec et al., 1996). There are four members of the GDNF family of ligands, each of which exhibit receptor selectivity towards one of the four GFRα's. GDNF preferentially binds GFRα-1 and the remaining ligands, neurturin, artemin and persephin each bind preferentially to GFRα-2-4 respectively (Airaksinen and Saarma, 2002). The GDNF family of ligands are protective to those fibres expressing the receptor for it, in that selective cell death can be averted following their administration (Averill et al., 2004; Bennett et al., 2006; Leclere et al., 2007). The purinergic receptor P2X3, a two transmembrane ligand-gated cation channel, is expressed on 98% of IB4-binding afferents (Vulchanova et al., 1997; Vulchanova et al., 1998). Non-peptidergic, P2X3 immunoreactive afferents can be described as C-fibres due to their small diameter cell bodies, restrictive distribution in inner lamina II of the spinal cord and a lack of overlap with Aδ afferents terminating in deeper lamina II. The endogenous ligand for P2X3, ATP, is released from target tissue in response to either cell damage or membrane depolarization (Burnstock, 2000). The ATP-selective purinergic receptor subtypes found on rat non-peptidergic sensory afferents (either P2X3 or P2X2), can form homo or heterotrimeric receptor-channels (Burnstock, 2000; Honore et al., 2002; Jarvis, 2003). It has also been suggested that the P2X3 or P2X2/3 receptor-channels can be associated with mechanical allodynia (Tsuda et al., 2000). Other purinergic receptors, such as the GPCR P2Y receptors can be stimulatory or inhibitory based on the Gα protein and, like the ion channel P2X receptors, can be distributed through the peripheral nervous system on neurons or non-neuronal immune cells such as microglia (Gerevich and Illes, 2004). The bradykinin receptors are divided into two types, B1 and B2 and respond to bradykinin released by target non-neuronal cells following nerve injury. The B1 receptor, not normally expressed on nociceptive afferents, is upregulated following nerve injury on non-peptidergic afferents and

specifically in response to increased levels of available GDNF (Vellani et al., 2004).

1.4.4.4.2. Peptidergic

1.4.4.4.2.1. Central Terminations

The peptidergic C-fibres terminate within lamina I and outer lamina II (IIo). They form monosynaptic connections with NK-1R expressing projection neurons.

1.4.4.4.2.2. Peptide Content

The peptidergic afferents, as their name suggests, are peptide rich. This means that they express a number of neuropeptides which are important to the transmission of nociceptive information such as sP, CGRP, vasoactive intestinal peptide (VIP), galanin, and the neurotrophic factor BDNF (Averill et al., 1995; McMahon et al., 1999).

1.4.4.4.2.3. Receptor Content

There exists overlap in the receptor expression between peptidergic C-fibres and nociceptive Aδ primary afferents, this includes the capsaicin receptor TRPV1 (Caterina et al., 1997), the Nav channels 1.7, 1.8 & 1.9 (Dib-Hajj et al., 2010), and the acid-sensing ion channels (ASICs) (Leffler et al., 2006). The peptidergic C-fibres are responsive to trophic factors released from their innervated target tissue and this is conferred by the expression of Trk receptors. Small diameter dorsal root ganglion neurons have been demonstrated to express the $\alpha2_A$ adrenergic receptor ($\alpha2_A$-AR) in conjunction with the delta-opioid receptor on sP containing afferents implicating its expression on peptidergic C- and Aδ-fibres (Riedl et al., 2009). It has been demonstrated using *in situ* hybridization and immunohistochemistry that two of the three primary subtypes of the α2-AR, $\alpha2_A$ and $\alpha2_C$ are those principally found on nociceptive primary afferent neurons (Cho et al., 1997). The α2-AR is a GPCR coupled to a Gi pathway so that stimulation of these receptors with low levels of their endogenous ligand, norepinephrine, is inhibitory. When clonidine, an α2-AR agonist, is

peripherally administered to neuropathic pain patients, the effects are analgesic (Lavand'homme and Eisenach, 2003). The α1-AR is a Gq-coupled GPCR, meaning that upon agonist binding, activates PLC increasing intracellular levels of IP_3 and calcium. When the antagonist, phentolamine, is peripherally administered to patients experiencing neuropathic pain, the effects are analgesic (Kim et al., 1993). Unfortunately, the distribution of the α1-AR receptors on sensory afferents in the skin has not been adequately described because of lack of a suitable antibody. The bradykinin B2 receptor is constitutively expressed and is upregulated following injury, more specifically in response to increased levels of NGF (Dray and Perkins, 1993; Lee et al., 2002; Perkins et al., 1993).

1.4.5. Autonomic Nervous System

The autonomic nervous system is divided into the parasympathetic and the sympathetic nervous systems. The focus of this discussion will be the sympathetic nervous system which innervates the glabrous skin. Hairy skin in the head region only (such as that found in the lower-lip area) receives innervation from the parasympathetic as well as the sympathetic nervous system (Ramien et al., 2004). The parasympathetic and sympathetic nervous systems can also be divided based on their relative responsiveness to trophic factors, similar to that observed by the peptidergic and non-peptidergic primary afferents. The parasympathetic nervous system is responsive to the GDNF family of trophic factors whereas the sympathetic is responsive to neurotrophins such as NGF. The local production of these trophic factors has been attributed to the surrounding Schwann cells (Gonzalez-Martinez et al., 2003). The post-ganglionic sympathetic efferents synthesize and release norepinephrine, in an activity dependant manner (which the exception of those that innervate sweat glands, which produce acetylcholine). Norepinephrine is synthesized within post-ganglionic efferents in a number of enzymatically catalyzed steps. The first of which is the hydroxylation of tyrosine to L-DOPA by tyrosine hydroxylase, followed by its decarboxylation to dopamine by pyridoxal phosphate and DOPA decarboxylase and concluded by its oxidation to norepinephrine by dopamine β-hydroxylase. The presence of these enzymes is exploited through the application of specific

antibodies towards either tyrosine hydroxylase or dopamine β-hydroxylase for the use in immunohistochemistry. The transport of norepinephrine is via the vesicular monoamine transporter 2 (VMAT2) which is again specific to sympathetic efferents in the periphery (Nirenberg et al., 1996; Weihe and Eiden, 2000; Weihe et al., 1994). Sympathetic innervation within the glabrous skin is normally restricted to blood vessels found in the lower dermis (Ruocco et al., 2002; Yen et al., 2006). Sympathetic efferents are exquisitely responsive to nerve growth factor (NGF) (Levi-Montalcini, 1976; Levi-Montalcini and Angeletti, 1963b). This responsiveness is conveyed through the expression of the nerve growth factor receptors p75 and TrkA (Chao, 1994; 2003; Chao and Hempstead, 1995; Naska et al., 2010).

1.5. Neurotrophins

The neurotrophin family is made up of four members, NGF, brain derived neurotrophic factor (BDNF), neurotrophin-3 (NT-3) and neurotrophin-4 (NT-4). The cognate receptors for these neurotrophins are the tropomyosin receptor kinases (Trk) A, B and C. TrkA, which exhibits high affinity for NGF, TrkB which is selective for BDNF and also binds NT-4, and TrkC which binds NT-3. Neurotrophins are all able to exert pro-survival or supportive effects during development and adulthood respectively and insufficiency of each of the them can lead to impairment of the peripheral or central nervous systems (Chao, 2003).

1.5.1. Nerve Growth Factor

Nerve growth factor (NGF) in its mature form is a 13kDa peptide. The human structure has been resolved in its homodimeric form when bound to

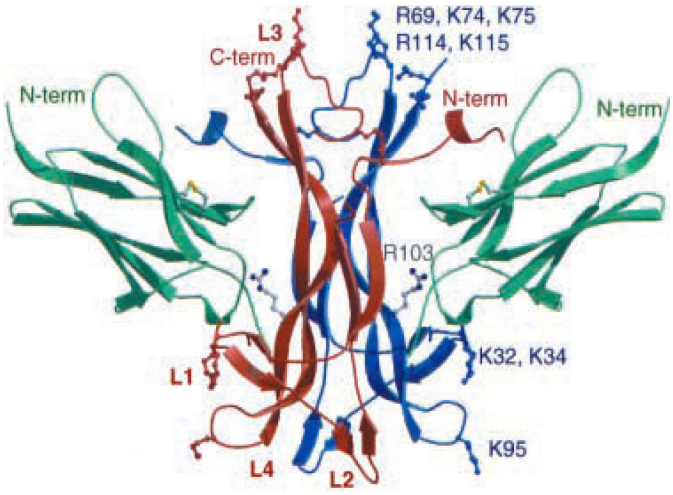

Figure 4: Crystal structure of NGF. Existing as dimer (blue and red) in complex with TrkA-D5 (green). Central core of NGF made up of β-sheets and loops L2 and L4 interact with TrkA-D5. (From Wiesmann C, 1999)

the extracellular (D5) domain of TrkA. The NGF inflexible core is made up of a pair of double-stranded, twisted β-sheets, which confers the structural integrity as well as a hydrophobic core, a cysteine-knot, and reverse turn at one end and three β-hairpin loops at the other (see Figure 4). Two NGF molecules assemble in parallel to form the homodimer which essentially resembles a bat with wings, where the torso of the bat is the β-sheets and forms the essential contact with TrkA (McDonald et al., 1991; Wiesmann et al., 1999).

1.5.2. History

Nerve growth factor, through the pioneering work of Rita Levi-Montalcini, was initially found to be the secreted agent from mouse sarcoma cells. This soluble factor promoted significant neurite outgrowth of sympathetic and sensory ganglia obtained from chick and human embryo and the neurite outgrowth can be attenuated by a sequestering antibody (Cohen et al., 1954; Levi-Montalcini and Booker, 1960). This diffusible factor was later found to exist in large quantities in snake venom and adult mouse submaxillary glands (Cohen, 1960; Cohen and Levi-Montalcini, 1956). The significance of her work, then with Victor Hamburger, provided evidence that, during development, nerve cells depend on target derived trophic factors. These trophic factors convey the signal to developing cells to survive rather than undergo apoptosis. The first such factor

to be identified during her work with Stanley Cohen was NGF. The Nobel Prize in Physiology or Medicine was awarded in 1986 to Stanley Cohen and Rita Levi-Montalcini for their work (Newmark, 1986).

1.5.3. Nerve Growth Factor Receptors

There are two primary receptors for nerve growth factor; p75 and TrkA. TrkA is a single transmembrane receptor tyrosine kinase which either heterodimerizes with p75 (a member of the tumour necrosis factor receptor family) or homodimerizes depending on cell surface concentrations. TrkA is a 140kDa protein when fully glycosylated and expressed on the cell surface, whereas the 110kDa form is an immature, incompletely glycosylated, variant (Vaegter et al., 2011).

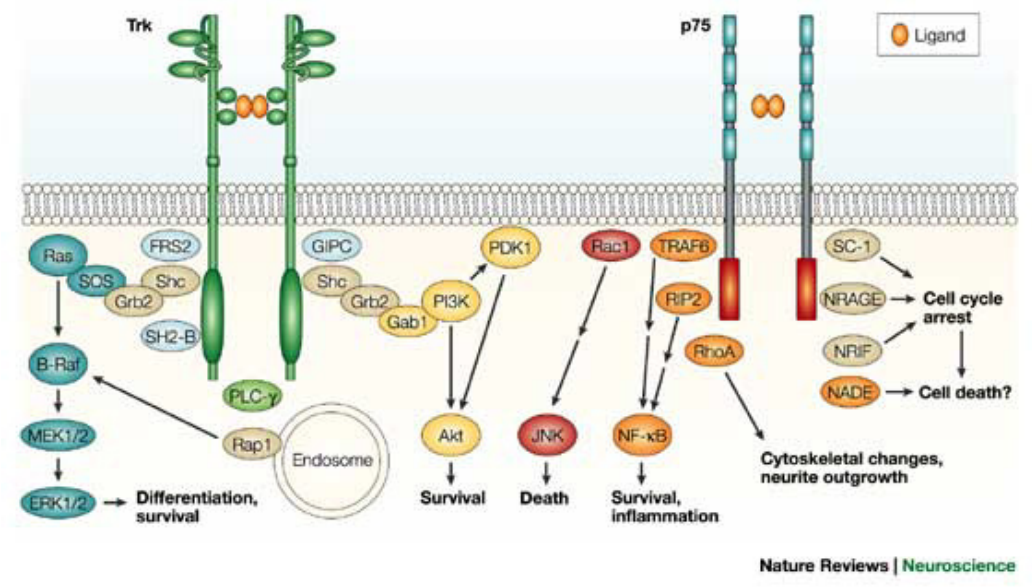

Figure 5: Signalling cascades of both p75 and TrkA upon NGF binding. TrkA can induce three signalling cascades: Erk1/2, PLC-γ and PI3K pathways culminating in survival and differentiation. p75 activation involves NF-kB and JNK pathways. (From Chao, MV., 2003)

The TrkA receptor is made up of two cysteine rich domains (D1 & D3) that flank three leucine-rich motifs (D2) in the extra-cellular N-terminal domain followed by two immunoglobulin-like regions D4 and D5 which form the essential contact with NGF. The transmembrane domain is followed by the intracellular non-catalytic juxtamembrane domain wherein the first of five phosphorylated tyrosines are located (Tyr490). The catalytic kinase domain is home to Tyr670, 674/5 and finally the C-terminal tail Tyr785. Phosphorylated Tyr490 and 785 are key binding spots for signalling molecules whereas the Tyr670, 674 and 675 play an autoregulatory function as part of the kinase catalytic domain (Reichardt, 2006). TrkA binds NGF with high affinity (Kd ~10^{-11}M) however, in certain situations, NT-3 can also bind TrkA and this binding differentiates endosomal signalling (in the case of NGF) from a more limited cell surface signalling in the case of NT-3 (Ivanisevic et al., 2007; Kuruvilla et al., 2004). Upon ligand binding by NGF to the extracellular domain (specifically the D5 domain) stabilization of the flexible NGF is conferred, but also a conformational change of TrkA is induced and results in trans-autophosphorylation of the five tyrosine residues (Kaplan and Stephens, 1994; Patapoutian and Reichardt, 2001). The signalling cascades induced by ligand binding include Erk, PI3K and PLC-γ (see Figure 5) (Chao, 2003; Nicol and Vasko, 2007). Phosphorylated Tyr490 recruits the SHC adaptor protein in conjunction with SOS and Grb-2 which then initiates binding of Gab-1 and PI3K. PI3K produces many lipid products which induce the recruitment of molecules such as the Akt kinase to the membrane where it can then phosphorylate a number of pro-survival molecules such as IκB which then recruits the transcription factor NF-κB. BAD, when phosphorylated by Akt, associates with 14-3-3 proteins and prevents binding of BAD to Bcl-xL, a pro-apoptotic family of proteins (Patapoutian and Reichardt, 2001). Phosphorylation of the Tyr785 residue recruits PLC–γ and is activated by TrkA's kinase function. PLC-γ then hydrolyses phosphatidylinositides to generate diacylglycerol (DAG) and inositol tri-phosphate (IP_3) which in turn induces the release of intracellular calcium stores. P13K can also be activated by the Ras/Raf/Erk cascade. This

leads to phosphorylation of the transcription factor, CRE-binding protein (CREB) (Patapoutian and Reichardt, 2001).

P75 is a low-affinity neurotrophin receptor which binds each neurotrophin equally, namely, NGF, BDNF, NT-3 and NT-4 (Kd ~10^{-9}M). The extracellular domain is made up four cysteine-rich motifs, a single transmembrane domain and an intracellular `death domain` which propagates its pro-apoptotic signalling cascade. The binding ratio of p75 and TrkA to a NGF dimer is still not fully agreed upon, however some suggest that it is a p75 dimer which complexes with the TrkA dimer to induce a conformational change in the TrkA dimer which enhances the binding affinity of TrkA (Chao, 2003; Reichardt, 2006). The p75 mediated signalling cascade (see Figure 5) is principally through the neurotrophin-receptor-interacting MAGE homologue (NRAGE) and leads to cell cycle arrest. As well, neurotrophin activation can lead to recruitment of the Rac1 adaptor protein and subsequent activation of the JNK pathway, ultimately activating p53 leading to apoptosis (Chao, 2003; Reichardt, 2006). Unfortunately, p75 signalling is not quite so simple, and it has been reported that in some cases, p75 activation by NGF is able to induce cell survival (Hempstead et al., 1991; Massa et al., 2006). To moderate either p75 or TrkA signalling when each are bound by NGF, the binding affinity of p75 to the mature NGF is such that signalling will preferentially occur via the TrkA cascade. As well, TrkA signalling pathways such as PI3K inhibit those activating the JNK pro-apoptotic cascade initiated through p75 (Reichardt, 2006). However, it has recently been discovered that sortilin, a pro-apoptotic receptor which principally associates with p75, is found on all tissues in which either p75 or TrkA is found (Kiss et al., 2010; Vaegter et al., 2011). This receptor not only promotes apoptosis when associated with p75 but can enhance the anterograde receptor transport of TrkA via heterodimerization to promote cell survival and to ensure receptor localization at synapses (Vaegter et al., 2011). p75 exhibits non-selective, low binding affinity for all mature neurotrophins, however it displays a much higher binding affinity for their precursors, the secreted proneurotrophins (Harrington et al., 2004; Lee et al., 2001).

1.5.4. proNGF

The precursor to the mature form of nerve growth factor is proNGF. ProNGF has been suggested to be either mildly neurotrophic or strongly pro-apoptotic, depending on the experimental protocols and researcher (Clewes et al., 2008; Fahnestock et al., 2004; Nykjaer et al., 2004). The complex of proNGF and p75 has been resolved and it is shown that it is a 2:2 complex in contrast to the monovalent binding of mNGF to p75 (Feng et al., 2010). The precursor form of NGF has always been thought of as an intracellularly-matured peptide processed by a furin convertase (Seidah et al., 1996). NGF levels are modulated by tumor necrosis factor (TNF)-α and interleukin (IL)-1 in non-neuronal, target tissue (Hattori et al., 1993; Heumann et al., 1987b; Lindholm et al., 1987). Mast cells not only synthesize NGF, but are positively regulated by it, such that increased NGF availability increases mast cell infiltration and degranulation releases NGF (Aloe and Levi-Montalcini, 1977; Leon et al., 1994). NGF is also produced by Schwann cells, fibroblasts, keratinocytes and vascular endothelium, all of which have contact with TrkA and p75-expressing peripheral neurons and sympathetic efferents (Heumann et al., 1984; Heumann et al., 1987b; Scholz and Woolf, 2007; Stucky et al., 1999; Verge et al., 1989a). It has also been recently shown that proNGF is released by cultured human keratinocytes (Dallos et al., 2006) and cleaved within the extracellular space of CNS neurons to its mature form (Bruno and Cuello, 2006; Lee et al., 2001). The processing enzymes of proNGF include plasmin which directly cleaves proNGF to its mature form and matrix metalloprotease-9 (MMP-9) which degrades any residual mNGF remaining in the extracellular space (Bruno and Cuello, 2006). It has also been demonstrated that the processing enzymes are released in response to elevated levels of IL-1 and TNF-α (Bechtel et al., 1996; Han et al., 2005; Zhou et al., 2009).

1.5.5. Positive Roles of NGF

Following nerve injury, a process called Wallerian degeneration occurs. Within minutes of the nerve injury there is an immune and glial cell reaction in which macrophages infiltrate the area. The damaged axon begins to denervate its Schwann cells which then, due to the lack of contact, secrete MMPs. MMPs

break down the basal lamina of endoneurial blood vessels which in addition to the secreted vasoactive mediators such as CGRP, sP and bradykinin, promote plasma extravasation and vasodilatation. This in turn further propagates the immune reaction of allowing passage of circulating macrophages, T lymphocytes and mast cells to the damaged area and contributes to the generation of a neuro-inflammatory reaction to injury (Scholz and Woolf, 2007). As macrophages clear the myelin debris, myelinating and non-myelinating Schwann cells de-differentiate, proliferate and reorganize around the denervated territory, and throughout this progress increase surface p75 receptor expression (Ribeiro-da-Silva et al., 1991; Scholz and Woolf, 2007). Infiltrated macrophages and mast cells release the pro-inflammatory cytokines IL-1, IL-6, IL-1β and TNF-α as well as NGF. These molecules not only promote further macrophage infiltration but also increase the synthesis and release of NGF and GDNF by Schwann cells (Moore et al., 2002). It has also been suggested that it is the loose association of NGF by p75 on the surface of the reorganized Schwann cells which promote regrowth and survival of the intact TrkA-expressing peripheral nerves (Ramer et al., 1997; Taniuchi et al., 1986). The trophic factor gradient is reduced after persistent denervation or after axon contact has been re-established and homeostasis is returned (Johnson Jr et al., 1988). When Wallerian degeneration is delayed in a mutant strain of mice, macrophage recruitment is reduced, myelin sheaths and axons persist, although regeneration is impaired (Ramer et al., 1997). When exogenous NGF is applied to injured peripheral neurons, the overall loss of CGRP-immunroreactive peptidergic afferents is attenuated, an observation that supports the neuroprotective role of NGF (Bennett, 1998; Derby et al., 1993; Donnerer, 2003; Ljungberg et al., 1999; Schicho et al., 1999). Other trophic factors implicated in sensory afferent regeneration include GDNF. The administration of GDNF prevents injury associated mechanical sensitivity possibly through the prevention of upregulated sodium channels (Boucher et al., 2000; Nagano et al., 2003). The administration of GDNF, unlike NGF, does not promote axon sprouting but is efficacious in a neuroprotective manner (Leclere et al., 2007).

1.5.6. Role of NGF in Pain

In contrast to the apparent protective effects of increased levels of GDNF, prolonged increase in NGF promotes stimulus-induced hypersensitivity. Stimulus-induced hypersensitivity is commonly associated with either thermal (cold or heat) or mechanical hypersensitivity. Mice engineered to over express NGF demonstrate a two-fold increase in the number of sensory DRG axons, hyperinnervation of CGRP-immunoreactive afferents in the skin, sprouting of sympathetic efferents around sensory DRG and sensitivity to applied mechanical and thermal stimuli (Albers et al., 1994; Davis et al., 1993; Jarvis, 2003; Stucky et al., 1999). Increased availability of NGF to intact TrkA-expressing terminals leads to NGF being taken up by them and retrogradely transported to the cell body. It was initially suggested that it is this heightened concentration of NGF in DRG that would promote sprouting of sympathetic efferents around myelinated and unmyelinated TrkA-expressing cell-bodies (Ramer and Bisby, 1997a; Ramer et al., 1999; Ramer et al., 1997). However, an alternative and more likely hypothesis is that following injury, local macrophages and satellite cells surrounding DRG increase local production of NGF, which would lead to sympathetic sprouting around DRG cells (Ramer et al., 1998b). Retrograde transport of NGF from the target tissue is increased in pathological conditions and in turn increases the synthesis of CGRP, sP and BDNF in TrkA expressing medium and small diameter primary afferents (Donnerer et al., 1992; Obata et al., 2003). NGF is responsible for sensitizing nociceptive afferents, leading to lowered activation threshold. Acute heat sensitivity is conferred through the sensitization of the TRPV1 receptors in part by NGF through the phosphorylation of the TRPV1 receptor via the PI3K pathway (Zhang et al., 2005; Zhu and Oxford, 2007). The other method by which NGF confers long-term or sustained sensitivity to applied heat is by increasing the amount of cell-surface TRPV1 receptors via the p38 pathway (Ji et al., 2002). It was recently demonstrated that a site mutation in NGF did not interfere with its ability to bind to TrkA and retained its neurotrophic effects. However, this mutation was unable to induce a mechanical allodynia response within 5hrs following sub-cutaneous injection to a

mouse hind-paw. This observation is particularly important because it raises the exciting possibility that the induced effects on pain originate from a pathway independent from one involved in cell-survival. The pain-related mechanism involves the PLC-γ pathway (initiated by phosphorylation of Tyr785 on TrkA), resulting in release of intracellular calcium stores and further activation of PKC, suggesting the direct stimulatory effects on the sensory neuron could be stunted (Capsoni et al., 2011). The mechanisms underlying NGF-mediated mechanical sensitivity could involve PKC in which as-yet unidentified receptor cation channels responsible for transducing this stimuli are both upregulated and inserted into the membrane following NGF priming prior to mechanical activation (Di Castro et al., 2006). Unfortunately, compared to the information available on the mechanisms underlying alterations in thermal perception, there is a paucity in available information on mechanotransduction and the involvement in which increased NGF levels may alter it. Studies in which selective blockade of a variety of known receptor channels such as the TRPs, ASICs or Navs, fail to completely abrogate the mechanotransduction signal (Drew et al., 2007; Lin et al., 2009). NGF may acutely modulate the sodium channel thresholds by activating downstream kinases such as the ERK1/2 and p38 kinases which in turn phosphorylate Nav 1.7 and affect gating properties leading to hyperexcitability (Stamboulian et al., 2010). NGF acting through p38 does not alter gating properties of Nav 1.8 but increases current density (Hudmon et al., 2008; Stamboulian et al., 2010).

1.6. Methods Used

1.6.1. Immunohistochemistry

One of the principal techniques employed through the course of this dissertation is light microscopy of fixed tissue using immunohistochemical techniques.

1.6.1.1. History

Original immunohistochemical methods were based on the observation that antibodies against cell surface antigens could be used to visualize their

distribution in mammalian tissue. The requirements were that the antibody be retained to the tissue during the chemical processing required to visualize its distribution. There also needed to be a stable association between the antibody and its fluorescent label and that this be a specific reaction restricted to the properties of the antibody rather than that of the label (Coons et al., 1942). This first fluorescent label was fluorescein isocyanate, a derivative of the now commonly used fluorescein thioisocyanate (FITC) (Coons and Kaplan, 1950). However, it wasn't until the development of target-specific antibodies that indirect immunofluorescence really developed (Geffen et al., 1969). Once the reliable and rational development of monoclonal antibodies was perfected, this allowed for yet a higher degree of resolution and reproducibility within this emerging technique (Cuello et al., 1979).

1.6.2. Quantifiable Behavioural Analysis

One of the major developments in pain research was the ability to quantify the basic observation that animals in pain were sensitive to evoked stimuli. Unfortunately, since animals are not able to directly communicate to the observing researcher that the application of various stimuli induces discomfort, we are left with indirect methods such as averaging withdrawal frequencies or withdrawal latencies. Both of these methods are based on the premise that if an applied stimuli causes pain, the animal will withdraw the limb from the applied stimuli. It is the stimulation of the sensory afferents discussed earlier that initially transmit this signal through to higher order neurons and networks where it is then processed in the brain and the eventual withdrawal response is measured. It is the basis of this response which reaffirms the importance of studying the changes most intimately responsible for the initial perception of painful stimuli.

1.6.2.1. History

Maximilian von Frey, an Austrian-German physiologist, introduced the sensory specificity theory in 1895. This implied that there were discrete regions in the skin which were innervated and were responsible for specific sensations such as heat, cold, touch and pain. Von Frey initially used camel hairs calibrated

such that a known force applied to each hair would be required to bend it and these were later modified and retained the name 'von Frey hairs'. In pain research, this quantified the response frequencies associated with force applied to be able to determine relative mechanical sensitivity (Chaplan et al., 1994; Randall and Selitto, 1957). Another method which significantly contributed to the quantification of behavioural assessments was the Hargreaves method by which a focused beam of light is applied to the foot of unrestrained animals. The time it took for the animal to withdraw his paw from this light was measured as withdrawal latency. Paw withdrawal latencies or thresholds from an applied stimuli following induction of either neuropathic or inflammatory conditions were quantified and these latencies or thresholds can be significantly modified based on application of anti-inflammatory or analgesic agents (Hargreaves et al., 1988).

1.7. Animal Models of Neuropathic Pain

The development of animal models of any disease state is very important for elucidating mechanisms underlying various disease states as well as the modification of various aspects of its presentation through pharmacological manipulations.

1.7.1. Nerve Injury

Prior to 1988 (the year in which the first model of mononeuropathy was introduced) animal models of peripheral neuropathic pain were restricted to neuroma models, which developed following complete transection of peripheral nerves, and dorsal root rhizotomy, in which the spinal roots of the DRG terminals were transected. As well, other animal models of pain were developed based on disease states (e.g. diabetes), administration of toxins (e.g. mercury poisoning or lead administration) or inflammatory reactions (e.g. carrageenan), but these were adequate only to study the pathology of the nerves, as they did not induce a consistent pain state (Bennett and Xie, 1988; Thomas, 1971). Dorsal root rhizotomy resulted in autotomy (or the self-cannibalism of the affected limb) as well as perceived stimulus-evoked sensitivity and spontaneous pain as demonstrated by excessive scratching of the affected area (Sweet, 1981). This

model represented a specialized case in human patients of brachial plexus avulsion in which a complete deafferentation occurs in the periphery. Due to the apparent insensitivity or dysesthesia as demonstrated by the significant autotomy associated with this animal model, the rhizotomy model could not be used for generalized chronic pain studies (Sweet, 1981).

1.7.1.1. Chronic Constriction Injury Model of Peripheral Mononeuropathy

In 1988, Bennett and Xie were successfully able to reproduce the more pertinent aspects of a painful peripheral mononeuropathy commonly associated with causalgia or other traumatic and entrapment nerve injuries in rats (Bennett and Xie, 1988). The advantages to this model were the reduction in behaviour severity observed following rhizotomy, and ease of reproduction (in contrast to the neuroma models). The chronic constriction injury (CCI) model consisted of the application of four loose chromic gut ligatures tied around the common sciatic nerve so that they did not themselves constrict the nerve. The localized inflammatory reaction following the application of the foreign chromic gut ligatures would induce a self-strangulation of the nerve against the applied ligatures. The result of the inflammation and self-strangulation is associated with the induction of Wallerian degeneration described earlier. The behavioural correlates to this model was a long-lasting (~11wks) sensitivity of the affected hind-paw to noxious heat stimuli, sensitivity to applied noxious chemical stimuli (mustard oil) and sensitivity to cold stimuli (Bennett and Xie, 1988). The consequential development of stimulus (heat, cold and tactile) evoked hypersensitivity, as well as the perceived spontaneous pain experienced by the experimental animals, led researchers to investigate the underlying neurological and morphological changes which could explain this. In the early 1990s, a number of important studies conducted at the light and electron microscopic levels recorded the spectrum of fibre loss following the application of the CCI as well as the histological changes occurring within the sciatic nerve immediately distal to the site of injury. It was found that anywhere from 71-94% fibre loss at its peak was observed within the myelinated afferent population following application of the CCI (Basbaum et al., 1991; Coggeshall et al., 1993; Guilbaud et

al., 1993). The unmyelinated afferents, for reasons not fully understood, seemed to be fairly resilient towards the nerve injury in that a peak loss of only 34-74% has been reported. It has been noted that during the progression of the injury, an increase in thinly myelinated axons occurs from approximately two weeks onward. However, it cannot be ascertained whether these regenerated afferents are clearly Aβ or Aδ as these afferents are inherently altered in their conduction properties due to the injury. The alterations in myelin thickness make accurate physiological recordings from the regenerating thinly myelinated afferents and identification of them under the electron microscope unreliable. The variation within the degree of fibre loss has been associated with inter-laboratory changes in tightness of the applied ligatures, where tighter ligatures are associated with a model more closely approximating an axotomy and looser ligatures with an incomplete, partial nerve injury. It is this variation that led Mosconi and Kruger (1996) to develop a model in which the chromic gut ligatures were replaced with a fixed-diameter polyethylene tubing (cuff model) (Mosconi and Kruger, 1996).

1.7.1.2. Cuff Model of Neuropathic Pain

The cuff model of neuropathic pain was developed with the expectation that it would be interchangeable in terms of behavioural correlates and degree of fibre loss with the original CCI. As well, it would have the advantage of standardizing the degree of injury to the sciatic nerve with the objective of investigating the peripheral mechanisms of neuropathic pain (Mosconi and Kruger, 1996). The general similarities between the two models include development of nocifensive behaviour, significant increase in the ratio of small, unmyelinated afferents to large/medium diameter myelinated afferents as well as enclosure of the applied ligatures (or cuff in this case) by a dense network of connective tissue. A marked degree of Wallerian degeneration followed the application of the polyethylene cuff indicated by degenerated axon profiles, disrupted myelin sheaths as well as proliferated Schwann cells containing myelin debris and macrophage infiltration was observed (Mosconi and Kruger, 1996). A variation of this model was developed by Pitcher and Henry (2004) to exploit the reproducibility of the original cuff model for the long term persistence of

mechanical sensitivity. These authors adapted the original Mosconi and Kruger model to apply only one polyethylene cuff around the common sciatic nerve as opposed to four. This was done to reduce the relative degree of trauma to the nerve inherent in the application process itself while still maintaining the prolonged mechanical sensitivity (Pitcher and Henry, 2004). It is this modified version of the Mosconi and Kruger model which has been used in our lab and for the work conducted in this thesis.

1.8. Mechanisms of Neuropathic Pain in Animal Models

The many theories which try to explain the development and maintenance of neuropathic pain include discussions on centrally and peripherally mediated mechanisms (Sandkuhler, 2009). The scope of this introduction will be mostly restricted to peripheral mechanisms. The basic premise for most of these theories is that, following nerve injury, there exist a local imbalance within the periphery of cytokines, trophic factors and other pro-inflammatory mediators (e.g. protons and ATP). This, combined with the injury to the nerve itself, results in an acute response to this imbalance. However, it is the maladaptive changes occurring within the peripheral nervous system which perpetuates the neuropathic pain condition. The general definitions used to describe the behavioural correlates following onset of pathological pain have been previously mentioned briefly in this General Introduction:

Allodynia: when a stimulus not known to activate nociceptive afferents begins to elicit a painful response. This represents an altered quality in sensation as defined by the 2011 IASP guidelines. This innocuous touch is considered to be that which would normally be sufficient to generate action potentials from LTM primary afferents (Sandkuhler, 2009).

Hyperalgesia: a heightened response to adequate stimulation required to elicit a painful response. The stimulation applied does not change in modality meaning that prior to and after injury, the response remains painful however it is the threshold which is lowered in order to elicit the painful response.

1.8.1. Sympathetic Involvement

As mentioned earlier, the sympathetic nervous system is normally involved in maintaining vascular tone and evoking appropriate responses when fight or flight mechanisms are activated. Sympathetic activity in normal circumstances plays no role in propagating pain signalling. However, following application of a variety of nerve injury models, sympathetic involvement has been described. Hallmarks of sympathetic involvement in pain maintenance can include rekindling of spontaneous pain and mechanical sensitivity following administration of a sympathetic block by local injection of norepinephrine. As well, some patients experiencing neuropathic pain claim that being startled by a sharp noise or emotional arousal exacerbates their pain (Bennett, 1991). The painful sensations following administration of norepinephrine can be reversed by pharmacological agents which can block α-adrenoreceptors such as phentolamine (Ali et al., 2000), or transient depletion of norepinephrine from its stores within the post-ganglionic efferents such as that which follows treatment by guanethidine. Guanethidine acts to deplete the local stores of norepinephrine from sympathetic terminals (Maxwell, 1982).

Among the original observations to explain the inappropriate involvement of the sympathetic nervous system in the maintenance of neuropathic pain was the formation of sympathetic baskets, following application of a spinal nerve ligation, around medium to large diameter cell bodies in the DRG (McLachlan et al., 1993). The animal models which have been used to study the involvement of the sympathetic nervous system in either the generation or maintenance of neuropathic pain have been based on the nerve lesion models such as that involving the ligation and transection of the sciatic and saphenous nerves. The injection of guanethidine post-operatively in this ligation/transection model reduces the incidence of autotomy and this observation lends support to the hypothesized sympathetic involvement. The Seltzer model (aka partial nerve ligation model), in which the sciatic nerve is partially ligated, demonstrated an almost complete ablation of the nerve-injury evoked sensitivity to heat and mechanical stimuli by post-operatively injected guanethidine (Shir and Seltzer,

1991). Data from other models such as the spinal nerve ligation (SNL) in which L5 and L6 spinal nerves are ligated, again demonstrated reduction of the ensuing mechanical allodynia following sympathectomy. However, thermal sensitivity was less affected following sympathectomy (Chung et al., 1993; Kim et al., 1993). In the SNL model, excitability parameters were recorded from DRG cell bodies following either direct electrical stimulation of the sympathetic sprouts or chemical activation by either ATP or norepinephrine. Following stimulation, it was shown that only large and medium diameter cell bodies demonstrated a reduced threshold for activation and it is these cells around which sympathetic basket formation was observed (McLachlan et al., 1993; Xie et al., 2010). Following administration of guanethidine to rats having received CCI, an only partial alleviation of spontaneous pain and mechanical sensitivities was observed but, cold allodynia was reduced (Perrot et al., 1993). CCI does induce sympathetic basket formation around DRG neurons; however an association with either small, medium or large diameter cell bodies is not clear (Ramer and Bisby, 1997c).

It has also been suggested that the relative degree of inflammation associated with the applied nerve injury in animal models is related to the degree of sympathetic basket formation and spontaneous activity of DRG afferents (Xie et al., 2006). Not only does the sprouting within the DRG occur following application of nerve injury or direct irritation by inflammatory agents, but our lab has consistently demonstrated a direct interaction between peptidergic afferents (which also express α_2-AR) (Riedl et al., 2009) and sympathetic efferents as early as 2-4 weeks either following chronic inflammation (Almarestani et al., 2008) or CCI (Grelik et al., 2005b; Yen et al., 2006). These results point not only to a method by which sympathetic excitation may drive inappropriate sensation via activation of large or medium diameter cell bodies in an experimental setting, but also point to a more direct excitation between sympathetic efferent interaction with small diameter peptidergic afferent peripheral terminals in the skin. Potential mechanisms driving the sprouting of the efferent terminals to either the DRG or upper dermis include the elevated levels of NGF following nerve damage

(Grelik et al., 2005b; Ramer et al., 1997; Ramer et al., 1998a; Ramer et al., 1998b; Yen et al., 2006). In experiments using engineered mice in which the development of Wallerian degeneration is delayed, there was a lack of regenerative peripheral sprouting of the damaged axons, as well as attenuation of evoked pain-related behaviour and sympathetic basket formation around DRG cell bodies (Ramer et al., 1997). The reverse is also true, being that if NGF is over-expressed, sympathetic efferents are present in small amounts in uninjured DRG. However, following application of nerve injury, the consequential basket formation is amplified (Ramer et al., 1998a).

A number of theories by which this inappropriate association between sympathetic efferents and sensory afferents contribute to either the maintenance or generation of neuropathic pain have been proposed. For example, following this association, upon stimulation of the sympathetic nervous system, norepinephrine and ATP are co-released and act on nearby receptors (Burnstock, 2000; Gibbins and Morris, 1997; Park et al., 2000). Expression of the α–AR on medium-large diameter cell bodies has been suggested to increase (Birder and Perl, 1999). However, conclusive evidence suggesting that local release of norepinephrine acting on these sites on the cell body and being sufficient to generate action potentials is lacking. An alternative hypothesis could be entertained, namely, that the interaction sufficient to generation action potentials within sensory afferents may rest within the periphery. It has been demonstrated that clonidine, an α_2-AR agonist, is antinociceptive peripherally via a G_i pathway (Lavand'homme and Eisenach, 2003; Ma et al., 2005). It has also been proposed that the nociceptive mechanism of norepinephrine (via α_1-AR) is synergistic with P2X3 receptors through its co-release with ATP from sympathetic efferents (Maruo et al., 2006). Following application of the CCI to the mental nerve, we have observed a close association between sprouted sympathetic fibres and P2X3-IR non-peptidergic afferents in the skin of the lower lip (Taylor and Ribeiro-da-Silva, 2011). However, a hypothesis to explain the underlying mechanisms driving the association between the non-peptidergic C-fibres and sympathetic

efferents is lacking. The observation is particularly novel given the lack of common trophic factor support to each the non-peptidergic C-fibres and sympathetic efferents.

1.8.2. Protein Expression Changes

It has also been proposed that, following nerve injury, there is a phenotypic switch as a result of the change in the microenvironment surrounding the uninjured nerves, in which neuropeptides not normally expressed by some non-nociceptive primary afferents are newly expressed. For example, it has been suggested that sP is expressed by Aβ-fibres after injury (Neumann et al., 1996) however this has not been confirmed (Hughes et al., 2007). It has also been suggested that TRPV1 expression is shifted from predominantly small and medium diameter afferents to large diameter afferents following SNL and PNL (Hudson et al., 2001; Ma et al., 2005), the significance of which would be a new sensitivity of large-diameter afferents to activation by high temperatures. Changes in expression of sodium channels have been described in many nerve injury models in which a dramatic upregulation of Nav 1.7, redistribution of Nav 1.8 (Gold et al., 2003) in sensory afferents and a *de novo* expression of Nav 1.3 (which is normally down-regulated after embryonic development) (Dib-Hajj et al., 2010). Sensitization of the TRPV1 channels has been suggested to be mediated through the increased expression of peripheral NGF. The acute sensitization of peripheral nociceptors by NGF is driven, in part, by activation of the kinase domain of the TrkA receptor which is able induce the phosphorylation of other membrane channels through the PI3K pathway and lower their threshold of activation. The contribution of TrkA activation to chronic sensitization is mediated through TrkA activation of signalling pathways to increase expression of receptor channels such as TRPV1 at peripheral terminals (Zhu and Oxford, 2007; Zhuang et al., 2004). In contrast, GDNF not only protects against injury-associated nerve loss (Bennett et al., 1998b) but has contradictory roles in the prevention or development of evoked pain-related behaviours. Indeed, when administered to naïve rats, GDNF was pro-nociceptive (Albers et al., 2006; Bogen

et al., 2008; Malin et al., 2006) and when administered following SNL, PNL or CCI was analgesic (Boucher et al., 2000; Sakai et al., 2008).

1.8.3. Inappropriate Innervation

Further hypotheses explaining the onset and maintenance of neuropathic pain focus on the inappropriate innervation changes following application of nerve injury models. For example, postulated changes occurring in the CNS included the suggestion that sprouting of A-fibres from deeper layers onto the superficial dorsal horn contributed significantly to the mechanism underlying the development of mechanical allodynia. This was to support a suggestion wherein LTM Aβ-fibres would make *de novo* connections with nociceptive higher-order pathways (Woolf et al., 1992). It was originally thought that Aβ-fibers were the only fiber type able to take up the cholera toxin subunit B molecule used to trace the myelinated afferents, but following injury it was demonstrated that C-fibers also developped this ability thus disproving the sprouting theory (Santha and Jancso, 2003). In light of this discovery, it has been accepted that sprouting of myelinated afferents into lamina II is minimal at best following nerve injury using alternative methods (Bao et al., 2002; Hughes et al., 2003).

With respect to changes in the periphery, our lab and others (Ma and Bisby, 2000) have demonstrated that a disequilibrium in skin sensory innervation correlated with the onsetof evoked pain-related behaviour associated with the progression of animal models of neuropathic and chronic inflammatory pain (Almarestani et al., 2008; Grelik et al., 2005b; Ruocco et al., 2000; Yen et al., 2006). A local disequilibrium in sensory innervation has been hypothesized to contribute to the development of mechanical and thermal sensitivity by exposure of polymodal C-fibres to a permissive environment of a sensitizing, proinflammatory soup in which these molecules are effective in reducing the threshold for generation of action potential in response to normally innocuous stimuli.

However, there exist many more theories as to the generation or maintenance of neuropathic pain, including but not limited to disinhibition of lamina I spinal cord neurons via a BDNF-mediated mechanism in which KCC2

levels are decreased. This would result in a decrease in GABA's inhibitory properties on inter- and projection neurons (Coull, 2003; Coull et al., 2005). Chronic activation of peripheral immune cells and long-term release of proinflammatory mediators may also contribute to sustained spontaneous activity and reduced activation thresholds of primary afferents (Zhang and De Koninck, 2006).

1.9. Presentation of the Problem

Collectively, these observations suggest that the problem of neuropathic pain is multi-faceted. The number of potential mechanisms to explain neuropathic pain continues to grow. However, often conflicting results arise from the research and the ability to generalize our findings is limited. We are restricted on many sides, namely by the extent to which our animal models adequately reflect the true pathology exhibited by man. Our lab had initially described sprouting of peptidergic afferents in close apposition to sympathetic efferents following application of a nerve injury model. We hypothesized that the gross morphological changes in the peptidergic population would develop quickly following application of the CCI and that these changes in the peptidergic fibre population would be permanent. The initial observations of the peptidergic fibre population were made directly, but those of the non-peptidergic were made using a method of exclusion. We hypothesized that the non-peptidergic C-fibres would respond similarly in that a sprouting would occur within two months following nerve injury. We also sought to ascertain whether the myelinated fibres were permanently diminished in glabrous skin. As well, it was also important to consider the similarities (and differences) in two very similar models of neuropathic pain with respect to their peripheral innervation changes and behavioural correlates. The initial observations made at the ultrastructural level by electron microscopy suggested that a comparable loss of myelinated and unmyelinated afferents existed. The application of the polyethylene cuff, to be considered an interchangeable model to the chromic-gut based chronic constriction injury model, should elicit similar changes in peripheral innervation. For example, we hypothesized that an almost complete ablation of myelinated

afferents would be observed in the upper dermis of the glabrous skin, peptidergic afferents would sprout and increase in fibre density within the upper dermis. As well, the two models should be comparable in terms of mechanical and thermal sensitivity. Many of these changes in peripheral innervation have been hypothesized to be driven by the local expression of NGF; an adequate study of its non-neuronal cellular distribution with respect to its responsive fibre population has not been adequately performed due to limitations in immunohistochemical methods. We sought to examine the relative distribution of proNGF which should be found in higher concentrations in the cell cytoplasm and thus be amenable to localization by immunohistochemical techniques. We hypothesized that the heightened cellular production of proNGF (which can be inferred to be representative of mNGF non-neuronal tissue distribution) should be closely associated with those fibres responsive to it.

Chapter Two

Delayed reinnervation by non-peptidergic nociceptive afferents of the glabrous skin of the rat hindpaw in a neuropathic pain model

Jennifer Peleshok and Alfredo Ribeiro-da-Silva

The Journal of Comparative Neurology (2011) 519(1):49-63

2.1. Abstract

Painful peripheral neuropathies have been associated with a reorganization of skin innervation. However, the detailed changes in skin innervation by the different afferent fibre types following a neuropathic nerve injury have never been characterized in an animal model of neuropathic pain. Our objective was to thoroughly characterize such changes in the thick skin of the foot in a well established rat model of neuropathic pain, namely the chronic constriction injury (CCI) of the sciatic nerve. We used the immunofluorescence detection of CGRP, purinergic receptor P2X3 and NF200 as markers of peptidergic nociceptive fibres, non-peptidergic nociceptive C fibres and myelinated afferents, respectively. We observed that CCI operated animals developed significant mechanical allodynia and hyperalgesia as well as thermal hyperalgesia. At 3 days following nerve injury, all CCI operated animals had a significant decrease in the density of fibres immunoreactive (IR) for CGRP, P2X3 and NF200 within the upper dermis. A recovery of CGRP-IR fibres occurred within 4 weeks of nerve injury and sprouting above control levels was observed at 16 weeks. However, the myelinated (NF200-IR) fibres never recovered to control levels within a period of 16 weeks following nerve injury. Interestingly, the P2X3-IR fibres took considerably more time to recover than the CGRP-IR fibres following the initial loss. A loss in P2X3-IR fibres persisted to 16 weeks and recovered to levels above that of control at 1.5 years following nerve injury. Further studies are required to clarify the relevance of these innervation changes for neuropathic pain generation and maintenance.

2.2. Introduction

Neuropathic pain occasionally develops following injury to peripheral nerves; however, its pathophysiology is poorly understood. Several animal models of neuropathic pain have been developed in an attempt to provide some insight into the mechanisms that lead to the initiation and maintenance of this type of pain. The first animal model of neuropathic pain to be developed (Bennett and

Xie, 1988) is still extensively used today. This model is based on the unilateral application of four loose chromic gut ligatures around the rat sciatic nerve (CCI model). Although the application of nerve lesions is known to induce changes in both the peripheral and central nervous systems (Woolf and Salter, 2000), in this study we focused on changes occurring within the periphery following application of the CCI to the sciatic nerve.

There are three principal fibre types innervating the glabrous skin of the rat hind paw which are of particular interest to this study: the unmyelinated peptidergic fibres, the unmyelinated non-peptidergic C-fibres, and the myelinated A-fibres. The peptidergic fibres are so called due to their expression of neuropeptides, in particular substance P (SP) and calcitonin gene-related peptide (CGRP). These fibres also express the high affinity neurotrophin receptor TrkA and thus are responsive to nerve growth factor (NGF). The non-peptidergic C-fibres do not express TrkA and thus are not responsive to NGF, but in turn bind the isolectin B4 (IB4) and are responsive to the neurotrophic factor glial cell-line derived neurotrophic factor (GDNF) (Molliver et al., 1997; Priestley et al., 2002). The purinergic receptor P2X3 has been found to be almost exclusively localized to these fibres and as such can be used as a marker for the non-peptidergic C-fibre population (Bradbury et al., 1998). P2X3 is a two-transmembrane, nonselective cation channel gated by ATP. ATP is co-released with noradrenaline from sympathetic fibres (Burnstock, 2004), and following tissue damage is released by injured cells where it signals through P2X3 receptors on sensory neurons (Zhao et al., 2008). ATP has been shown to be pro-nociceptive because noxious responses are evoked following its administration (Bland-Ward and Humphrey, 1997). Application of a P2X3 antagonist following nerve injury is analgesic (Jarvis et al., 2002). Retrograde tracing has established IB4 as being a marker for the non-peptidergic population of C-fibres (Plenderleith and Snow, 1993); however, due to limitations using IB4 as a histochemical marker for this fibre population in the skin, antibody alternatives have been sought. As such, we have used P2X3 as a marker of this population and have recently published the distribution of P2X3-immunoreactive (IR) fibres within the skin of naïve animals. We have shown that

within the glabrous skin of the rat hind paw; there is a much denser innervation of the epidermis by P2X3-IR fibres compared to the peptidergic, CGRP-IR fibres (Taylor et al., 2009b). Neurofilament-200 (NF200) has been described as a marker for large and medium diameter myelinated fibres (Lawson et al., 1984), and was shown to be a reliable marker of these fibres even after injury (Ruscheweyh et al., 2007).

The pathological changes in the sciatic nerve immediately distal to the site of injury following application of the CCI model have been well studied at the light and electron microscopic levels (Coggeshall et al., 1993). However, because the sciatic nerve is a mixed nerve, electron microscopy studies alone cannot differentiate between sensory and motor fibres. It has been shown that myelinated fibres are the most dramatically affected with some groups reporting an almost 99% fibre loss distal to injury (Basbaum et al., 1991). The unmyelinated fibres are less drastically affected in that anywhere from 37-55% fibre loss has been reported (Basbaum et al., 1991). Electron microscopy has shown that disturbances of the integrity of the sciatic nerve begin as early as three days post-injury (Coggeshall et al., 1993). It is important to note that application of peripheral neuropathic pain models results in a spectrum of changes specific to that particular model (Sandkuhler, 2009). Therefore, we will restrict the scope of this paper to discussing our results in context to those results published using the CCI model.

We have previously reported the morphological changes which occur within the upper dermis of the glabrous skin of the rat hind paw following application of the CCI to the sciatic nerve (Yen et al., 2006). However, in that study we restricted our analysis to two fibre populations: the CGRP immunoreactive (IR) peptidergic fibres and the sympathetic fibre population, as detected by immunoreactivity to dopamine β-hydroxylase (DBH). We had shown an initial decrease in the peptidergic population at 2 weeks post-injury followed by sprouting persisting to 20 weeks. The sympathetic fibres, which were normally sparse within the upper dermis, increased considerably in number from

2 weeks and persisted to 20 weeks post injury (Yen et al., 2006). However, changes in other fibre populations were not investigated.

In the current study, we expanded the previous data (Yen et al., 2006) by investigating the morphological changes within the upper dermis for non-peptidergic C-fibres, as well as the myelinated A-fibres, from 3 days up to 1.5 years post-CCI.

2.3. Materials and Methods

In total, 76 male Sprague-Dawley rats (Charles River Canada), weighing between 150-175g, were used for this study. All animals were maintained on a 12-hour light/dark cycle and allowed access to food and water ad libitum. All animal protocols were approved by the McGill University Animal Care Committee and followed the guidelines of the Canadian Council on Animal Care and the International Association for the Study of Pain.

Peripheral Nerve Lesions

Animals were randomly assigned to receive either the chronic constriction injury operation or sham operation. All animals were deeply anaesthetized with isoflurane. In total, 34 rats received the sham operation and 42 received the chronic constriction injury of the common sciatic nerve, as described in detail by Bennett and Xie (1988). Briefly, the left common sciatic nerve was exposed at the mid-thigh through the biceps femoris and all surrounding fascia was removed. Proximal to the trifurcation of the sciatic nerve, four ligatures (4-0 chromic gut, Ethicon) were tied loosely around the nerve with 1 mm spacing in between. The incision was closed in layers using absorbable sutures (Vicryl, Ethicon). The animals assigned to sham-operated groups underwent the above mentioned procedures with the exception of the application of the chromic gut ligatures.

Behaviour

Two groups of animals (CCI- and sham-operated) were tested for mechanical allodynia and hyperalgesia as well as thermal hyperalgesia to ensure application of the CCI to the sciatic nerve was successful in inducing a painful neuropathy. All animals (23 in total) were tested between 9 AM and 4 PM. Animals were allowed to habituate to the quiet testing room for 10-30 min prior to

being placed in clear plastic cages on a wire mesh screen for the mechanical sensitivity testing. After another habituation period of 30 min, baseline measurements were established over the course of three consecutive daily trial periods. Any animals which had abnormal baseline withdrawal thresholds for either mechanical or thermal stimulation were removed before the application of the nerve injury to ensure that there was no error introduced due to an underlying sensory abnormality of the animal. Using this guideline, three animals were removed before being assigned to groups. 4 g and 15 g von Frey filaments were applied to the rear paw foot pad five times and held for five seconds for each application. Care was taken to ensure that the application of the von Frey filaments were restricted to the area of the paw surrounded by tori. This was repeated five times, contra to ipsi, where each animal was tested randomly. All reactions to the applied filament were recorded and averaged. The outliers (defined as being greater than two standard deviations from the mean) were removed prior to statistical analysis. The 4 g filament was used to ascertain mechanical allodynia and the 15 g mechanical hyperalgesia. Following mechanical sensitivity assessments, the rats were placed in clear plastic chambers on the surface of a Hargreaves thermal hyperalgesia plate. The rats were allowed to habituate to the chambers and the plastic surface was cleared of all defecation. A focused beam was applied to the plantar surface of both the contra and ipsi rear paw. The beam had a surface temperature of 31oC and a cut off of 20.48 sec. Each rat was tested three times on each of the ipsi and contra rear paw surfaces and the times at which the rat raised his paw and broke the beam path were recorded and averaged. Values greater than two standard deviations from the mean were removed from the analysis. The average withdrawal latencies from the ipsilateral CCI operated paws were calculated as percent difference from the ipsilateral sham-operated controls where the sham-operated latencies were taken as 100%. After baseline, animals were tested at 7, 10, 15 and 21 days after surgery.

Animal perfusion and histological processing

Animals were sacrificed after periods of 1.5yr, 16wks, 8wks, 4wks, 2wks, 7d and 3d post-surgery. Rats were administered Equithesin (6.5mg chloral hydrate and 3mg sodium pentobarbital) in a volume of 0.3mL, i.p., per 100g body weight. Once animals were deeply anaesthetized, they were transcardially perfused with vascular rinse (0.1% w/v sodium nitrite in a phosphate buffer) followed by histological fixatives (3% paraformaldehyde, 15% saturated picric acid in 0.1M phosphate buffer pH 7.4) for 30min. The glabrous skin from the left hind paw, specifically the thin skin surrounded by the tori targeted during behaviour testing, was removed to post-fix for 1hr and replaced by 30% sucrose in 0.1M phosphate buffer for cryoprotection. Tissue was embedded in an optimum cutting temperature medium (OCT, TissueTek), cut using a cryostat (Leica) at a thickness of 50µm and processed as free floating sections. Sections were then placed in an antifreeze solution (a mixture of 37.5% ethylene glycol and 37.5% sucrose in PBS) and stored at -20oC until used.

Immunohistochemistry

Sections were then washed in PBS for 30 min. Subsequently, PBS with 0.2% Triton X-100 (PBS-T) was used to dilute the immunoreagents and for washing. Sections were then treated with 50% ethanol for 30 min followed by 1 hour incubation in PBS-T containing 10% (v/v) normal serum of the species used to generate the secondary antibody to reduce non-specific staining. Subsequently, sections were incubated with primary antibodies (diluted in PBS-T) either overnight or for 48hrs (in the case of P2X3) at 4^{o}C. The following primary antibodies were used: polyclonal rabbit anti-calcitonin gene related peptide (CGRP; 1:2000, Sigma), monoclonal mouse anti-neurofilament-200 (NF200; 1:2 Abcam, Cambridge MA). After washing, the sections were incubated with secondary antibody diluted in PBS-T for two hours at room temperature. The following secondary antibodies were used: for NF200 staining, a highly cross-adsorbed goat anti-mouse IgG conjugated to Alexa 596 (1:800, Molecular Probes, Eugene, OR) and for CGRP, a goat anti-rabbit conjugated to Alexa 488 (1:800, Molecular Probes, Eugene, OR). Sections were washed and mounted on gelatin-coated slides and coverslipped using Aquapolymount (Polysciences; Warrington,

PA). In the case of P2X3 staining, after 30 min incubation with ethanol, sections were treated with 0.3% hydrogen peroxide solution for 10min. Following a 30min PBS and 30min PBS-T wash, sections were then blocked with normal serum as described above and incubated for 48hrs at 4oC with a guinea-pig anti-P2X3 primary antibody (1:25 000, Neuromics; Edina MN). The sections were then washed and incubated for 90min with a biotin-conjugated donkey anti-guinea-pig IgG (1:200, Jackson Immunoresearch, West Grove PA), washed for 30min with PBS-T and incubated for 1hr with Vectastain Elite ABC kit (1:250, Vector Laboratories, Burlingame, CA). The P2X3 signal was amplified using a tyramide treatment (1:75, Perkin-Elmer; Norwalk, CT) for 7min. Streptavidin conjugated to Alexa 488 (1:200, Molecular Probes; Eugene OR) was applied to the sections for 2hrs. Finally, the sections were washed and mounted as described above.

Sections from 6 sham-operated and 6 animals with CCI lesions from the 4 week time point were processed for a double labelling of CGRP and the pan-neuronal marker, Protein Gene Product 9.5 (PGP9.5). For this, sections were processed as described above; however, the initial antibody incubation was with a mixture of a guinea-pig anti-human CGRP antibody (1:4000, Bachem; Torrance CA) and an anti-PGP 9.5 antibody generated in rabbit (1:800, Cedarlane; Burlington Ont.). After washing, the sections were incubated with a mixture of highly-cross adsorbed goat anti-rabbit IgG conjugated to Alexa Fluor 488 (1:800, Molecular Probes) and donkey anti-guinea-pig antibody conjugated to rhodamine red-X (1:400, Jackson Immunoresearch). After washing, the sections were mounted as described above.

Images for the Figures

Pictures for the figures of this publication were taken as Z-stacks of confocal optical sections using a Zeiss LSM 510 confocal microscope equipped with argon and helium neon lasers applying a 40X water-immersion objective. Images were exported directly in TIFF format and adjusted using Adobe Photoshop CS4 for brightness and contrast.

Primary Antibody Characterization

CGRP (rabbit): The anti-CGRP antibody raised in rabbit was purchased from Sigma (C8198, lot 013K4842). It was generated against synthetic rat CGRP conjugated to KLH. The specificity was tested via dot-blot and the antibody was found to recognize rat CGRP conjugated to bovine BSA; recognition of human CGRP and β-CGRP (conjugated to bovine BSA) was also observed (data supplied by Sigma). Specificity was also assessed by immuocytochemistry using free-floating sections of rat glabrous skin, and the staining was completely abolished when the antibody was pre-adsorbed with rat CGRP (Yen et al., 2006). This antibody has been used extensively in our lab as a marker of peptidergic fibres in rat spinal cord, DRG and skin (Almarestani et al., 2008; Bailey and Ribeiro-da-Silva, 2006; Dickson et al., 2006; Grelik et al., 2005a; Grelik et al., 2005b; Lorenzo et al., 2008; Taylor et al., 2009; Yen et al., 2006).

CGRP (guinea-pig): The anti-CGRP antibody raised in guinea-pig was purchased from Bachem (T-5027, lot A00098-2). It was generated against a synthetic peptide from human α-CGRP with the following sequence: H-Ala-Cys-Asp-Thr-Ala-Thr-Cys-Val-Thr-His-Arg-Leu-Ala-Gly-Leu-Leu-Ser-Arg-Ser-Gly-Gly-Val-Val-Lys-Asn-Asn-Phe-Val-Pro-Thr-Asn-Val-Gly-Ser-Lys-Al a-Phe-NH2. The antibody has 100% reactivity with human and rat α-CGRP, human CGRP (8-37), chicken CGRP, and human β-CGRP. It has 0.04% cross-reactivity with human amylin and 0% cross-reactivity with rat amylin and with human and salmon calcitonin as determined by radioimmunoassay (manufacturer's technical information). Although Western blot information was not available, the immunostaining has been localized in the skin to IB4 negative C-fibres, and fibres innervating blood vessels in rats (Fundin et al., 1997; Rice et al., 1997) and in monkeys (Paré et al., 2007). Experiments from our lab have demonstrated that double staining using the rabbit anti-CGRP described above stains the same structures as does this one (data not shown).

Purinergic receptor P2X3: The polyclonal anti-P2X3 antibody was raised in guinea-pig (Neuromics, GP10108, lot 400457) against the intracellular C-terminal domain of rat P2X3, specifically against the sequence

VEKQSTDSGAYSIGH corresponding to amino acids 383-397. Specificity was confirmed by preadsorbing the antibody with the peptide immunogen (20 µg/ml) prior to staining trigeminal ganglia of rat; no staining was observed (Dellarole and Grilli, 2008; Ichikawa and Sugimoto, 2004).

Neurofilament 200 (NF-200): The anti-NF200 antibody (Abcam, ab910, also known as RT97, lot 671264) recognizes the heavy chain of neurofilaments in myelinated fibres. It is a monoclonal antibody generated from the immunization of mice with Triton X-100 insoluble rat brain protein (Wood, 1981). It was later shown by epitope mapping that this antibody targets the carboxy domain of the 210 kDa, high molecular weight neurofilament protein in human and bovine samples (Anderton et al., 1982). The antibody was used to correlate the diameter and conduction velocity to neurofilament status, in large and medium-diameter rat primary afferents to confirm that it recognizes both Aβ and Aδ fibres (Lawson and Waddell, 1991).

PGP 9.5: The rabbit anti-PGP 9.5 antibody (Ultraclone code RA95101) was generated by repeated injection of purified whole human PGP 9.5 in Freund's Adjuvant into rabbits. The antibody cross-reacts with PGP 9.5 protein in all mammalian species (manufacturer's technical information). By western blot it recognizes a band at 38kDa from human and rat skin, and preadsorption with purified PGP 9.5 completely abolished this recognition (Doran et al., 1983; Thompson et al., 1983). Immunohistochemical staining with this antibody in either rat or human skin was absent following preadsorption with purified human PGP 9.5 protein (Doran et al., 1983; Thompson et al., 1983).

Quantification of fibre density

Micrographs were obtained using a Zeiss Axioplan 2 imaging fluorescence microscope equipped with a high-resolution color digital camera, using a 40X Plan-Fluotar oil-immersion objective. The Carl Zeiss Axiovision 4.8 software (Zeiss Canada) was used to obtain the images. Six experimental animals were used for each time point. Six sections per sampled animal and four images per section were taken making a total of 144 images per time point. The observer who took the images was blinded as to the experimental groups, and the codes

broken only after all data were collected. The images were quantified for fibre density of P2X3, CGRP and NF200 immunoreactivity. The innervation density of the upper dermis, defined as the area within 150μm from the dermo-epidermal junction, was measured as previously described in one of our publications (Yen et al., 2006). The images were exported as TIFF files to an MCID Elite image analysis system (Imaging Research Inc., St. Catharines, Ont., Canada). We used a function of the MCID software to detect fibres. Following detection, fibres were skeletonized to one pixel in width. Segments shorter than 5 μm were excluded from the measurements, to ensure only bona fide fibres were measured. Fibre length was measured in μm and divided by the live frame area (μm^2) to determine total fibre length per unit area. A one-way ANOVA with Bonferroni correction was used for statistical analyses. Graphs were plotted using GraphPad Prism version 5.

2.4. Results

Behaviour Testing

All CCI operated animals developed significant ipsilateral mechanical hyperalgesia at day 7 post-injury which was more pronounced at days 15 through 21 (Figure 1A). Mechanical allodynia reached significance (compared to sham) at fifteen days post-injury and remained significant to day 21 (Figure 1B). The heat hyperalgesia graph was plotted by adjusting all CCI responses (both ipsilateral and contralateral paws) to that of sham, where sham is 100% and all others comparisons made to the matched time point. Heat hypersensitivity developed at day 7 and persisted to day 21 post-injury (Figure 1C).

Morphological Observations

In sham-operated animals, the peptidergic fibres, as detected by CGRP immunoreactivity, formed a dense plexus along the dermo-epidermal junction with the occasional isolated CGRP-IR fibre protruding from this plexus into the epidermis (Figure 2A). The plexus at the dermo-epidermal junction originated from fibres travelling in small nerves from the lower dermis (Figure 2A). At 3 days post-lesion, there was a dramatic loss of CGRP staining, with a partial recovery from 7 to 14 days post-lesion (Figures 2B-D). This overall reduction in

the innervation density of the upper dermis at early time points was particularly marked along the dermo-epidermal junction, and resulted from a loss of fibres in the small nerve bundles. Furthermore, the remaining fibres appeared thinner (Figure 2C). Importantly, CGRP-IR fibres were no longer observed in the epidermis. However, at four weeks post-surgery the innervation within the upper dermis returned to the characteristic CGRP-IR innervation pattern seen in the sham operated animals (Figure 2E); as well, there was a partial return of the epidermal innervation of these fibres at this time point. This innervation pattern did not change 8 weeks post-surgery compared to that of either sham-operated controls or to that observed at 4 weeks post-injury (Figures 2F). There was a hyperinnervation by CGRP-IR fibres compared to that of sham-operated controls at 16 weeks post-injury (Figure 2G). At 16 weeks post-injury the network of CGRP-IR fibres throughout the upper dermis was denser and more widespread compared to that of sham-operated animals. There was a full recovery of the epidermal innervation by these fibres at 16 weeks post-injury. This hyperinnervation was still detected at 1.5 years post-lesion (Figure 2H). These changes were quantified and the data shown in Figure 5A.

In sham-operated animals, the non-peptidergic fibre population, as detected by P2X3 immunoreactivity, mimicked that of the peptidergic in that both were most dense at a plexus along the dermo-epidermal junction (compare Figures 2A and 3A). We observed a higher number of P2X3-IR fibres within the epidermis than of CGRP-IR fibres (Figures 2A and 3A). Unfortunately, because of background fluorescence of the epidermis after application of the TSA protocol, this observable difference between the CGRP- and P2X3-IR fibres was not quantifiable. The plexus of P2X3-IR fibres along the dermo-epidermal junction was much denser compared to the CGRP-IR fibres, but only the occasional P2X3-IR fibre was seen in the lower regions of the upper dermis (Figure 3A). The changes following CCI were much more dramatic compared to those of the peptidergic fibre population in that the decrease in non-peptidergic innervation of the upper-dermis was initially greater and lasted longer compared to the peptidergic population (Figure 5B). At day 3, day 7 and 2 weeks post-

lesion there was an almost complete ablation of the P2X3-IR fibres within the upper dermis as well as throughout the epidermis (Figures 3B-D). Four weeks post-injury, the immunoreactivity returned but very few actual fibres were detected; those that remained were located along the dermo-epidermal junction (Figure 3E). A small recovery was detected at 8 weeks, although the density was well below sham levels and most fibres occurred along the dermo-epidermal junction. Still, almost no P2X3-IR non-peptidergic C-fibres were detected in other areas of the upper dermis and none in the epidermis (Figure 3F). At sixteen weeks post surgery, the P2X3-IR non peptidergic C-fibre innervation was significantly below sham density. At this time point a small recovery was observed compared to the previous time point, but only the occasional fibre was found in the epidermis (Figure 3G). In contrast, 1.5 years after injury there was a hyper-innervation compared to sham, by P2X3-IR fibres in the upper dermis (Figure 3H), although the innervation of the epidermis was still less than in sham animals (Figure 3A). The quantitative changes in the innervation of the upper dermis by P2X3-IR fibres are shown in Figure 5B.

Myelinated afferents were detected by immunoreactivity to the neurofilament heavy chain of molecular weight ~200kDa (NF200). However, it should be noted that such a staining does not allow the differentiation of Aβ from Aδ fibres. In sham-operated animals, these fibres were found in bundles in small cutaneous nerves throughout the upper dermis, with only an occasional isolated fibre appearing to travel alone (Figure 4A). These fibres were found to be distributed equally throughout the upper dermis with no preference to the dermo-epidermal junction. Virtually no NF200-IR fibres penetrated the epidermis. At 3, 7 days and 2 weeks following nerve lesion, there were almost no detectable NF200-IR nerve fibres throughout the upper dermis (Figure 4B-D). At 8 and 16 weeks post-injury an occasional NF200-IR fibre was seen within the upper dermis. These isolated fibres were sparse (Figures 4F-G). The loss in fibre density was approximately 96% up to 8 weeks post-injury at which time the loss was 78% (Figure 5C).

In an attempt to confirm whether the P2X3-IR and NF200-IR fibre losses were bona fide losses rather than a down regulation of phenotypic markers, we performed a double-labelling for CGRP and the pan-neuronal marker PGP 9.5, in 6 sham animals and in 6 CCI rats from the 4 week time point (Figure 6). In the dermis of sham-operated rats, there were thick bundles of PGP 9.5-IR fibres; some of these fibres were also labelled for CGRP (Figure 6A; double arrows). In the epidermis, fine terminal branches of fibres solely immunoreactive for PGP 9.5 could be observed (Figure 6A; green arrowheads). In contrast, in the CCI animals, most fibres observed in the dermis and the occasional fibre found in the epidermis co-localized PGP 9.5 and CGRP immunoreactivities (Figure 6B; yellow arrows). The occasional fibre solely immunoreactive for PGP 9.5 in the dermis possessed rather large varicosities (Figure 6B; green arrows).

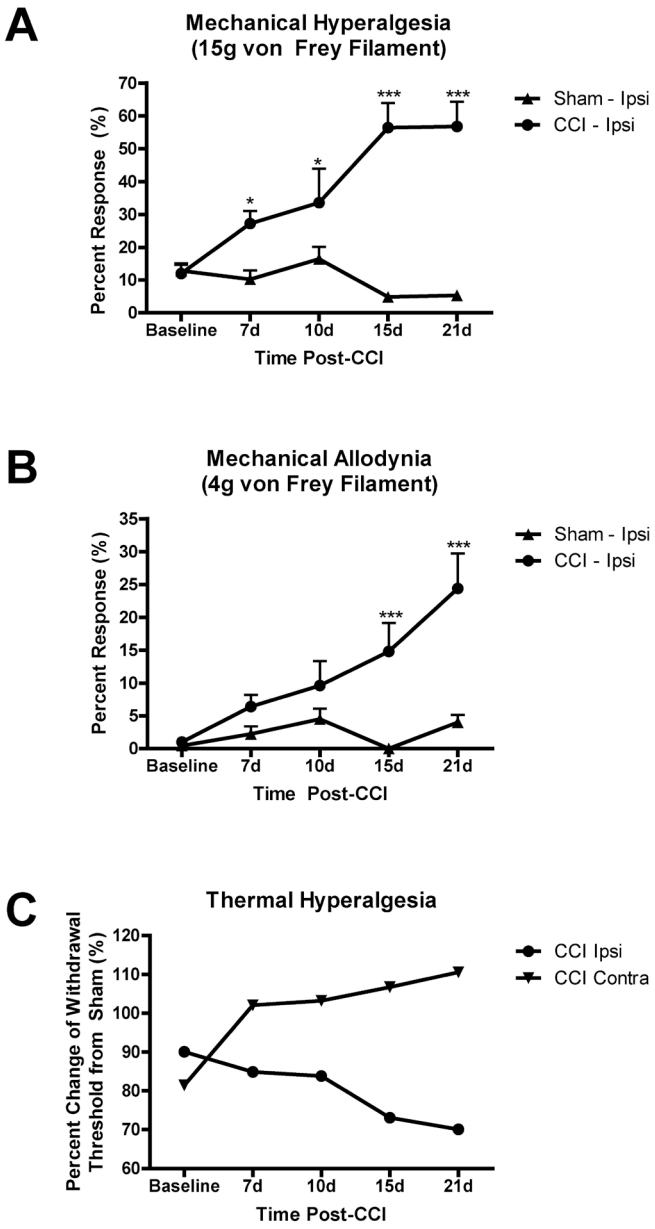

Figure 1. **Behavioural changes following CCI**. **A:** Response frequency of CCI and sham operated Sprague-Dawley rats to application of repeated stimulation of ipsilateral hind paw with 15g von Frey filament as a measurement for mechanical hyperalgesia. *$p \leq 0.05$ by 2 way ANOVA with Bonferroni post-hoc. All comparisons were made against time-matched sham-operated controls. **B:** Response frequency of CCI and sham operated Sprague-Dawley rats to application of repeated stimulation of ipsilateral hind paw with 4g von Frey filament as a measurement of mechanical allodynia. ***$p \leq 0.001$ by 2 way ANOVA with Bonferroni post-hoc comparisons. **C:** Change in withdrawal frequency taken as a percent change of each time point with respect to the matched sham time point. Withdrawal frequency was measured using the Hargreaves method for thermal hyperalgesia.

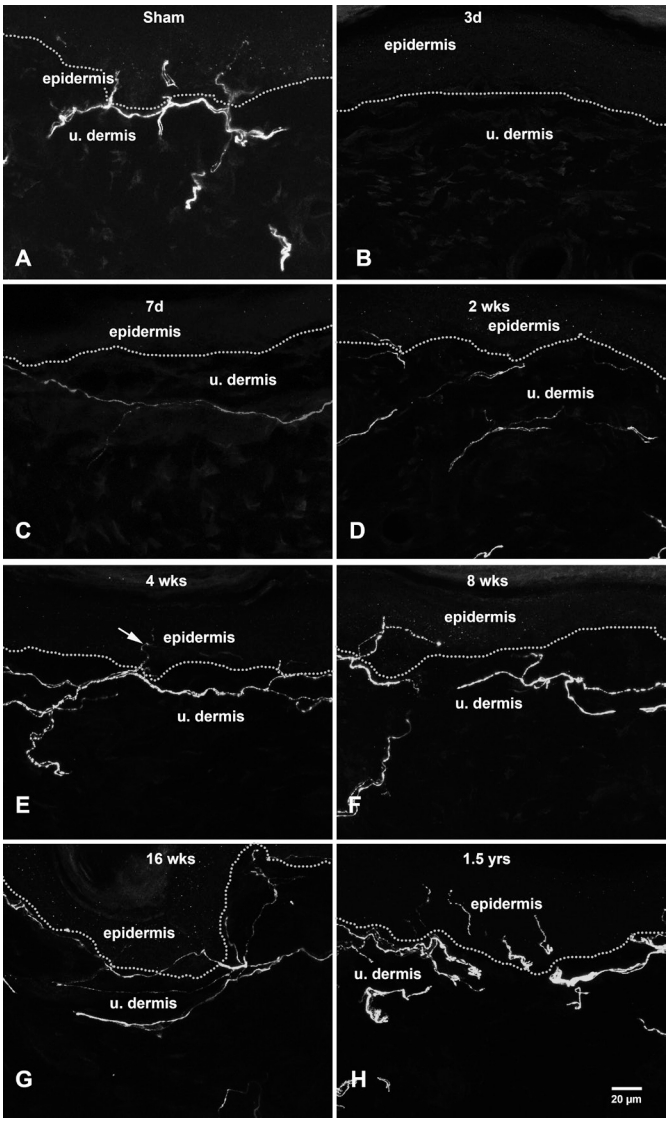

Figure 2. Confocal images of representative skin sections immunostained for CGRP from sham-operated animals and rats from 3 days to 1.5 years post-CCI. **A**: In sham-operated animals note the fiber plexus along the dermo-epidermal junction. Arrow points to an isolated CGRP-IR fiber within the epidermis. **B**: At 3 days post-CCI, note the virtual absence of CGRP-IR fibers in this field. **C**: At 7 days post-CCI, occasional fibers were observed along the dermo-epidermal junction. **D**: At 2 weeks post-CCI, note that thin fiber networks can now be observed within the upper dermis. **E & F:** Note a network of CGRP-IR fibers throughout the upper dermis, but concentrated at the dermo-epidermal junction at 4 & 8 weeks post-CCI; arrow indicates one of the occasional fibers in the epidermis (at 4 weeks). **G**: A thick network of CGRP-IR fibers of higher density than that of sham animals was seen 16 weeks post-CCI. **H**: Note the dense network of CGRP-IR at 1.5 years post-lesion. Dashed line represents the dermo-epidermal junction.

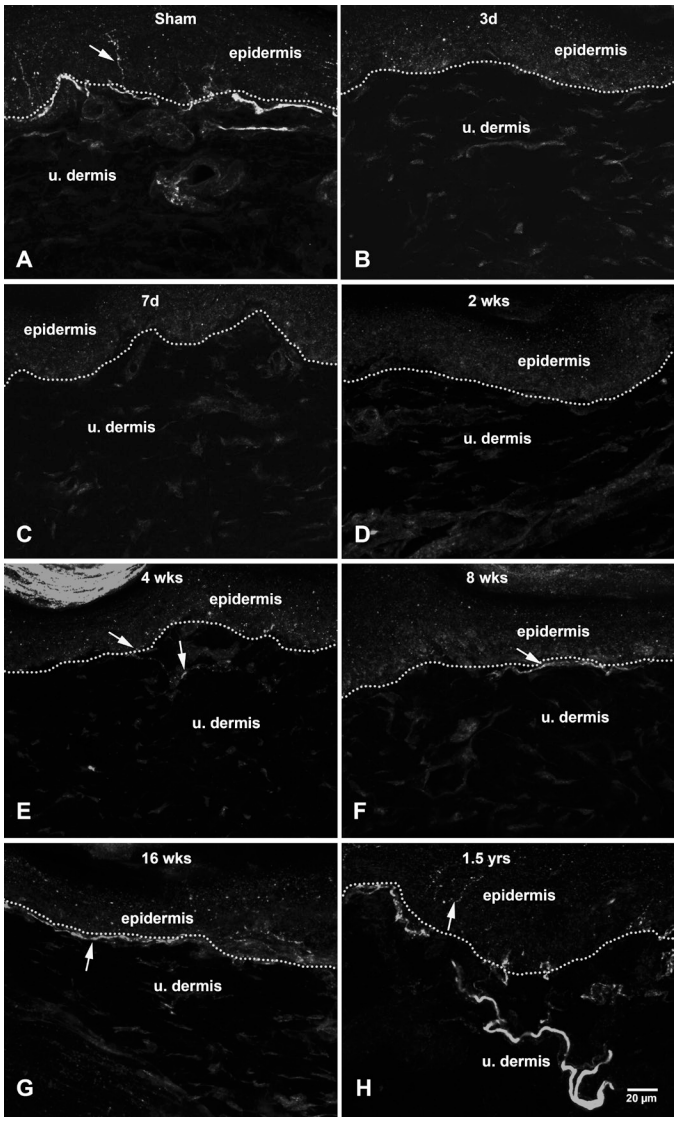

Figure 3: Confocal images of representative skin sections immunostained for P2X3 from sham-operated animals and rats from 3 days to 1.5 year post-CCI. **A**: Section from sham-operated animal showing P2X3-IR fibers localized almost exclusively along the dermo-epidermal junction with many projections from the thicker fibers into the epidermis (arrow). **B**: At 3 days post-CCI there was an almost complete absence of P2X3-IR fibers. **C & D**: At 7 & 14 days post-CCI no significant P2X3 immunoreactivity was observed. **E**: At 4 weeks post-CCI, P2X3-IR fibers was observed to be sparse (arrow) and patchy in appearance. **F**: At 8 weeks post-CCI, some longer fibers (arrow) were detected. **G:** At 16 weeks post-CCI, P2X3-IR fibers were still well below sham levels, but were clearly more abundant than at earlier time points, particularly at the dermo-epidermal junction. **H**: At 1.5 years post-CCI P2X3-IR fibers formed bundles within the upper dermis in addition to the plexus at the dermo-epidermal junction; some fibers penetrated the epidermis (arrow). Dashed line represents the dermo-epidermal junction.

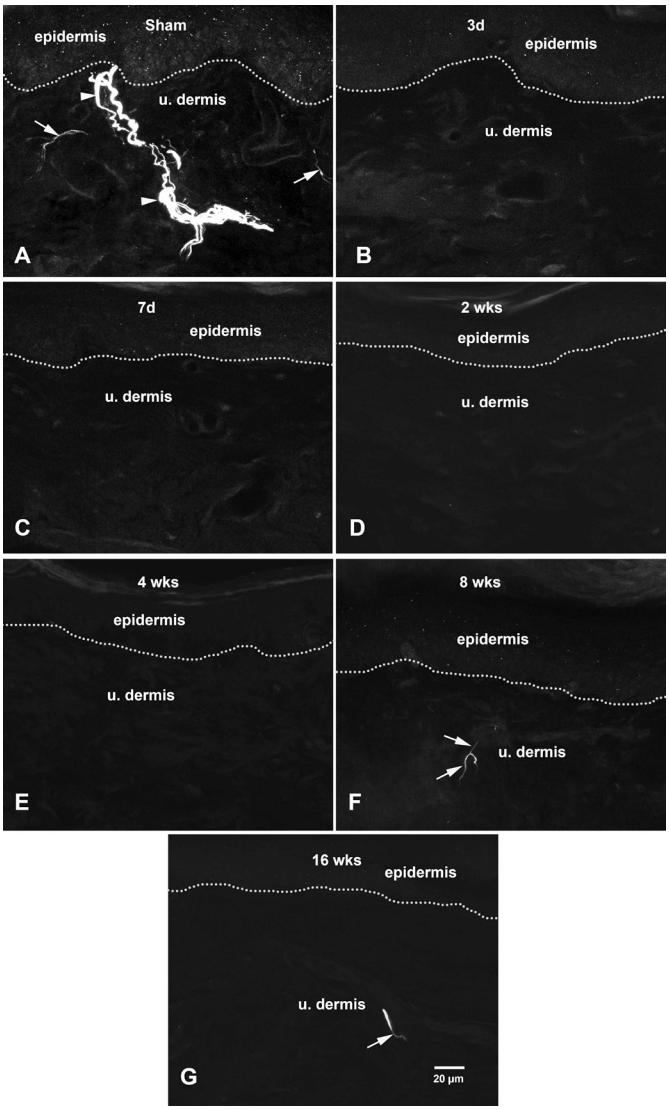

Figure 4: Confocal images of representative skin sections immunostained for NF200 from sham-operated animals and rats from 3 days to 16 weeks post-CCI. **A**: Section from a sham-operated animal showing NF200-IR fibers travelling in thick bundles through the upper dermis (arrowhead) or independently (arrow). **B-E**: From 3 days through 4 weeks post-CCI note the absence of NF200-IR fibers. **F & G**: At 8 & 16 weeks post-CCI thin, isolated NF200-IR fibers were occasionally seen within the upper dermis. U. dermis = upper dermis. Arrows indicate isolated fibers. Dashed line represents the dermo-epidermal junction.

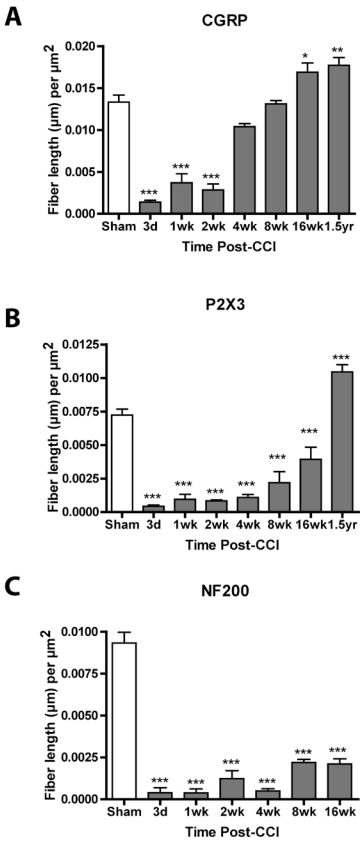

Figure 5: Average fiber density within the upper dermis in sham operated and CCI animals at several time points. Quantification of innervation of the upper dermis from sham operated and CCI animals on 3 days through 1.5 years after surgery (n=6 per time point). Fibers were measured by means of an MCID image analysis system, as described in the Materials and Methods, in an area within 150 µm from the dermo-epidermal junction. **A:** Quantification of CGRP-IR fibers within the upper dermis from rats at 3 days to 1.5 years post-CCI compared to sham operated controls. At 3d post-injury density was significantly reduced and returned to levels of sham operated controls at 4 and 8 weeks post-CCI. At 16 weeks post-CCI there was a significant sprouting sustained to 1.5yr post-CCI. **B:** Quantification of P2X3-IR fibers in the upper dermis from 3 days to 1.5 years post-CCI, compared to sham. At 3 days post-CCI, P2X3-IR fiber density was significantly reduced and remained well below sham values until 16 weeks post-injury. At 1.5yr post-CCI there was a significant increase in fiber density compared to that of sham. **C:** Quantification of NF200-IR myelinated A-fibers within the upper dermis. Rats were sampled from 3 days to 16 weeks post-CCI and values compared to those of sham operated controls. At 3 days post-CCI NF200-IR fibers were undetectable and remained very low in density until 8 weeks post-injury, when there was a small increase in density. For each immunostaining, statistical comparisons were done by means of a one-way ANOVA followed by Bonferroni post-hoc comparisons to sham. *$p \leq 0.05$; **$p \leq 0.01$; ***$p \leq 0.001$.

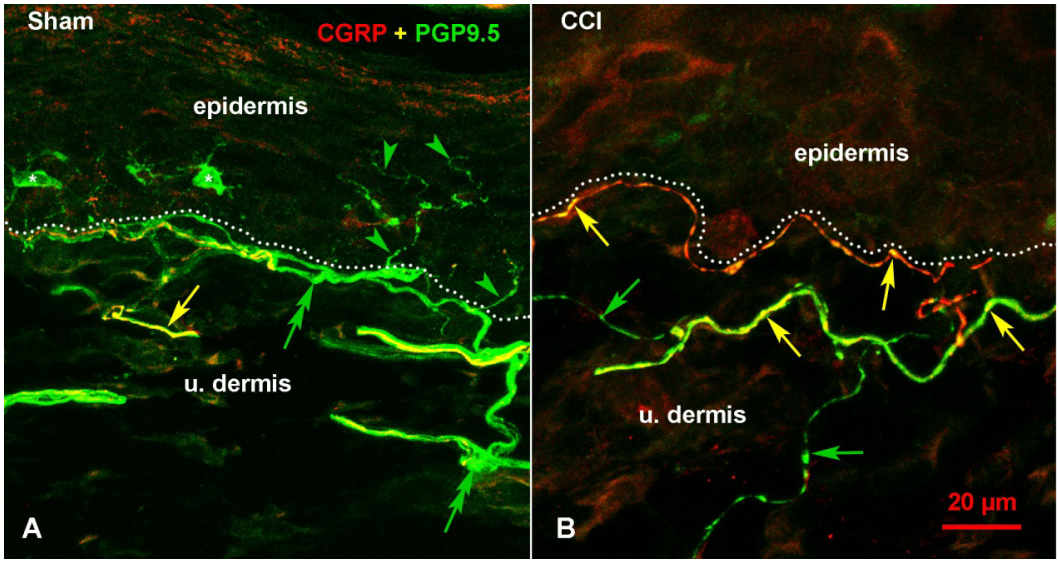

Figure 6: Double labelling for PGP-9.5 (in green) and CGRP (in red) in sham and CCI animals, at 4 weeks post-lesion. A: In a sham animal, note the thick bundles of PGP immunoreactive fibre bundles (double arrows) traveling in the upper dermis and along the dermo-epidermal junction, from which fibres penetrate into the epidermis (arrowheads); although individual fibres are difficult to detect at this magnification, some fibres co-localize CGRP immunoreactivity (yellow color from the co-localization). **B:** At 4 weeks post-CCI, note the heavy depletion of PGP-9.5 fibres from the epidermis and upper dermis; indeed the few remaining fibres in the dermis co-localized CGRP immunoreactivity (yellow arrows), with the exception of two that might represent sprouting sympathetic fibres (green arrows). Confocal z-stacks (of 20 optical sections). U. dermis = upper dermis. Dashed line represents the dermo-epidermal junction. Asterisks indicate PGP 9.5-IR Langerhans cells.

2.5. Discussion

In this study, we investigated the changes in the sensory innervation of the skin of the rat hind paw following application of a CCI to the common sciatic nerve, at time points from 3 days to 1.5 years. The main findings were: 1) an initial loss and subsequent persistent hyper-innervation by peptidergic nociceptive afferents (Figure 5A); 2) an early loss of non-peptidergic C-fibres followed by a very slow recovery and late sprouting (Figure 5B) and 3) a dramatic and permanent loss of myelinated afferents (Figure 5C).

In our study, we relied on phenotypic markers (CGRP, P2X3 and NF200) to identify specific fibre populations. Therefore, we cannot rule out the possibility that the expression level of those markers in the fibres may fall below detection levels following nerve lesion, although the fibres may still be anatomically present. This possibility is easier to accept for the expression of CGRP and P2X3 than for NF200, as the latter is a structural protein and very low levels of it would affect the integrity of the fibre itself. To address this issue, we used an extra marker. PGP9.5 is a pan-neuronal marker and detects all axons, independently of being sensory, motor or autonomic, and has been used in many studies to detect overall levels of innervation (Oaklander, 2001) including studies from our own lab (Grelik et al., 2005a; Taylor et al., 2009). Therefore, we decided to assess the overall skin innervation at 4 weeks post-CCI using PGP9.5 immunoreactivity, and compare it to sham, to confirm whether the profound fibre loss of NF200-IR and P2X3-IR at 4 weeks was genuine. As described in the Results section, we observed an extensive depletion of PGP 9.5-IR fibres in the CCI animals, and most of the fibres which remained co-localized CGRP immunoreactivity, the only fibre population that showed considerable recovery at the 4 week time point. Moreover, the very few fibres in the dermis which were immunoreactive for PGP 9.5-only were thin and with large varicosities and therefore might represent sprouted sympathetic fibres. Lastly, the few fibres that penetrated the epidermis were double-labelled for PGP9.5 and CGRP (Figure 6B). These data provide strong evidence in support of a bone fide fibre loss following CCI, which does not represent a decrease in marker immunoreactivity.

Our data on myelinated afferents in the upper dermis of the plantar surface on the paw differs from that of other studies which focused on myelinated fibre counts on mixed nerves immediately distal to the lesion (Basbaum et al., 1991; Coggeshall et al., 1993; Guilbaud et al., 1993). The differences lie in that we assessed fibre density using an immunological marker (NF200) of myelinated fibres, and that the measurements were made in the skin itself, not in the lesioned nerve. Our results are compatible with those which performed fibre counts on the sciatic nerve revealing that the myelinated fibres are preferentially affected over unmyelinated following nerve injury where an almost complete loss was seen of the former (Basbaum et al., 1991; Carlton et al., 1991; Coggeshall et al., 1993; Guilbaud et al., 1993). Unfortunately, none of the above studies counted peptidergic (identified by either CGRP or SP labelling) or non-peptidergic afferent fibres distal to the lesion.

To date, very few articles have examined the terminal field territory of sciatic nerve fibres in the skin. A previous article from our laboratory detailed the innervation changes in the sympathetic and peptidergic fibre populations following application of the CCI (Yen et al., 2006). In that study, we were able to provide initial results showing the sprouting of the peptidergic fibres. Additionally, we described a de novo invasion of the upper dermis by sympathetic fibres, where they established close appositions with the peptidergic afferents. Interestingly, these ectopic sympathetic fibres did not innervate blood vessels, as they normally do in the lower dermis, but wrapped around the peptidergic fibres. However, we had not investigated the initial morphological changes at early time points, nor had we studied the very long time points post-lesion. Lastly, we had not investigated the changes in the non-peptidergic subpopulation of C-fibres. This latter population of nociceptive primary afferents has been difficult to label in the skin, but we have recently optimized a protocol which allowed us to carry out a comprehensive study of the skin innervation in normal rats using P2X3 immunoreactivity as a marker (Taylor et al., 2009). At present, we are still limited in the markers we can use, as NF200 does not allow us to discriminate Aβ from Aδ afferents in the skin. The current study will thus need to be expanded

when proper markers of myelinated fibre subpopulations become available. Other than our own investigations, one other study used both the CCI and partial sciatic nerve ligation models to investigate the changes at 4 and 14 days post-lesion in the innervation of the skin footpads by fibres immunoreactive for CGRP, SP and PGP-9.5 (Ma and Bisby, 2000). While the study by Ma and Bisby (2000) used the thick skin of the footpad, we used exclusively the skin in between the tori, which is the area where we apply the von Frey hairs for behaviour testing. In doing so, we are able to measure changes in innervation in the exact region in which neuropathic pain is being assessed. Furthermore the study by Ma and Bisby (2000) was restricted to two time points and only used the markers PGP-9.5, SP and CGRP. In doing so, they could only identify in the dermis the peptidergic fibre population, as PGP9.5 labels all fibres independently of them being sensory, motor or autonomic. It is interesting to note, however, that the changes in the CGRP innervation that Ma and Bisby (2000) reported in the CCI model at the 4 and 14 day time points are similar to those we observed, although it appears that we had less variability from animal to animal (see Figure 5A).

Changes in myelinated fibres

The drastic initial decrease in immunoreactivity for the three fibre populations we studied (peptidergic, non-peptidergic and A-fibres) is in agreement with the changes previously observed in the sciatic nerve itself distal to the lesion (Basbaum et al., 1991). Based on the pathological observations carried at the EM levels on the nerve distal to the lesion, it is likely that the initial fibre loss is caused by Wallerian degeneration. The time course of fibre degeneration at the sciatic nerve proper has been proposed as follows. Within the first five days there is extensive axonal degeneration that remains until two weeks post-injury. From two weeks up to four months, there is a regeneration of the intact nerves as well as a remyelination of injured afferents. These myelinated afferents do not fully regain their entire myelin sheath (Guilbaud et al., 1993).

The ultrastructural analysis of the sciatic nerve revealed that distal to the lesion, ultrastructural changes occurred, and regenerative fibres differed from their original state (Basbaum et al., 1991; Coggeshall et al., 1993). These studies

have shown that in the nerve distal to the lesion, from 4 to 14 weeks post-injury, there was fibre remyelination. Regenerating myelinated fibres did not regain a myelin sheath of the same thickness as uninjured fibres and as a result appeared thinner following nerve lesion. On the contrary, injured unmyelinated fibres regenerated to an appearance approximating that of their naïve state (Coggeshall et al., 1993). Additionally, it has been shown that only ~50% of those myelinated fibres which were lost shortly after CCI application regenerated (Guilbaud et al., 1993). In agreement with these data, we observed an initial almost complete loss of myelinated fibres in the skin, as detected by NF200 immunoreactivity. This was followed by the late reappearance of some fibres, which were usually thin. However, the density of myelinated fibres detected at 8-16 weeks post-lesion was only about 25% of sham levels, suggesting that many regenerated fibres might not reach the skin.

Changes in Non-Peptidergic and Peptidergic Nociceptive Afferents

One of the novel observations of this study is that the peptidergic and non-peptidergic C fibres recovered from an initial loss in density of innervation at very different rates. While the initial loss of both small diameter fibre populations within one week of injury was similar (Figures 3A and 3B), there was a major difference in their recovery. At one month post injury the peptidergic population had recovered to pre-lesion levels, whereas the non-peptidergic only did so at a period after 16 weeks and only at the 1.5 year post-lesion time-point did we detect a density above sham levels (Figure 5B). How these differences in the rate of recovery between these two populations of nociceptive fibres affects the maintenance of the neuropathic pain is at present unknown. Following application of a CCI lesion, administration of exogenous GDNF prevented the development of the lesion-induced mechanical sensitivity (Nagano et al., 2003). These data are consistent with another publication in which the administration of GDNF prevented the development of pain-related behaviour after the application of two separate neuropathic pain models; pain related thresholds in control animals were not affected (Boucher et al., 2000). In contrast to what happened following GDNF application, administration of NGF function blocking peptides or

antibodies to the TrkA receptor attenuated nerve injury induced nociception (Bennett et al., 1998a; McMahon et al., 1995). Following injury, NGF is released by Schwann cells, invading macrophages and fibroblasts (Ramer and Bisby, 1997a). NGF acts in a multitude of different ways in the PNS following nerve injury. NGF upregulates CGRP and SP and is capable of preventing neuronal death (McMahon and Priestley, 1995). Therefore, NGF and GDNF may have opposite effects on pain-related behaviour after injury. The available evidence indicates that NGF is pro-nociceptive, whereas GDNF seems to have no direct effects on nociception, unless there is a lesion. The fact that GDNF mRNA is known to be upregulated in Schwann cells distal to the injury site and that such upregulation persists after lesion (Hammarberg et al., 1996) would suggest that GDNF is related to the non-peptidergic fibre regrowth following lesion. There is evidence from in vitro studies that non-peptidergic, IB4 binding neurons do not express integrin and GAP-43, which would render them less capable of axonal regrowth (Leclere et al., 2007). In the same study, the co-culture of DRG neurons with lesioned sciatic nerve explants revealed much lower levels of GDNF than NGF in the medium. As a result IB4-positive neurites grew much less than other neurites, suggesting that levels of GDNF available after nerve lesion may be too low for proper regrowth of this class of primary afferent (Leclere et al., 2007). This finding is consistent with our own in that the nonpeptidergic population displays a slower degree of recovery. The concentration of GDNF released by surrounding cells is currently unknown, as this concentration has been too small to accurately record.

We have previously shown that after CCI sympathetic fibres sprout and establish close appositions with the peptidergic afferents in the upper dermis (Yen et al., 2006). The sprouting of sympathetic fibres after CCI was initially reported surrounding DRG cells (McLachlan et al., 1993), followed by reports in the thin skin of the rat lower lip after complete transection (Ruocco et al., 2002), CCI lesion of the mental nerves (Grelik et al., 2005b) and in the thick skin of the hind paw of rats following CCI of the sciatic nerve (Yen et al., 2006). This sprouting of sympathetic fibres within the upper dermis has been proposed as a morphological

basis for sympathetically maintained pain, and may have a major role in the onset of the neuropathic pain in the CCI model (Yen et al., 2006). Therefore, based on the data from the current study, we could infer that if the sympathetic system does play a major role in the triggering and maintenance of the hyperalgesia and allodynia, it should be mostly by effects of released neurotransmitters on peptidergic afferents, as the density of the non-peptidergic fibres remains rather low until after 16 weeks (Figure 5). However, the possibility remains that the persisting P2X3-IR fibres have an abnormal function. Indeed, it has also been demonstrated that following nerve injury there is a sensitization of P2X3 receptors in the skin (Chen et al., 2005). Furthermore, ATP, the endogenous ligand of the P2X3 receptor, is co-released with noradrenaline (NA) by sympathetic afferents in the peripheral nervous system (Burnstock, 1999). There is also some evidence that α1-adrenergic receptors are present on P2X3 positive, non-peptidergic afferents within the peripheral nervous system (Meisner et al., 2007). And it has been shown that following sciatic nerve ligation there is an enhanced responsiveness of P2X3 expressing neurons in the DRG to noradrenaline (Maruo et al., 2006). Therefore, the small number of persisting and sprouting P2X3 afferents may respond to substances released by the sympathetic fibres, thus contributing to the pain.

Significance of skin innervation changes

In this animal model, the mechanical hyperalgesia and thermal hypersensitivity started at 1 week post-lesion and peaked at 2 weeks. In contrast, the mechanical allodynia started only at 2 weeks. As discussed above, it is possible that the sprouted sympathetic fibres, described in our previous study (Yen et al., 2006), play a role in the triggering of these behaviour changes. Specifically, the onset of mechanical allodynia(and of a steep increase in mechanical and thermal hyperalgesia) occurs when newly sprouted sympathetic fibres wrap around the peptidergic afferents at 2 weeks post-lesion (Yen et al., 2006). The extremely low density of myelinated afferents as seen from 3 days post-lesion may be surprising, as thick myelinated afferents are often considered to mediate peripheral stimulus-evoked mechanical allodynia (Woolf and

Mannion, 1999). However, this almost complete depletion concurs with studies in the sciatic nerve, which at 2 weeks post-CCI show a near complete loss of large myelinated fibres distal to the lesion (Basbaum et al., 1991; Munger et al., 1992). Therefore, our data gives further support to the hypothesis that thick myelinated afferents are not directly involved in the mediation of the allodynia triggered by peripheral innocuous stimuli. Instead, allodynia may rather result from lowering of thresholds of activation of nociceptive fibres. Central mechanisms at the level of the spinal cord, particularly a loss of inhibition (Coull et al., 2005) certainly play a role in the triggering and maintenance of the pain-related hypersensitivity displayed by these animals, but the discussion of such mechanisms is beyond the scope of this article. The long-lasting changes in innervation we report in this study do not correlate with maintenance of chronic pain in these animals, as studies using this model have shown that withdrawal reflexes return to normal after 1-2 months (Bennett and Xie, 1988; Coggeshall et al., 1993). Thus despite the persisting loss of thick afferents and persistent hyper-innervation by peptidergic afferents and sympathetic fibres, CNS compensatory mechanisms likely play a major role in returning tested pain-related behaviours to normal. However, this conclusion is based on the responses to stimulus-evoked tests, and though these thresholds return to normal this not does indicate that the animals are pain-free. Indeed, the possibility remains that these animals display some sort of persistent spontaneous pain, an issue that needs to be clarified in further studies.

Conclusions

In conclusion, we have shown that after CCI there is a differential effect of the nerve injury on three fibre populations. We observed a rather quick recovery of the peptidergic (CGRP-IR) fibre population, whereas the non-peptidergic (P2X3-IR) fibre and myelinated (NF200-IR) A-fibre populations recovered much later (the former) or never (the latter). Further studies are required to clarify the physiological meaning of these observations.

Connecting Paragraph – Chapter 2 to Chapter 3

Peripheral nervous system alterations following application of a single nerve injury models are often extrapolated to those alterations purported to occur following the application of other nerve injury models. Within the scope of constriction injury models of the sciatic nerve, two commonly used ones are the chromic gut based classical CCI model as well as that based on the application of a polyethylene cuff. Both models were developed as a mild, long term constriction injury model. In the previous chapter, we described the changes which occur at both early and late time points reflecting a permanent change in peripheral innervation following the application of the chromic gut based CCI. A natural tendency is to suppose that the changes observed in the CCI model should be applicable to other constriction-injury based neuropathic pain models, more specifically following the application of the polyethylene cuff. Following this train of thought, we hypothesize that the behavioural and morphological correlates following the application of a polyethylene cuff based constriction injury should be comparable to those following the application of the classical chromic gut-based model. For the purposes of our studies, we focus on the changes in peripheral innervation specifically of the glabrous skin and this focus is extended to include a comparative examination of evoked pain behaviour following the application of these two constriction-injury based models.

Chapter Three

Comparative study of two chronic constriction injury neuropathic pain models

Jennifer C. Peleshok, Abeer W. Saeed and Alfredo Ribeiro-da-Silva

(Submitted to Journal of Comparative Neurology)

3.1. Abstract

This study compared the behavioral and morphological changes in the glabrous skin of the rat hind paw in the original chronic constriction injury (CCI) model of neuropathic pain to those in the polyethylene cuff model. Male Sprague-Dawley rats were anesthetized prior to the unilateral application of 4 loose chromic gut ligatures (CCI model) or a fixed diameter polyethylene cuff to the common sciatic nerve. Behavioral characterization of the animals was done through 2 weeks to 16 weeks to study evoked responses to thermal (Hargreaves) and mechanical (von Frey) stimulation. At several times points from 2-16 weeks, the animals were perfused with histological fixatives and the glabrous skin of the hind paws was processed for immunofluorescence using antibodies against CGRP, P2X3 and NF200 as markers, respectively, of peptidergic nociceptive fibers, non-peptidergic C-fibers and myelinated afferents. We observed a transient thermal hyperalgesia in both cuff and CCI animals, whereas mechanical hyperalgesia persisted to the 16 week time point only in the cuff operated animals. A transient loss and sprouting of peptidergic fibers occurred in the CCI group compared to a mild, static loss in the cuff. The non-peptidergic C-fibers in the cuff model underwent a mild loss and return to sham levels compared to the sustained loss observed in CCI animals. The myelinated fiber population saw a drastic and sustained loss in CCI operated animals compared to a gradual loss in the cuff animals. Our data indicates that the cuff and CCI models represent two different models of neuropathic pain.

3.2. Introduction

The development of the first animal model of neuropathic pain (Bennett and Xie, 1988) represented a considerable breakthrough in pain research. It is based on the unilateral application of four chromic gut loose ligatures around the common sciatic nerve of the rat. The chronic constriction injury (CCI) model provides a tool to accurately replicate, in an animal setting, some of the clinical features of the neuropathic pain seen in humans in order to study its mechanisms. The application of the chromic gut ligatures led to the development of hypersensitivity towards applied mechanical and thermal stimuli, as a

consequence of the edema and self-strangulation of the nerve (Bennett and Xie, 1988). This original CCI model was found to lead to variability from group to group in terms of degree of fiber loss and behavioral responses to evoked stimulation (Basbaum et al., 1991; Coggeshall et al., 1993). This inter-lab variability was attributed to differences in the tightness of the applied ligatures in which tighter ligatures generated dramatic fiber loss and severe behavioral profile compared to those applied more loosely. To eliminate such variability, a supposedly equivalent model based on the application of fixed diameter polyethylene cuffs around the sciatic nerve was developed (Mosconi and Kruger, 1996). Although the original cuff model is based on the application of 4 individual cuffs, the model was subsequently modified to include a single longer cuff (Pitcher et al., 1999). Models of neuropathic pain have been described in terms of their behavioral correlates, extent of nerve damage, degree of immune cell activation, and firing properties of neurons.

Our lab has used both the classical CCI and cuff models (Bailey and Ribeiro-da-Silva, 2006; Peleshok and Ribeiro-da-Silva, 2011; Yen et al., 2006). Using the chromic gut CCI in combination with immunocytochemical methods, we have demonstrated a marked loss of peptidergic sensory fibers within the glabrous skin of the rat hind paw followed by a sprouting of them (Yen et al., 2006).

Some studies in the literature have used the cuff model as if it were the equivalent of the classical CCI (Coull et al., 2005; Coull et al., 2003) As some preliminary data from our lab suggested that there were substantial differences between the two models, from duration of allodynia to changes in peripheral innervation, we decided to carry out a behavioral and morphological comparative study of the two models.

3.3. Materials and Methods

In total, 106 male Sprague-Dawley rats (Charles River Canada), weighing between 150-175g, were used in this study. All animals were maintained on a 12-hour light/dark cycle and allowed access to food and water *ad libitum*. All animal protocols were approved by the McGill University Animal Care Committee and followed the guidelines of the Canadian Council on Animal Care and the International Association for the Study of Pain. Raw data from CCI operated animals was adapted and expanded from a prior publication (Peleshok and Ribeiro-da-Silva, 2011).

Peripheral Nerve Lesions

Animals were randomly assigned to receive either a traditional CCI, constriction injury with application of polyethylene cuff (cuff) or a sham operation. All animals were deeply anaesthetized with isoflurane. In total, 28 rats received the sham operation, 36 received the cuff injury and 35 received the CCI to the common sciatic nerve, as described in detail in previous publications (Pitcher and Henry, 2004; Pitcher et al., 1999). Briefly, the left common sciatic nerve was exposed at the mid-thigh through the biceps femoris. All surrounding fascia was removed to allow free passage of blunt glass probes. Proximal to the trifurcation of the sciatic nerve, four ligatures (4-0 chromic gut, Ethicon) were tied loosely around the nerve with 1 mm spacing in between. For the cuff surgery, a single 2 mm section of PE-60 polyethylene tubing (Intramedic PE-60, Fisher Scientific Ltd., Montreal Qc) was placed at the same location proximal to the trifurcation of the sciatic nerve as that for the chromic gut ligatures. The incision was closed in layers using absorbable sutures (Vicryl, Ethicon). The animals assigned to sham-operated groups underwent the above mentioned procedures with the exception of the application of either the chromic gut ligatures or polyethylene cuff.

Behavior

All animals (36 in total) were tested between 9 AM and 4 PM. Animals were allowed to habituate to the quiet testing room for 10-30 min prior to being placed randomly in clear plastic cages on a wire mesh screen for the mechanical

sensitivity testing. After another habituation period of 30 min, baseline measurements were established over the course of three consecutive daily trial periods alternating between experimenter on each test day. For example, behavior testing was conducted on all animals on Day 3 by JP and Day 7 by AS to minimize experimenter bias. Any animal which had abnormal baseline withdrawal thresholds for either mechanical or thermal stimulation was removed before the application of the nerve injury to ensure there was no error introduced due to an underlying sensory abnormality of the animal. Therefore, from the original 36 animals, 3 animals were excluded prior to assignment to operation group. Three groups of animals (11 CCI-, 12 cuff- and 10 sham-operated) were tested for mechanical allodynia and hyperalgesia as well as thermal hyperalgesia. 4 g and 15 g von Frey filaments were applied to the rear paw foot pad five times and held for five seconds for each application. Care was taken to ensure application of the von Frey filaments were restricted to the area of the paw surrounded by tori (Figure 1). This was repeated five times, alternating from the contralateral to ipsilateral paw, where each animal was tested randomly. All reactions to the applied filament were recorded and averaged. The outliers (defined as being greater than two standard deviations from the mean) were removed prior to statistical analysis. The 4 g filament was used to assess mechanical allodynia and the 15 g mechanical hyperalgesia (Flatters and Bennett, 2004; Zheng et al., 2011). Following mechanical sensitivity assessments, the rats were placed in clear plastic chambers on the surface of a Hargreaves thermal hyperalgesia plate. The rats were allowed to habituate to the chambers and the plastic surface cleared of all defecation. A focused beam was applied to the plantar surface of both the contra and ipsi rear paw. The beam had a surface temperature of 31^{o}C and a safety cut off of 20.48 sec. Each rat was tested three times on each of the ipsi and contra rear paw surfaces and the times at which the rat raised his paw and broke the beam path were recorded and averaged. Values greater than two standard deviations from the mean were removed from the analysis. The average withdrawal latencies from the ipsilateral injured paws were calculated as percent difference from the ipsilateral sham-operated controls

where the sham-operated latencies were taken as 100%. After baseline, animals were tested at 1 through 16 weeks post-surgery.

Animal Perfusion and Histological Processing

Animals were sacrificed after periods of 1, 2, 4, 8 and 16 weeks post-surgery. Animals used for behavioral testing were sacrificed at 16 weeks following final behavioral test. Rats were anesthetized with Equithesin (6.5mg chloral hydrate and 3mg sodium pentobarbital in a volume of 0.3mL, i.p., per 100g body weight) and transcardially perfused with vascular rinse (0.1% w/v sodium nitrite in a phosphate buffer) followed by 3% paraformaldehyde, 15% saturated picric acid in 0.1M phosphate buffer, pH 7.4, for 30min. The glabrous skin from the left hind paw, specifically the thin skin surrounded by the tori targeted during behavior testing, was removed, post-fixed by immersion in the same fixative of the perfusion for 1hr and immersed in 30% sucrose in 0.1M phosphate buffer for cryoprotection overnight at 4^{o}C. The excised region is depicted in Figure 1 as the grey rectangular region, surrounded by tori. Tissue was embedded in an optimum cutting temperature medium (OCT, TissueTek), cut using a cryostat (Leica) at a thickness of 50µm and the sections processed as free floating.

Immunohistochemistry

Sections were washed in 0.01 M phosphate buffered saline (PBS) for 30 min. Subsequently, PBS with 0.2% Triton X-100 (PBS-T) was used to dilute the immunoreagents and for washing. Sections were then treated with 50% ethanol for 30 min followed by 1 hour incubation in PBS-T containing 10% (v/v) normal serum of the species used to generate the secondary antibody to reduce non-specific staining. Subsequently, sections were incubated with primary antibodies (diluted in PBS-T) either overnight or for 48hrs (in the case of P2X3) at 4^{o}C. The following primary antibodies were used: polyclonal rabbit anti-calcitonin gene related peptide (CGRP; 1:2000, Sigma), and monoclonal mouse anti-neurofilament-200 (NF200; 1:2 Abcam, Cambridge MA). After washing, the sections were incubated with secondary antibody diluted in PBS-T for two hours

at room temperature. The following secondary antibodies were used: for NF200 staining, a highly cross-adsorbed goat anti-mouse IgG conjugated to Alexa 596 (1:800, Molecular Probes, Eugene, OR) and for CGRP, a goat anti-rabbit conjugated to Alexa 488 (1:800, Molecular Probes, Eugene, OR). Sections were washed and mounted on gelatin-coated slides and coverslipped using Aquapolymount (Polysciences; Warrington, PA). In the case of P2X3 staining, after 30 min incubation with 50% ethanol, sections were treated with 0.3% hydrogen peroxide solution for 10min. Following a 30min PBS and 30min PBS-T wash, sections were then blocked with normal serum as described above and incubated for 48hrs at 4^{o}C with guinea-pig anti-P2X3 primary antibody (1:25,000, Neuromics, Edina MN). The sections were then washed and incubated for 90min with biotin-conjugated donkey anti-guinea-pig IgG (1:200, Jackson Immunoresearch, West Grove PA), washed for 30min with PBS-T and incubated for 1 hour with Vectastain Elite ABC kit (1:250, Vector Laboratories, Burlington, Ont.). The P2X3 signal was amplified using a tyramide treatment (1:75, Perkin-Elmer; Norwalk, CT) for 7 min. Streptavidin conjugated to Alexa 488 (1:200, Molecular Probes; Eugene OR) was applied to the sections for 2 hours. Finally, the sections were washed and mounted as described above.

Images for the Figures

Images in the figures were obtained from the merging in a horizontal projection of Z-stacks of confocal optical sections, obtained using a Zeiss LSM 510 confocal microscope equipped with argon and helium neon lasers applying a 40X water-immersion objective. Images were exported directly in TIFF format and adjusted using Adobe Photoshop CS4 for brightness and contrast.

Primary Antibody Characterization

CGRP: The anti-CGRP antibody, raised in rabbit, was purchased from Sigma (C8198, lot 013K4842). It was generated against synthetic rat CGRP conjugated to KLH. The specificity was tested via dot-blot in which the antibody was found to recognize rat CGRP conjugated to bovine BSA; recognition of human CGRP and β-CGRP (conjugated to bovine BSA) was also observed (data

supplied by Sigma). Specificity was also assessed by immunocytochemistry using free-floating sections of rat glabrous skin, and the staining was completely abolished when the antibody was pre-adsorbed with rat CGRP (Yen et al., 2006). This antibody has been used extensively in our lab as a marker of peptidergic fibers in rat spinal cord, DRG and skin (Almarestani et al., 2008; Bailey and Ribeiro-da-Silva, 2006; Dickson et al., 2006; Grelik et al., 2005a; Grelik et al., 2005b; Lorenzo et al., 2008; Taylor et al., 2009; Yen et al., 2006).

Purinergic receptor P2X3: The polyclonal anti-P2X3 antibody was raised in guinea-pig (Neuromics, GP10108, lot 400457) against the intracellular C-terminal domain of rat P2X3, specifically against the sequence VEKQSTDSGAYSIGH corresponding to amino acids 383-397. Specificity was confirmed by preadsorbing the antibody with the peptide immunogen (20 g/ml) prior to staining trigeminal ganglia of rat; no staining was observed (Dellarole and Grilli, 2008; Ichikawa and Sugimoto, 2004).

Neurofilament 200 (NF-200): The anti-NF200 antibody (Abcam, ab910, lot 671264), (aka RT97), recognizes the heavy chain of neurofilaments in myelinated fibers. It is a monoclonal antibody generated from the immunization of mice with Triton X-100 insoluble rat brain protein (Wood, 1981). It was later shown by epitope mapping that this antibody targets the carboxy domain of the 210 kDa, high molecular weight neurofilament protein in human and bovine samples (Anderton et al., 1982). The antibody was used to correlate the diameter and conduction velocity to neurofilament status, in large and medium-diameter rat primary afferents, and it was confirmed that it recognizes both Aβ and Aδ fibers (Lawson and Waddell, 1991).

Quantification of fiber density

Micrographs were obtained on a Zeiss Axioplan 2 imaging fluorescence microscope equipped with a high-resolution color digital camera, using a 40X Plan-Fluotar oil-immersion objective. The Carl Zeiss Axiovision 4.8 software (Zeiss Canada) was used to capture the images. Six experimental animals were used for each time point. Six sections per sampled animal and four images per

section were taken making a total of 120 images per time point. The observer who took the images was blinded as to the experimental groups, and the codes broken only after all data were collected. The images were quantified for fiber density of P2X3, CGRP and NF200 immunoreactivity. The innervation density of the upper dermis, defined as the area within 150μm from the dermo-epidermal junction, was measured as previously described in one of our publications (Yen et al., 2006). The images were exported as TIFF files to an MCID Elite image analysis system (Imaging Research Inc., St. Catharines, Ont., Canada). We used a function of the MCID software to detect fibers. Following detection, fibers were skeletonized to one pixel in width. Segments shorter than 5 μm were excluded from the measurements, to ensure only bona fide fibers were measured. Fiber length was measured in μm and divided by the live frame area (μm^2) to determine total fiber length per unit area. Four frames from each of six sections taken from six animals per group were used.

Statistics

Data from fiber density analyses was analyzed using GraphPad version 5.0 using a 2-way ANOVA with a Bonferroni post-hoc analysis comparing each group to sham-operated controls.

Data Compilation

Previously obtained data from behavioral assessments (thermal hyperalgesia, mechanical allodynia and hyperalgesia) as well as select fiber density studies from CGRP, NF200 and P2X3 immunocytochemistry results from CCI operated animals were adapted and expanded from a previous publication (Peleshok and Ribeiro-da-Silva, 2011). Alterations being that the 3 days and 1.5 year time points from the prior publication were not used and behavioral time points were now extended up to 16 weeks post-injury, instead of only up to 21 days post-surgery in the previous publication. To demonstrate reproducibility, a new full cohort of 12 animals were operated for CCI and sham lesions and allowed to survive for 1 week (as described above), at which point tissue was processed for the immunocytochemical procedures described above.

3.4. Results:

Behavioral Testing

Mechanical allodynia and hyperalgesia were assessed for all three sets of animals, namely CCI-, cuff- and sham-operated. Mechanical allodynia was measured by the frequency with which an animal responds to the applied 4 g von Frey filament. Mechanical allodynia in the CCI became significant at 10 days post-lesion (Figure 2A). The mechanical allodynia associated with the cuff injury developed by 10 days post-injury (Figure 2B). By 4 weeks post-injury, the CCI-operated animals did not display any significant evoked behavior to the 4g filament whereas the mechanical allodynia observed in the cuff-operated animals persisted to the 16 week time point (Figure 2A and 2B). The CCI-operated animals responded to the application of the 15 g filament, indicative of mechanical hyperalgesia, with a significantly higher frequency of response at 7 days post-injury and attained a maximum of at 15 days post-injury (Figure 3A). In contrast, the cuff-operated animals developed a significantly higher response frequency at 10 days post-injury (Figure 3B). CCI-operated animals continued to display significant stimulus evoked sensitivity up to and including 8 weeks post-injury and returned to baseline values at 16 weeks post-injury (Figure 3A). However, cuff-operated animals maintained a significantly higher response frequency through to 16 weeks post-injury, with a minor decrease from a maximum attained at 21 days (Figure 3B).

Heat sensitivity was measured by application of a focused beam of light to the plantar surface of the rat hindpaw. The withdrawal latency was compared to the ipsilateral paw of sham-operated controls for all time-points (Figure 4A and B). The application of the CCI and cuff injuries induced a decrease in the time required to break the focused beam of light used to ascertain heat sensitivity. Withdrawal latencies were compared to sham-operated controls. By 10 days post-CCI, significant differences in heat withdrawal latencies were observed compared to the contralateral paw averaged to sham operated withdrawal latencies (Figure 4A). The significance increased through to 3 weeks post-injury after which point there was no significant difference compared to the contralateral side

for the remaining time points examined (Figure 4A). The cuff-operated animals developed significant decreases in withdrawal latency at 1 week post-injury and this continued to 3 weeks after which point no differences were observed compared to sham-operated controls (Figure 4B).

Immunocytochemistry

Immunocytochemical markers were used to label subpopulations of sensory fibers. CGRP-IR fibers in sham-operated animals formed a plexus along the dermo-epidermal junction (Figures 5A and 6A), from which a small number of individual fibers penetrated the epidermis. Following application of the CCI, the peptidergic fibers decreased in fiber density, and at 7 and 14 days post-injury there were few if any detectable fibers within the upper dermis (Figure 5B and C). However, after 2 weeks there was an increase in fiber density; at 8 weeks it reached sham levels and by 16 weeks there was a fiber density significantly higher than in controls (Figures 5D-F and 7). It should be noted that following application of the CCI there were few detectable CGRP-IR fibers within the epidermis throughout all time points examined (Figure 5B-F). In the animals which had received the cuff injury, the CGRP innervation followed a different sequence of morphological changes (Figure 6B-F). At 1 week post-injury there was a slight decrease in CGRP-IR fiber density in the upper dermis compared with that of sham-operated controls, but this was not significant because of increased variation between animals (Figures 6B and 7). However, from 2 weeks onwards there was a significant reduction in CGRP-IR fiber density compared to sham, from which there was no recovery through 16 weeks post-cuff (Figures 6C-F and 7).

The non-peptidergic C-fiber innervation, as revealed by P2X3 immunoreactivity, was mostly located in the epidermis and upper dermis, as we previous described (Peleshok and Ribeiro-da-Silva, 2011). In short, most P2X3-IR fibers in the dermis were located in the upper dermis, and formed a dense plexus along the dermo-epidermal junction (Figures 8A and 9A). The epidermal innervation by the P2X3-IR fibers was quite extensive. Thin projections from the fibers traveling along the dermo-epidermal junction penetrated into the epidermis.

At 1 week following application of the CCI, there were no observable P2X3-IR fibers in either the upper dermis, along the dermo-epidermal junction, or in the epidermis. This innervation profile persisted to 8 weeks post-injury when sparse P2X3-IR fibers were detected, mostly along the dermo-epidermal junction. At 16 weeks post-injury, more P2X3-IR fibers were detected in the upper dermis than at 8 weeks (Figure 8F), but values of density of innervation were still significantly less than in sham-operated controls (Figure 10). At either the 8 or 16 week time points, only the occasional P2X3-IR fiber was detected within the epidermis in contrast to the dense innervation seen in sham-operated controls (Figure 8E-F). Following application of the cuff injury, as in the CCI model, the innervation of the epidermis dramatically decreased to a point where very few fibers were observed compared to a very dense innervation in sham-operated controls (Figure 9). At 1 week post-cuff, there was no significant loss of non-peptidergic fiber innervation of the upper dermis and became significant at 2 weeks post-injury, when a further decrease in innervation density along the dermo-epidermal junction was observed (Figure 9B-C). The remaining fibers were very sparse and interspersed in contrast to the sham-operated and 1 week post-cuff animals. Also, at 2 weeks post-injury, the occasional P2X3-IR fiber was observed to innervate the epidermis (Figure 9C). These occasional intra-epidermal fibers were different from those seen in sham-operated controls in that they were not as clearly perpendicular to the dermo-epidermal junction and instead followed a more oblique path from the dermo-epidermal junction. At 4 and 8 weeks post-injury, the P2X3-IR fibers were more often found parallel to the dermo-epidermal junction than at 2 weeks (Figure 9D-E), and the innervation pattern was close to that observed in sham animals at 16 weeks post-cuff, although the scarcity of the intra-epidermal fibers still persisted (Figure 9F). Indeed, there was no significant recovery in the innervation of the epidermis by P2X3-IR fibers in the cuff model in spite of the observation that the P2X3-IR fibers remain in the upper dermis (Figure 9). Regarding measured changes in fiber density in the dermis, the animals receiving the cuff-injury developed a more moderate decrease at 1 week than the CCI rats, which was not significant when compared to sham-operated

controls (Figure 10). However, at 2 weeks following application of the cuff, the P2X3-IR fiber loss increased further compared to sham-operated controls (Figure 10). There was a subsequent recovery, with values of fiber density back to sham levels by 16 weeks (Figure 10).

We used NF200 as a marker for large and medium diameter myelinated sensory afferents. In sham-operated controls, these fibers were concentrated in bundles travelling in small cutaneous nerves in the dermis (Figures 11A and 12A), which continued in smaller nerves. In the terminal segments, these fibers run virtually isolated (Figures 11A and 12A). NF200-IR fibers were seldom seen in the epidermis. Within the first through fourth weeks following application of the CCI, almost no detectable NF200 immunoreactive fibers were found within the upper dermis (Figure 11B-D). This is confirmed by the highly significant drop in fiber density (Figure 13). However, there was a partial recovery at 8 and 16 weeks post-CCI (Figures 11E-F and 12). In contrast, the application of the cuff injury led to a considerably less drastic reduction in NF200-IR fibers, as residual fibers were detected at all time points (Figure 12B-F). The remaining NF200-IR fibers within the upper dermis following application of the cuff were part of smaller bundles and often run as single fibers. As well, these remaining fibers did not penetrate the dermo-epidermal junction into the epidermis.

As we re-used raw data from previous publication, we deemed it important to assess how reproducible the CCI immunocytochemical data was. For that, we processed for immunocytochemistry, using exactly the same markers, a new cohort of animals which received chromic gut CCI or a sham lesion at the one week time point. This new data were compared to the same data point from the previous set of animals. There were no differences observed in any of the afferent populations examined (Figure 14).

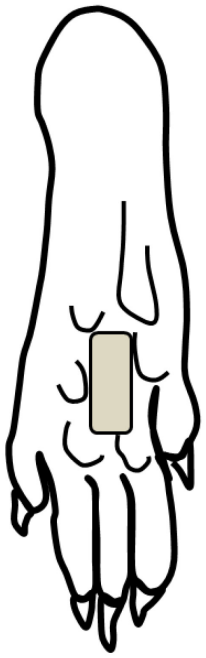

Figure 1: Region of rat hind paw thick skin sampled for immunocytochemistry. Skin samples were collected from the region of the plantar surface surrounded by tori which is outlined using a shaded box. This same area was used to focus the light beam for Hargreaves heat sensitivity test and for von Frey filament application

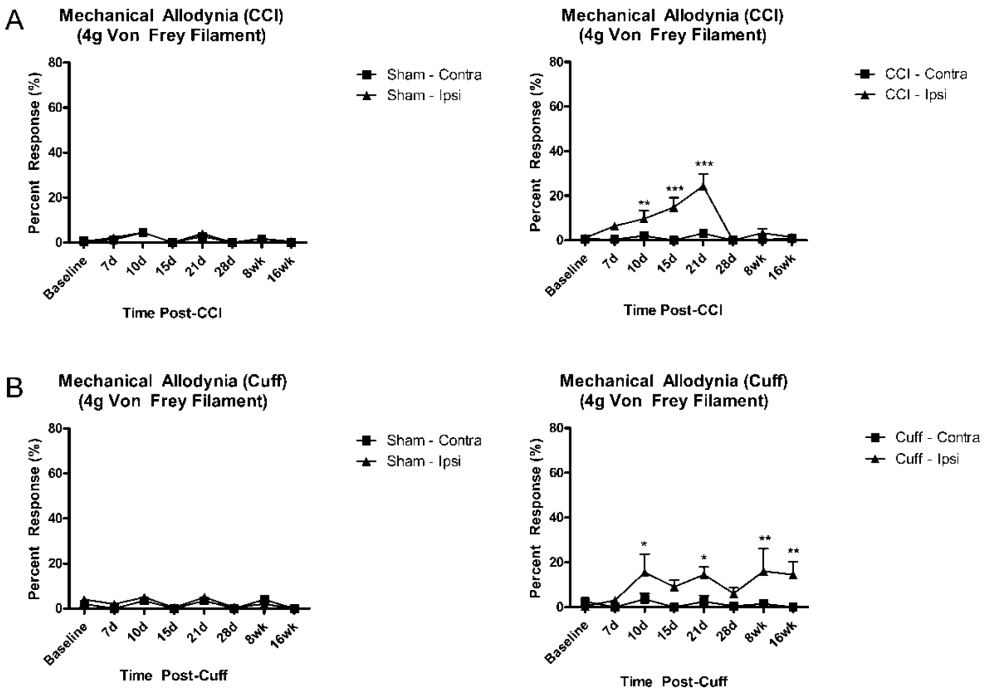

Figure 2: Mechanical allodynia time-course scores from baseline measurements to 16 weeks post-injury in lesioned and sham-operated rats. Mechanical allodynia was ascertained using a 4 g von Frey filament and average withdrawal frequency measured and calculated as total percent withdrawal frequency. All comparisons were made against the contralateral (unoperated) side. A) Mechanical allodynia development after chromic gut chronic constriction injury (CCI) attained significance at 10 days post-injury, peaked at 21 days and returned to baseline at 4 weeks post-injury. B) Mechanical allodynia after polyethylene cuff application also became significant at 10 days post-injury but significance was still observed at 16 weeks. *$p < 0.05$, **$p < 0.01$, ***$p < 0.001$; n = 8-10; mean + SEM comparisons made against baseline measurement.

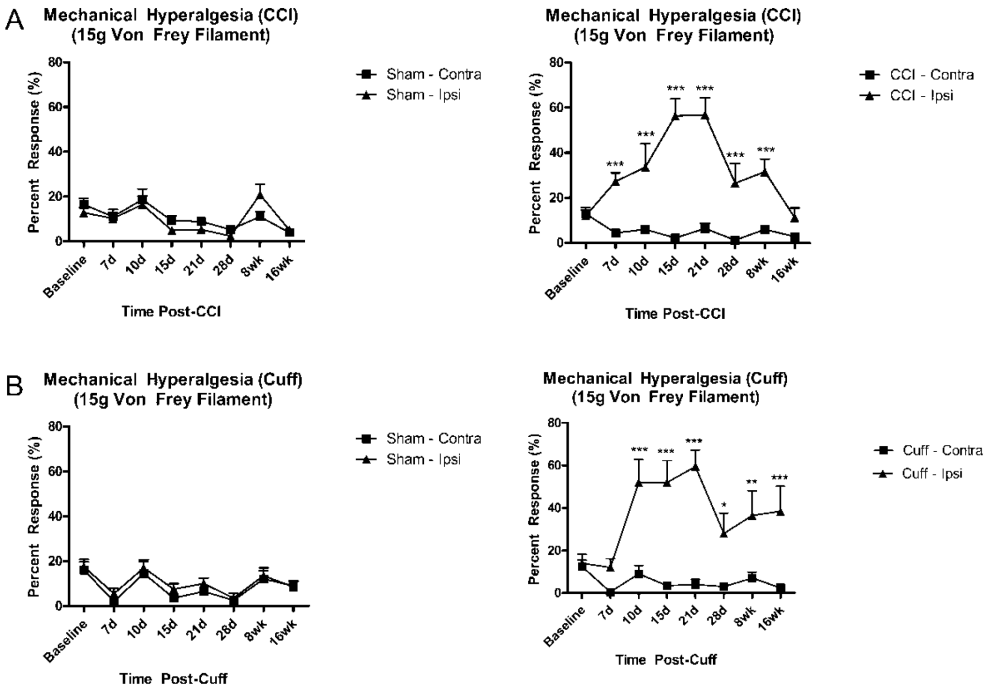

Figure 3: Mechanical hyperalgesia time course scores from baseline measurements to 16 weeks post-injury in lesioned and sham-operated rats. Mechanical hyperalgesia was ascertained using a 15 g von Frey filament and average withdrawal frequency measured and calculated as total percent withdrawal frequency. All comparisons were made against the contralateral side. A) Mechanical hyperalgesia development after CCI injury attained significance at 7 days post-injury and continued to increase in response frequency to 2 weeks. The values returned to baseline levels by 16 weeks post-injury. B) Mechanical hyperalgesia development after application of the polyethylene cuff attained significance only at 10 days post-injury but remained significant up to 16 weeks. *$p < 0.05$, **$p < 0.01$, ***$p < 0.001$; n = 8-10; mean + SEM; comparisons made against baseline.

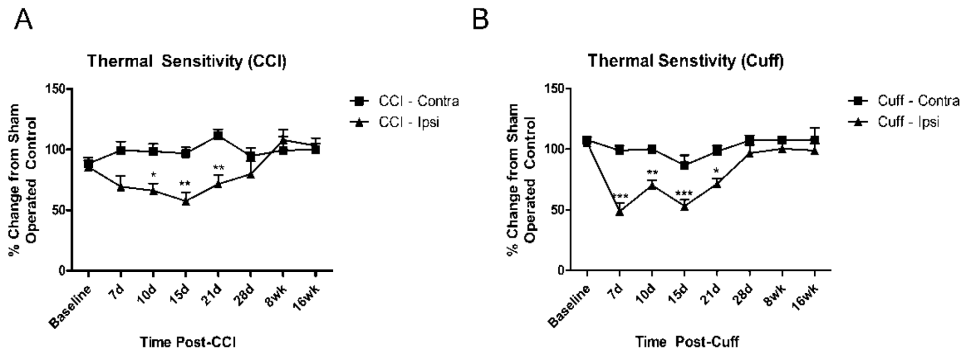

Figure 4: Thermal sensitivities were assessed by measuring withdrawal latencies of sham, CCI and cuff lesioned animals using the Hargreaves test. All response latencies were converted to percentages and further plotted as comparison to time matched sham-operated controls (for which response was set at 100%). A) Measurements of the ipsilateral hind paw in the CCI model animals showed a significant reduction of response latencies compared to sham operated control from 10 days to 3 weeks post-injury. This reduction resolved by 4 weeks post-injury. B) Measurements taken from animals receiving the polyethylene cuff injury showed a significant onset of thermal hyperalgesia at 7 days, although the subsequent pattern was the same as for CCI animals. *$p < 0.05$, **$p < 0.01$, ***$p < 0.001$; n = 8-10; mean + SEM; comparisons made against baseline.

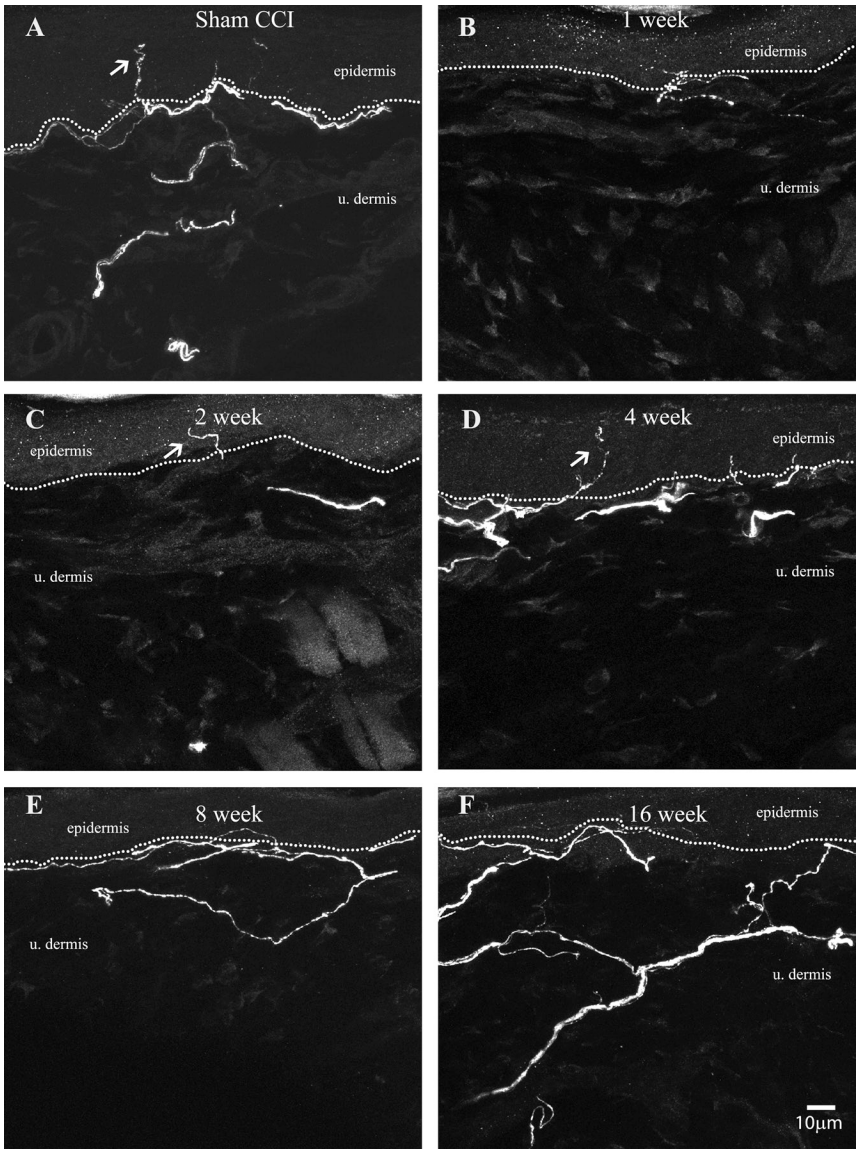

Figure 5: Peptidergic afferent innervation of the skin at each time point using immunoreactivity towards CGRP as a marker in the CCI model. All images were obtained using a confocal microscope and result from projection in horizontal plane of z-stacks of optical sections. A) Images from sham operated rats illustrate the occurrence of bundles of immunoreactive fibres in small cutaneous nerves, which join a dense fibre plexus close to or along the dermo-epidermal junction. Arrows point to the occasional CGRP-IR fibres penetrating into the epidermis. B and C) Following application of the CCI model, at 7 and 14 days post-lesion CGRP-IR fibres decreased significantly in number where only the occasional fibre was spotted close to the dermo-epidermal junction. In contrast to the sham-operated animals, few intra-epidermal afferents were observed. D-F) At later time points, there was recovery of the innervation, with hyper-innervation at 16 weeks.

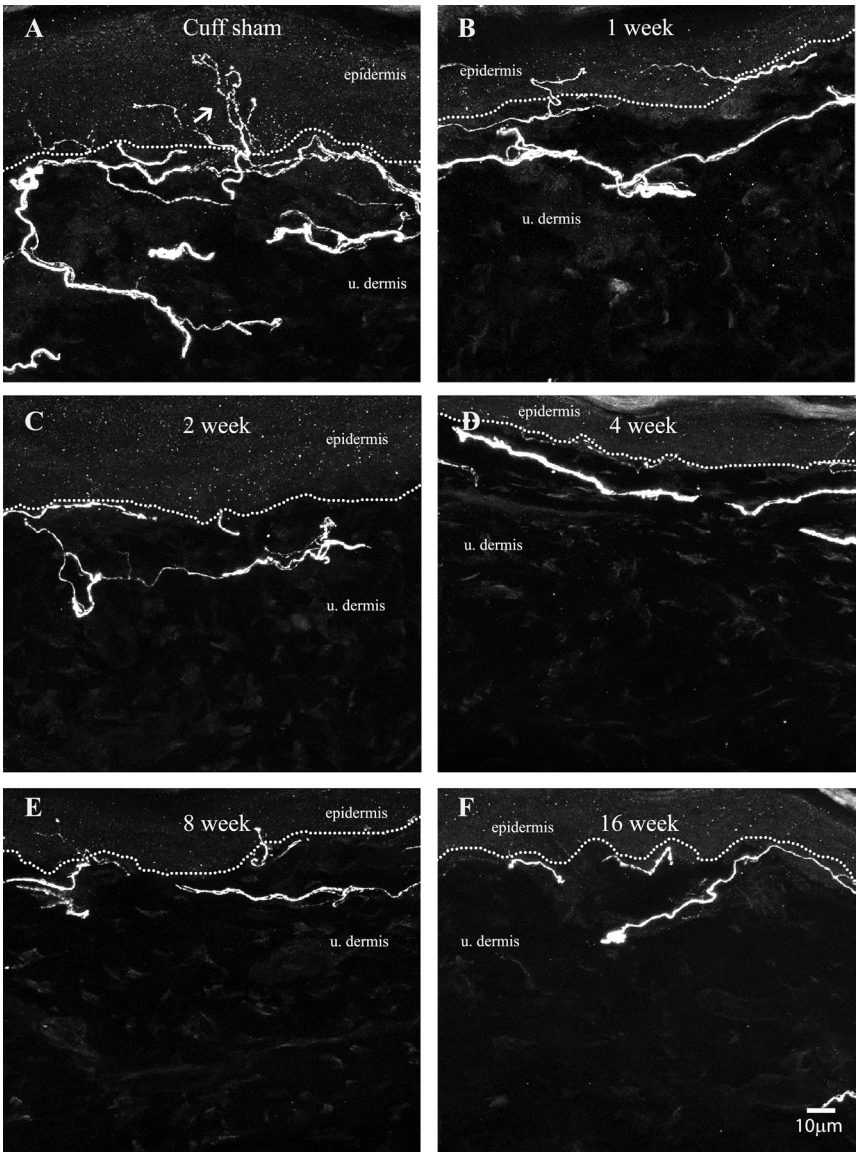

Figure 6: Peptidergic afferent innervation of the skin at each time point using immunoreactivity towards CGRP as a marker in the cuff model. All images were obtained using a confocal microscope and result from projection in horizontal plane of z-stacks of optical sections. A) In a sham-operated animal, note the abundant innervation of the dermis and the presence of intra-epidermal fibres (arrows). B) At one week post-lesion, there was no obvious loss in innervation. C-F) Subsequently, there was a substantial loss of innervation in the dermis with no apparent recovery up to 16 weeks. The epidermal innervation also was greatly decreased.

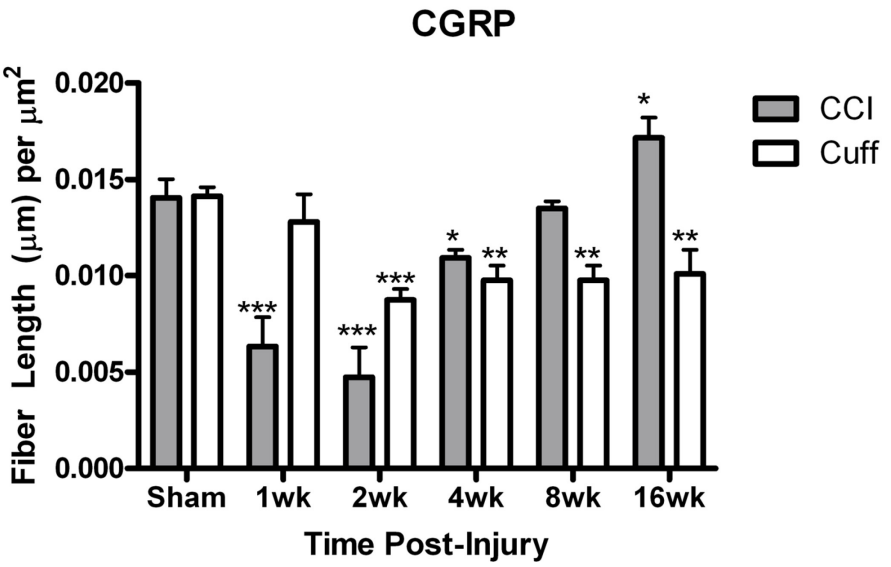

Figure 7: **Quantification of CGRP-IR fibre density - total area fibre length (μm)/total scanned area (μm$^{2)}$) - in the upper dermis.** All density comparisons were made to sham operated controls. Fibre density significantly decreased following application of the CCI model at one week post-injury, but not following the application of the cuff, where significant loss started at 2 weeks only. CCI animals had a recovery of CGRP-IR innervation by 4 weeks, with a density above sham levels at 16 weeks. The density of CGRP-IR fibres in animals with the cuff lesion had not recovered by 16 weeks and remained significantly lower than in sham operated controls. $p<0.05$, ** $p<0.01$, *** $p<0.005$; n=6; mean +SEM; comparisons made against sham operated controls.

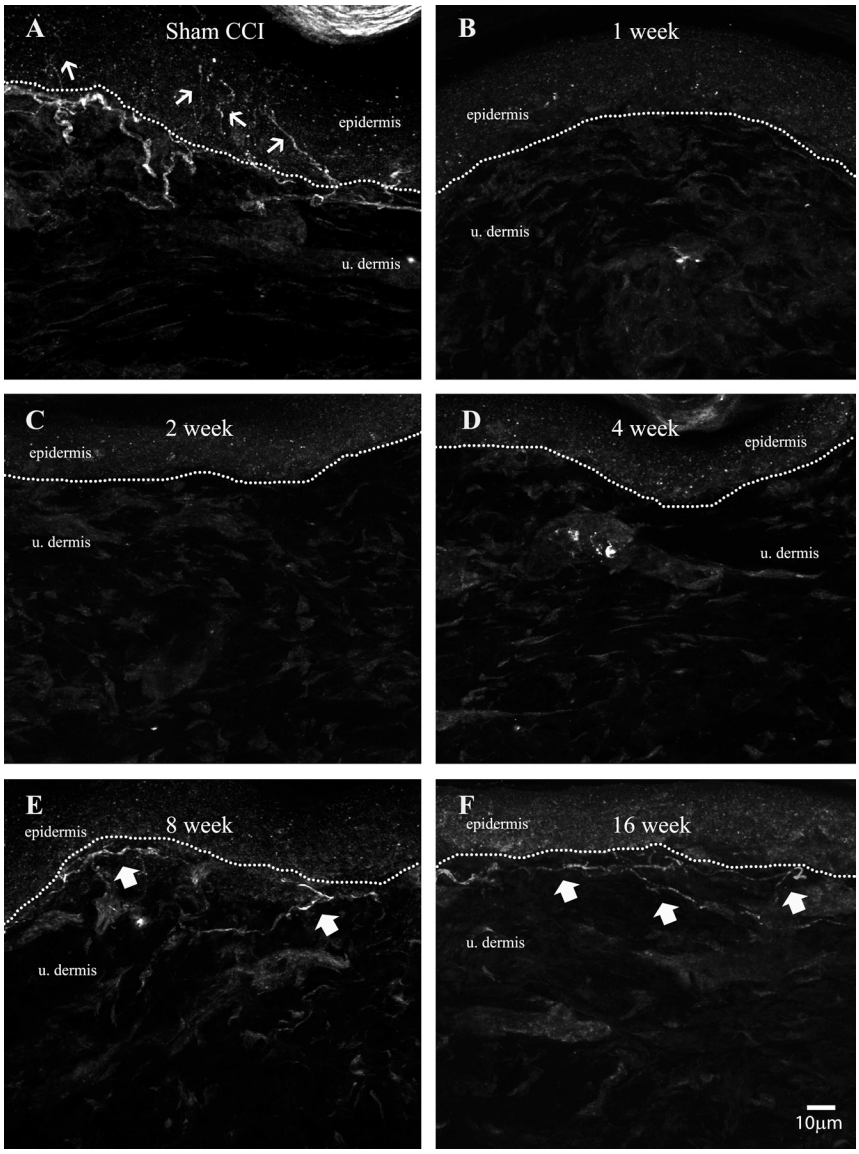

Figure 8: Non-peptidergic innervation of the skin at each time point using immunoreactivity towards the purinergic receptor P2X3 as a marker in the CCI model. All images were obtained using a confocal microscope and result from projection in horizontal plane of z-stacks of optical sections. A) In sham operated animals, note that the P2X3-IR innervation was particularly abundant in the upper dermis, with numerous fibres penetrating the epidermis (small arrows). B-D) In animals with a CCI lesion, there was a drastic decrease of P2X3-IR innervation starting at 1 week, with an almost complete depletion of fibres up to 4 weeks. E-F) At 8 weeks post-injury, only occasional fibres were spotted close to the dermo-epidermal junction, with a more marked recovery by 16 weeks. The intra-epidermal fibres were virtually undetected in CCI animals at all time points. Larger arrows indicate fibres in the upper dermis.

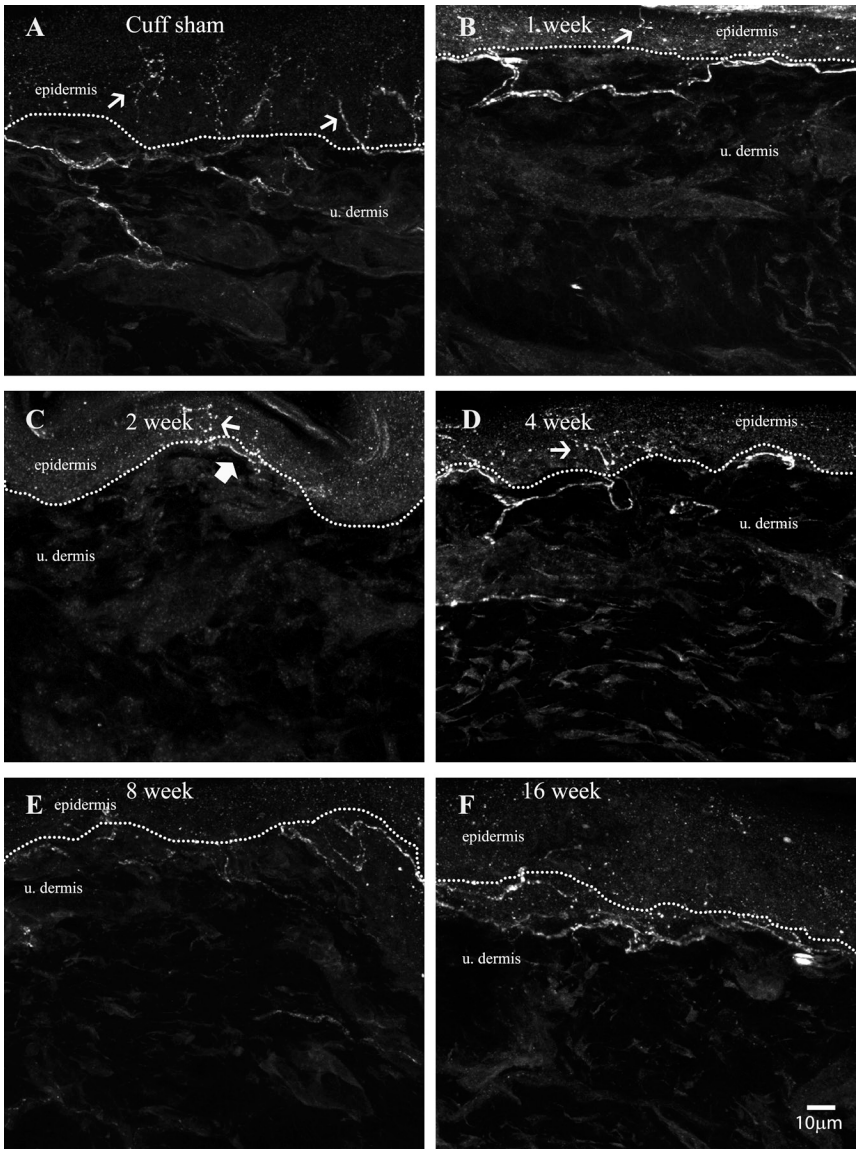

Figure 9: Non-peptidergic innervation of the skin at each time point using immunoreactivity towards the purinergic receptor P2X3 as a marker in the cuff model. All images were obtained using a confocal microscope and result from projection in horizontal plane of z-stacks of optical sections. B) Note that in the cuff model a mild decrease in dermal fibre loss is observed compared to sham-operated control and occasional fibres persist in the epidermis (small arrow). C) A dramatic loss of non-peptidergic C-fibres is observed within the upper dermis with few persisting along the dermo-epidermal junction (large arrow). D-E) Gradual return of non-peptidergic C-fibres observed along the dermo-epidermal junction. F) A return to sham operated control patterns at 16 weeks post-injury. In the cuff model, the intra-epidermal fibres were less than in shams but were still detected (small arrows).

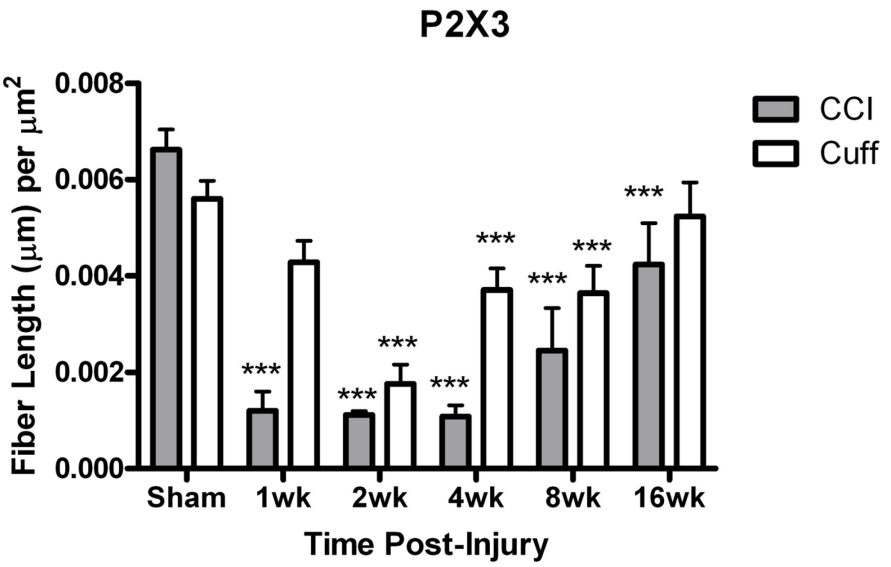

Figure 10: Quantification of P2X3-IR fibre density - total area fibre length (μm)/total scanned area (μm^2) - in the upper dermis. All density comparisons were made to sham operated controls. There was a drastic decrease in P2X3-IR fibre density in the CCI animals, starting at 1 week post-lesion, with recovery starting at 8 weeks. However, at 16 weeks values were still lower than in sham operated controls. In the animals with the cuff lesion, significant fibre density loss was also observed at one week post-injury and values returned to sham levels by 16 weeks. *$p < 0.05$, **$p < 0.01$, ***$p < 0.001$; n = 8-10; mean + SEM; comparisons made against sham operated controls.

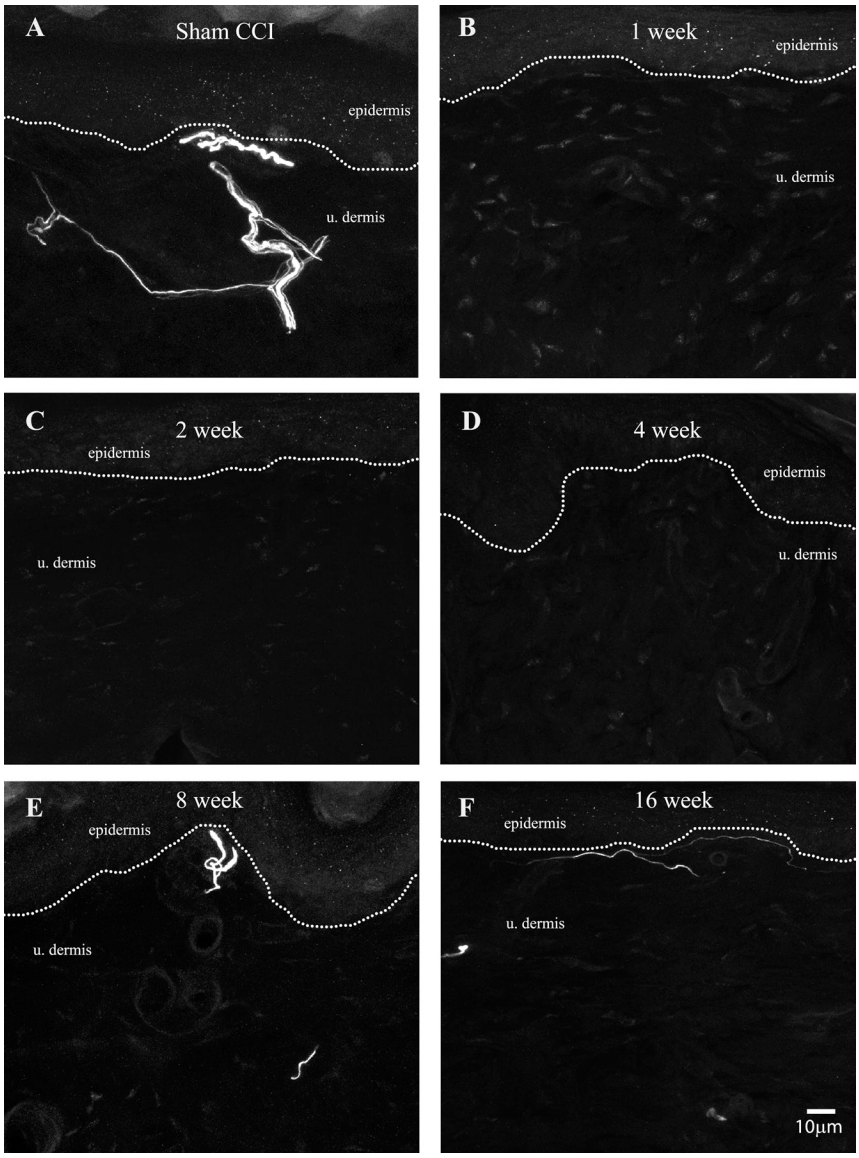

Figure 11: Myelinated afferent innervation of the skin at each time point using immunoreactivity for NF200 as a marker in animals with a CCI lesion. All images were obtained using a confocal microscope and result from projection in horizontal plane of z-stacks of optical sections. A) Images from sham operated animals show bundles of NF200-IR fibres in the dermis in cutaneous nerves, which continued into smaller nerves. The terminal segments represented just one or two NF200-IR fibres. NF200-IR fibres seldom penetrated the epidermis (none is shown). B-F) In lesioned animals, note the almost complete loss of NF200-IR at 1, 2 and 4 weeks, with few fibres observed at 8 and 16 weeks.

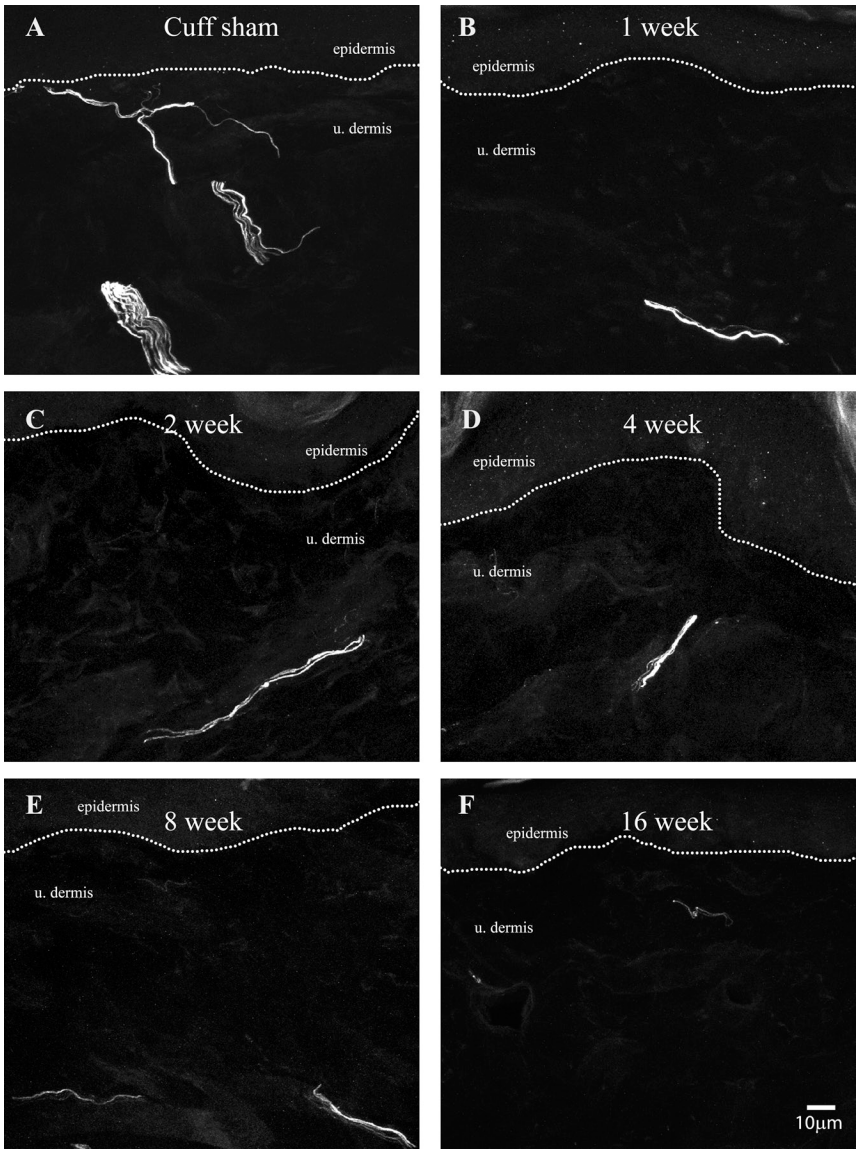

Figure 12: Myelinated afferent innervation of the skin at each time point using immunoreactivity for NF200 as a marker in animals with a cuff lesion. All images were obtained using a confocal microscope and result from projection in horizontal plane of z-stacks of optical sections. A) As in Figure 10, images from sham operated animals show bundles of NF200-IR fibres in the dermis in cutaneous nerves, which continued into smaller nerves. The terminal segments represented just one or two NF200-IR fibres. B-F) In animals with lesions, there was a very substantial loss of NF200-IR fibres, with a much lower number of immunoreactive fibres in the nerves and no recovery at any time. However, there was no virtual loss of innervation at the earlier time points like that observed following application of the CCI model.

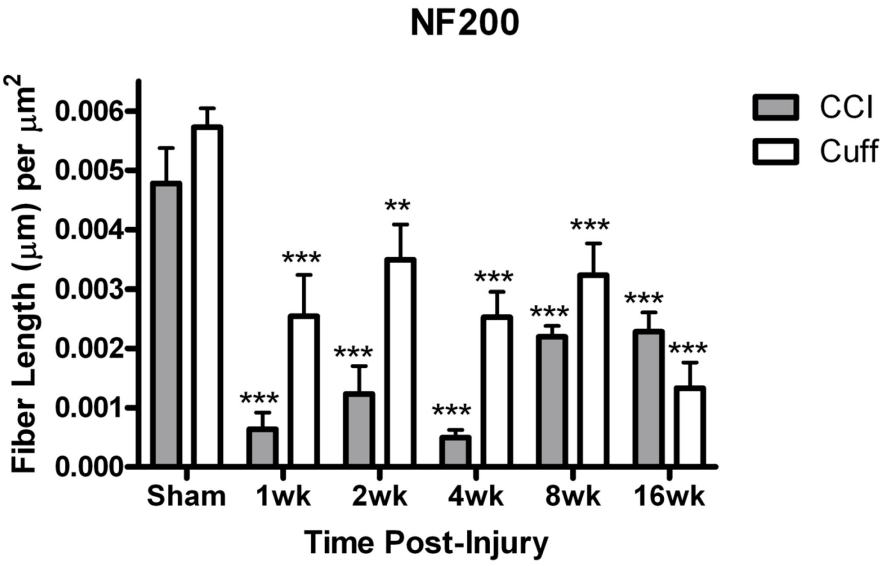

Figure 13: Quantification of NF200-IR fibre density - total area fibre length (μm)/total scanned area (μm^2) - in the upper dermis. All density comparisons were made to sham operated controls. In the CCI model, fibre density values significantly from 1 week post-lesion, with a slight recovery at 8 and 16 weeks. In the cuff model, the decrease was less marked, but there was no recovery. *$p < 0.05$, **$p < 0.01$, ***$p < 0.001$; n = 8-10; mean + SEM; comparisons made against sham operated controls.

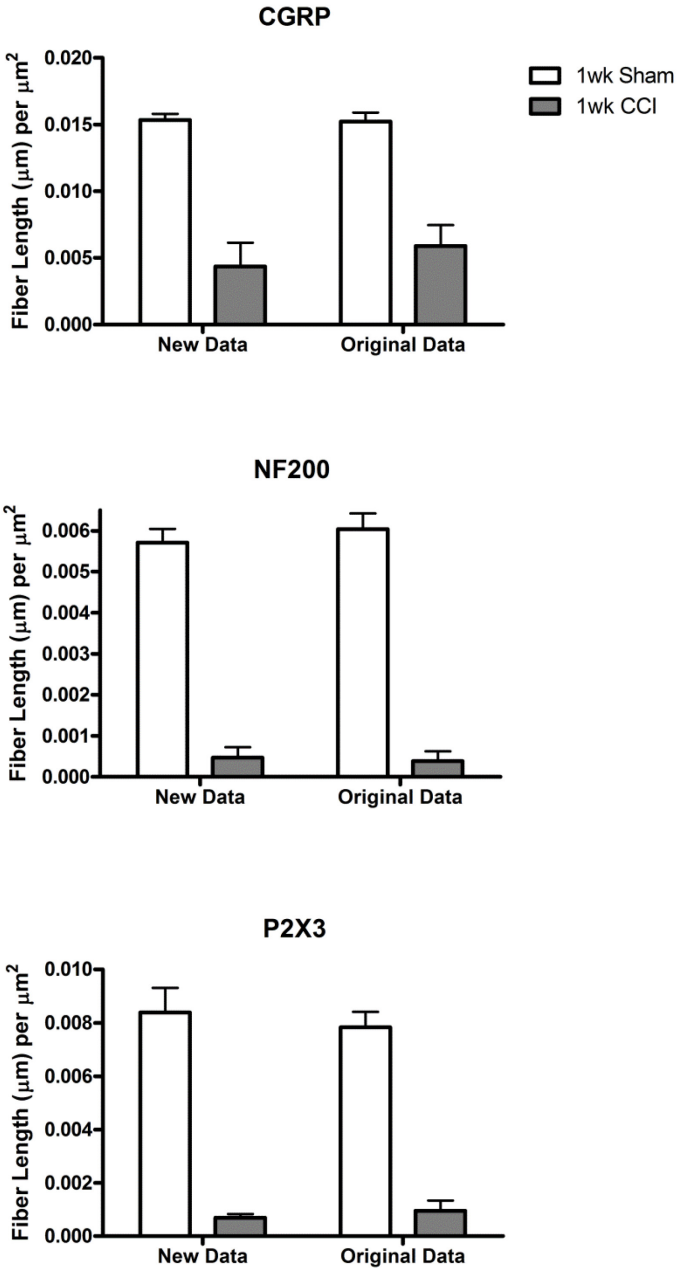

Figure 14: Comparison between previously obtained fibre density data and newly acquired fibre density data from CCI and sham animals at the 1 week time point. Values of fiber density from our previously publication (Peleshok and Ribeiro-da-Silva, 2011), shown in Figures 7, 10 and 13 (original data) were compared to values from a new group of animals (new data) to ascertain data reproducibility. Values were very similar and no significant differences were observed.

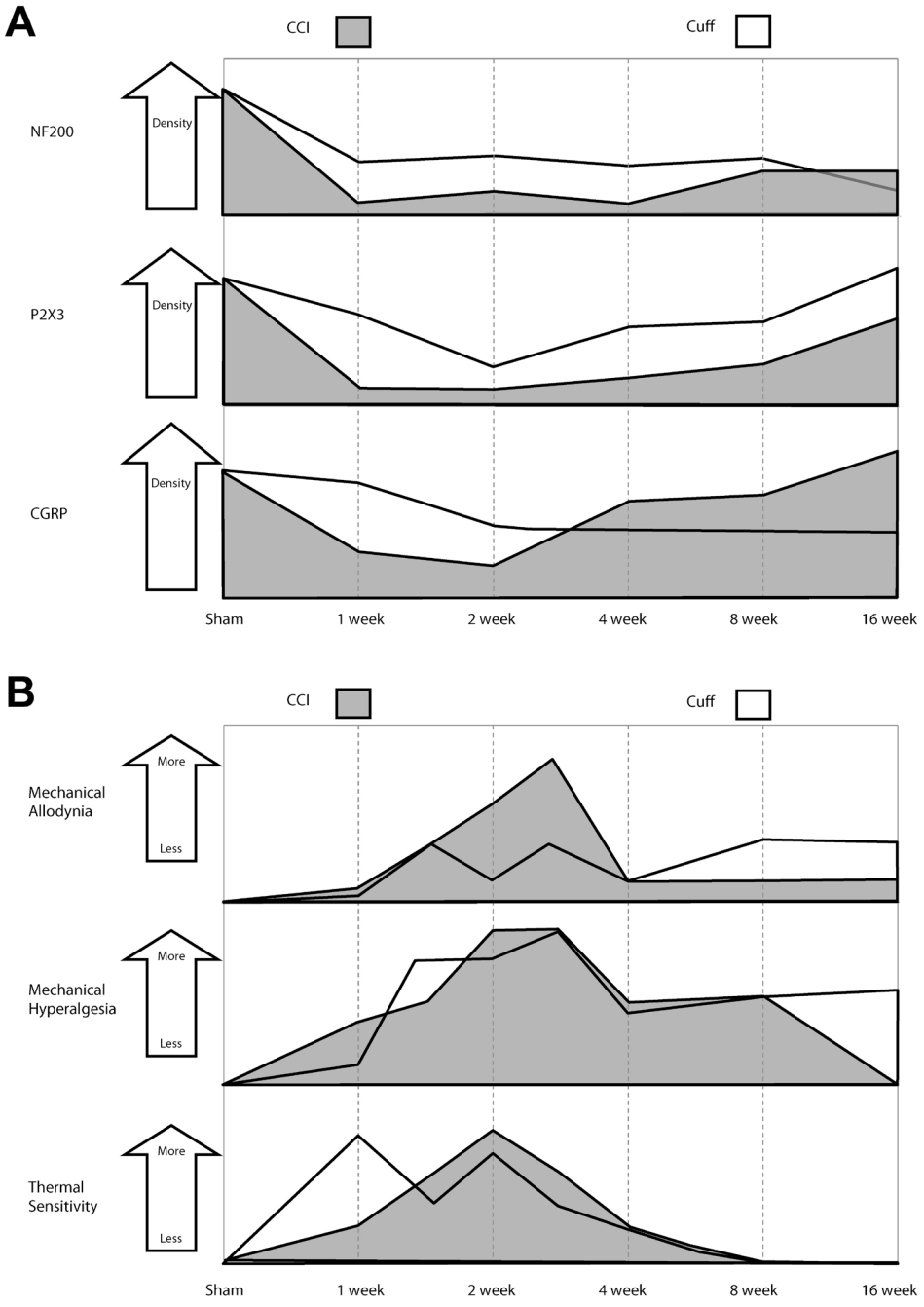

Figure 15: Graphical representation comparing changes over time in the fibre populations in the dermis (A) and in the pain-related behaviour (B), in the CCI and cuff models.

3.5. Discussion

The objective of the present study was to ascertain the differences and similarities underlying the two widely used chronic constriction injury models of the sciatic nerve, the classical CCI and the polyethylene cuff model. The principal findings were that 1) there were differences in duration of mechanical hypersensitivities between the two models whereas thermal sensitivity was comparable; 2) there was considerably less loss of non-peptidergic fibers in the cuff than in the CCI model with a late recovery; 3) there was a dramatic initial loss of peptidergic afferents followed by recovery above sham levels in the CCI model, compared with a less marked static loss in the cuff model; 4) there was an initial dramatic loss of myelinated afferents followed by a late partial recovery in the CCI model, compared with a less marked loss with no recovery in the cuff; and 5) there was a comparable drastic loss of epidermal innervation in both models. One possible criticism of this type of study is that we are using antibodies which recognize markers of fiber populations which can vary in expression with the lesions and become undetectable, although the fibers themselves persist. This issue has been addressed in a previous publication in which a double staining using CGRP as a marker for peptidergic afferents and PGP-9.5 as a pan-neuronal marker was conducted (Peleshok and Ribeiro-da-Silva, 2011). In that study, we demonstrated that 4 weeks after application of the classical CCI nerve injury, a time point in which only peptidergic afferents remained in the upper dermis, a drastic decrease in immunoreactivity for the pan-neuronal marker PGP-9.5 was observed. The remaining PGP-9.5-IR fibers co-localized CGRP immunoreactivity meaning that after nerve lesion the general loss in immunoreactivity could reasonably be attributed to fiber loss rather than a loss in phenotypic markers.

Pain-related behavior

The most significant difference between the two animal models was the persistence of mechanical hyperalgesia and allodynia to 16 weeks following application of the cuff model. A comparable persistence of mechanical hypersensitivity in the cuff model has been previously reported (Keller et al.,

2007; Pitcher and Henry, 2004; Pitcher et al., 1999). Indeed, in the CCI model, mechanical allodynia (as determined by the 4 g von Frey filament) resolved by 6 weeks (Figure 2 and 15) and mechanical hyperalgesia (as determined by 15 g von Frey filament) resolved by 16 weeks (Figure 3 and 15). This resolution of mechanical hypersensitivity sensitivity following application of the CCI has been previously reported in the literature (Kim et al., 1997; Munglani et al., 1995). In contrast, there were no dramatic differences in heat responses between the cuff and CCI-lesioned rats involving onset and resolution. These behavior differences, alongside the morphological differences that we were able to detect following application of the cuff and classical CCI models, may be the result of a basic difference between the two models, that the constriction is permanent in the cuff model, as the cuff is never removed, whereas the chromic gut is re-absorbed over time, although scar tissue remains, meaning that the constriction is never totally eliminated over time (Bennett and Xie, 1988). Therefore, the persistence of the constriction in the cuff model, which may be exacerbated by the continuous growth of the male rats, and the permanent irritation of the nerve may explain the absence of recovery of innervation by the peptidergic afferents and the persistence of the mechanical hyperalgesia and allodynia in this model (Keller et al., 2007; Pitcher and Henry, 2004; Pitcher et al., 1999). Previous reports indicate that following application of a non-re-absorbable polypropylene ligation of the sciatic nerve of rats, a significant alteration in the walking pattern was observed which persisted through 16 weeks post-injury in contrast to the resolution of this impairment following application of re-absorbable chromic gut ligatures (Kupers et al., 1992). Following application of the cuff, a sustained mechanical sensitivity was concomitant with microglial activation in which monocyte chemoattractant protein-1 (MCP-1) released from damaged neurons activated spinal microglia (Zhang and De Koninck, 2006). The above support the hypothesis that the classical CCI and the polyethylene cuff are two very different models of neuropathic pain, and that the mechanisms underlying them are not the same. One important issue is the differing degrees to which the myelinated afferents regress from the dermis. A prominent view regarding mechanical allodynia is that it is the

result of activity from Aβ-fibers that normally do not convey nociception (Campbell et al., 1988; Sandkuhler, 2009; Woolf and Doubell, 1994). However, it has also been suggested that a primary component in stimulus-evoked mechanical allodynia is decreasing activation thresholds of high-threshold mechanoreceptors on C-fibers (Song et al., 2003; Sandkuhler, 2009). This latter view gains support in light of our current and past work (Peleshok and Ribeiro-da-Silva, 2011), where the observation of an almost complete ablation of myelinated afferents was made at the time of mechanical allodynia onset using the CCI model (Figure 15). However, if this clearly indicates that we can have mechanical allodynia without A-fiber stimulation, it does not rule out a participation of A-fibers in it. Indeed, in the cuff model some A-fibers persisted at all time points (Figure 15). Of the two models, the classical CCI model is one in which a transient inflammatory response in conjunction with the dramatic loss of A-fibers suggests that the sensitization of C-fibers to normally innocuous mechanical stimuli would be the principle mechanism of action (Heumann et al., 1987b; Lindholm et al., 1987). The polyethylene cuff model is a more permanent one and the resulting inflammation may be less, concomitant with less myelinated fiber loss, likely accompanied by a moderate and persistent increase in target tissue cytokines and trophic factors which would help in sensitization of the remaining functional sensory afferents (Zhang and De Koninck, 2006). Using a cuff model of neuropathic pain, a significant decrease in threshold to generate action potentials has been shown for both C-fibers and A-fibers accompanied by an increase in Nav1.8 within the peripheral terminals of these fibers (Thakor et al., 2009). An increase in the expression of Nav1.8 within the uninjured C-fibers has also been suggested to contribute to the genesis of neuropathic pain in the CCI model, based on experimental evidence (Dong et al., 2007).

Epidermal Innervation

Skin biopsies from patients afflicted with neuropathic pain reveal a significant decrease in epidermal fiber innervation (Oaklander and Siegel, 2005). We have similarly demonstrated that in both the cuff and chromic gut CCI there is

also a significant and sustained loss of epidermal innervation. An adequate explanation as to the significance of this is lacking at this time.

Conclusions

In summary, we demonstrate that very similar models of neuropathic pain, both based on a mild constriction applied to the sciatic nerve, result in very different behavioral and morphological profiles. These data underlie the importance of not generalizing data obtained with a specific neuropathic pain model to other models, even if similar.

Connecting Paragraph – Chapter 3 to Chapter 4

From the previous two chapters, we can infer that innervation patterns within the skin could depend on relative changes in target tissue derived trophic factors. One such key trophic factor is nerve growth factor (NGF). It has been hypothesized that cellular targets within the periphery express NGF and a chemoattractant gradient forms by its association with p75 on the surface of Schwann cells. As a result of the recent availability of appropriate antibodies to be used for immunohistochemistry, we sought to describe the distribution of the precursor form of NGF, proNGF. We chose to use the epidermis and upper dermis as the tissue in which to study the distribution of proNGF given that it is this region where the innervation changes of both peptidergic sensory afferents and sympathetic efferents have been described. It is also this tissue which contains a variety of non-neuronal cells types that produce NGF. We chose to use the glabrous skin from both sham operated and CCI adult rats from one week to four weeks post-injury since the results from the previous chapters indicate that the peak changes in peptidergic afferent and sympathetic efferent innervation occurs at and prior to four weeks. We hypothesize that changes in the precursor form of NGF, proNGF, which exists in much higher levels than the mature form in cells, should be detectable. Alterations in its expression after injury should also be detectable, given that it is increased endogenous levels of NGF which are supposed to drive sprouting of peptidergic afferents and sympathetic fibres.

Chapter Four

Neurotrophic factor changes in the rat thick skin following chronic constriction injury of the sciatic nerve

Jennifer C. Peleshok and Alfredo Ribeiro-da-Silva

(Molecular Pain, under revision)

4.1. Abstract:

Cutaneous peripheral neuropathies have been associated with changes of the sensory fiber innervation in the dermis and epidermis. These changes are mediated in part by the increase in local expression of trophic factors. Increase in target tissue nerve growth factor in particular has been implicated in the promotion of peptidergic afferent and sympathetic efferent sprouting following nerve injury. The primary source of nerve growth factor has been cells found within the target tissue, namely the skin. Recent evidence regarding the release and extracellular maturation of nerve growth factor indicate that it is produced in its precursor form, released in an activity-dependant fashion and matured in the extracellular space. It is our hypothesis that the precursor form of nerve growth factor should be detectable in those cell types producing it and limitations in available immunohistochemical tools has restricted efforts in obtaining an accurate distribution of nerve growth factor in naïve as well as from skin from animal models of neuropathic pain. It is the objective of this study to delineate the distribution of the precursor form of nerve growth factor to those cell types expressing it, as well as describe its distribution with respect to those nerve fibers responsive to it. We observed a decrease in peptidergic fiber innervation at 1 week post-lesion followed by a recovery, correlating with protein levels of TrkA. ProNGF expression in animals having received the application of four loosely constrictive chromic gut ligatures placed around the common sciatic nerve, namely the chronic constriction injury (CCI) was significantly higher than in sham-operated controls from 1-4 weeks post-CCI. We also studied the distribution of proNGF immunoreactivity in sham and CCI-operated animals in the epidermis and dermis and found its expression to be increased in mast cells 1 week post-CCI and at later time points, in keratinocytes. P75 expression within the dermis and epidermis was significantly higher in CCI-operated animals than in controls and these changes were localized to neuronal and non-neuronal cell populations using specific markers for each. We describe proNGF expression by non-neuronal cells over time after nerve injury as well as the association of NGF-responsive fibers to proNGF-expressing target tissues. ProNGF expression

increases following nerve injury in those cell types previously suggested to express it.

4.2. Introduction:

Nerve growth factor (NGF) is a 13kDa neurotrophin (Holland et al., 1994). Its roles within the peripheral nervous system include the maintenance of the adult sensory afferents and sympathetic post-ganglionic efferents (Goedert et al., 1984; Goedert et al., 1981). During embryonic development, its expression is essential for the normal development and maturation of the sympathetic nervous system (Levi-Montalcini and Angeletti, 1963). Mice engineered to over-express NGF in keratinocytes were associated with increased peptidergic fiber density as well as inappropriate innervation by sympathetic efferents (Albers et al., 1994; Davis et al., 1997; Ma et al., 1995; Ribeiro-da-Silva et al., 2000). These mice were also shown to have heightened sensitivity to applied heat and mechanical stimuli (Davis et al., 1993). We have previously demonstrated that, following nerve injury, there was an increase in sympathetic and peptidergic innervation in skin, comparable to that occurring following the overexpression of NGF (Grelik et al., 2005a; Grelik et al., 2005b; Peleshok and Ribeiro-da-Silva, 2011; Ruocco et al., 2000; Yen et al., 2006). We have previously demonstrated that an increase in sympathetic and peptidergic innervation occurs following application of nerve injury models (Grelik et al., 2005a; Grelik et al., 2005b; Yen et al., 2006). These observed changes in NGF-responsive sympathetic and sensory fibers have been proposed to be mediated through the cell-surface NGF receptors, the high affinity receptor TrkA and the low-affinity pan-neurotrophin receptor p75 (Lumsden and Davies, 1983). In agreement with this, TrkA and, to a lesser extent, p75 were detected in both post-ganglionic sympathetic efferents and peptidergic sensory afferents (Verge et al., 1989a; Verge et al., 1989b). However, p75 was mainly expressed on Schwann cells, a cell type which is in direct contact with the nerve fibers (Ribeiro-da-Silva et al., 1991). Dimeric NGF binds its cognate receptor, TrkA and upon complex formation with p75, TrkA undergoes a conformational change enhancing its binding affinity for NGF (Barker, 2007; Chao, 2003; Reichardt, 2006; Wehrman et al., 2007). The half-life of NGF binding to p75 is

very rapid such that dissociation times have been estimated at < 3sec (Nicol and Vasko, 2007; Sutter et al., 1979; Wehrman et al., 2007). NGF is synthesized by a variety of peripheral cell types including mast cells, lymphocytes, keratinocytes and vascular endothelium in its precursor form proNGF (Aloe and Levi-Montalcini, 1977; English et al., 1994; Heumann et al., 1987a; Heumann et al., 1987b; Leon et al., 1994; Spitsbergen et al., 1995). The receptor p75 has a high affinity for proNGF, unlike its mature form (mNGF), and when ligand bound engages pro-apoptotic signaling cascades (Feng et al., 2010; Masoudi et al., 2009). Keratinocytes have been demonstrated to express a number of ligand-gated ion channels and that upon ligand binding, can cause membrane depolarization and release of a variety of factors including proNGF and ATP (Inoue et al., 2002; Kiss et al., 2010; Zhao et al., 2008). Within the extracellular space, proNGF is converted to its mature form, mNGF, through a protease cascade (Bruno and Cuello, 2006). The enzymes involved in this cascade include plasminogen, which is converted to its active form, plasmin, by either tPa or uPa. Plasmin in turn converts proNGF into its mature form, mNGF, and also converts proMMP-9 to its mature form, MMP-9, which in turn degrades mNGF (Bruno and Cuello, 2006; Lee et al., 2001). Previous literature describing the distribution of NGF in the periphery has been restricted to studies following injury, a point in which NGF is detectable within responsive nerve fibers (Wu et al., 2007) if we exclude an early study examining the distribution of NGF in keratinocytes (English et al., 1994). A clear differentiation between proNGF and mNGF could not be made in the above mentioned examples since the antibody used cannot differentiate the mature from the precursor form. Following nerve injury, Wallerian degeneration is triggered, a process necessary for those axons directly affected by the ligature and experiencing demyelination to be successfully cleared of myelin debris by recruited macrophages as well as for subsequent sprouting of uninjured axons (Ramer et al., 1997). During the process of Wallerian degeneration, macrophages and mast cells are recruited to the site of injury (Scholz and Woolf, 2007) where their phagocytic capabilities assist in clearing myelin debris (Scholz and Woolf, 2007). Activation of local Schwann cells is

followed by increased production of Il-1β and TNF-α, both of which increase transcription and translation of NGF within local cell types (Bergsteinsdottir et al., 1991; Hattori et al., 1993; Heumann et al., 1987b; Lindholm et al., 1987). This increase in peripheral Il-1β and TNF-α takes on additional significance when it is considered that they can lead to increases in proMMP-9 protein levels as well as its conversion to the mature form within skin; it has also been shown that cell surface plasmin levels were also increased following the increase in Il-1β and TNF-α (Bechtel et al., 1996; Han et al., 2005; Zhou et al., 2009). It has long been known which cell types are responsible for the production of NGF; however these studies have employed indirect methods such as culturing, *in situ* hybridization or over-expression systems (Bandtlow et al., 1987; Heumann et al., 1987a; Heumann et al., 1984; Scholz and Woolf, 2007).

NGF has been strongly implicated in both neuropathic and inflammatory pain conditions (Pezet et al., 2008; Pezet and McMahon, 2006; Pezet et al., 2001; Ro et al., 1999; Ugolini et al., 2007). It has been shown that following activation of Schwann cells as part of the Wallerian degeneration response, Schwann cells dramatically upregulate p75 on their cell surface (Ribeiro-da-Silva et al., 1991; Taniuchi et al., 1986; Taniuchi et al., 1988). The exact role of this upregulation has not been clearly defined, although it has been proposed that p75 in this case acts as a sequestering molecule to keep the increased NGF on the cell surface, to facilitate its function as a chemo attractant molecule for regenerating peptidergic afferents (Ramer and Bisby, 1997b; Taniuchi et al., 1988).

The increase in available NGF associated with both neuropathic and inflammatory pain has been well documented (Hefti et al., 2006; Herzberg et al., 1997; Hoheisel et al., 2007; Scholz and Woolf, 2007; Ugolini et al., 2007). Mice engineered to over-express NGF in keratinocytes not only develop hyperinnervation in the target tissue region by peptidergic afferents and sympathetic efferents but also display sympathetic basket formation around populations of dorsal root ganglia neurons (Albers et al., 1994; Ramer et al., 1998a).

Our lab has consistently demonstrated that following nerve injury there is a dramatic initial loss of myelinated and unmyelinated sensory afferents (Grelik et al., 2005a; Grelik et al., 2005b; Peleshok and Ribeiro-da-Silva, 2011; Yen et al., 2006). Four weeks following application of the chromic gut-based chronic constriction nerve injury, there was a return to sham operated control of peptidergic afferents followed by the development of a significant increase in peptidergic fiber density at later stages. We also detected a sprouting of sympathetic efferents into the upper dermis, a territory from which they are normally devoid, and which not only innervated areas of the dermis away from blood vessels but associated very closely with peptidergic afferents (Yen et al., 2006).

We undertook the current study to test the hypothesis that, following nerve injury, the innervation changes of peptidergic afferents and sympathetic efferents follow a change in expression of proNGF in the periphery and that this is closely associated with Schwann cell production of proNGF.

4.3. Materials and Methods:

In total, 60 male Sprague-Dawley rats (Charles River Canada), weighing between 150-175g, were used for this study. All animals were maintained on a 12 hour light/dark cycle and allowed access to food and water *ad libitum*. All animal protocols were approved by the McGill University Animal Care Committee and followed the guidelines of the Canadian Council on Animal Care and the International Association for the Study of Pain.

Peripheral Nerve Lesions

Animals were randomly assigned to receive either a traditional chronic constriction injury (CCI) or sham operation. All animals were deeply anaesthetized with isoflurane. In total, 30 rats received the sham operation and 30 received the CCI injury to the common sciatic nerve, as described in detail by Bennett & Xie (Bennett and Xie, 1988). Briefly, the left common sciatic nerve was exposed at the mid-thigh through the biceps femoris. All surrounding fascia was removed to allow free passage to blunt glass probes. Proximal to the

trifurcation of the sciatic nerve, four ligatures (4-0 chromic gut, Ethicon) were tied loosely around the nerve with ~1 mm spacing in between. The incision was closed in layers using absorbable sutures (Vicryl, Ethicon). The animals assigned to sham-operated groups underwent the above mentioned procedures with the exception of the application of the chromic gut ligatures.

Animal Perfusion and Histological or Western Blot Processing

Animals were sacrificed after periods of 1, 2, and 4 weeks post-surgery. Rats were administered Equithesin (6.5mg chloral hydrate and 3mg sodium pentobarbital) in a volume of 0.3mL, i.p., per 100g body weight. 3 animals per time point were perfused for immunohistochemical analysis. Once animals were deeply anesthetized, they were quickly transcardially perfused with vascular rinse (0.1% w/v sodium nitrite in a phosphate buffer) followed by histological fixatives (3% paraformaldehyde, 15% saturated picric acid in 0.1M phosphate buffer pH 7.4) for 30 minutes. The glabrous skin from the left hind paw, specifically the thin skin surrounded by tori, was removed, post-fixed for 1 hour in the same fixative used for the perfusion and placed in 30% sucrose in 0.1M phosphate buffer for cryoprotection overnight at 4^{o}C. Tissue was then embedded in an optimum cutting temperature medium (OCT, TissueTek), cut using a cryostat (Leica) at a thickness of 50µm and processed as free floating sections. A second cohort of 6 animals per time point were perfused for 30 seconds with ice cold saline to clear contaminating blood. The same region of glabrous skin as that used for immunohistochemistry was excised from the rat hind paw, snap frozen in liquid nitrogen and stored at -20^{o}C for no more than 10 days until processed for Western blot analysis.

Immunohistochemistry

Sections were washed in PBS for 30 minutes. In all subsequent steps, phosphate buffered saline (PBS) with 0.2% Triton X-100 (PBS-T) was used to dilute the immunoreagents and for washing. Sections were treated with 50% ethanol for 30 minutes followed by 1 hour incubation in PBS-T containing 10% (v/v) normal serum of the species used to generate the secondary antibody to

reduce non-specific staining. Subsequently, sections were incubated with primary antibodies (diluted in PBS-T) at 4^{o}C overnight (or 48 hours in the case of S100). The following primary antibodies were used: polyclonal guinea-pig anti-human calcitonin gene related peptide (CGRP; 1:4000, Bachem; Torrance CA), monoclonal mouse anti-dopamine β-hydroxylase (DBH; 1:5 MediMabs, gift of Dr. A. Claudio Cuello), polyclonal rabbit anti-proNGF (1:500, Alomone Labs, Israel), monoclonal mouse anti-p75 (MC192; 1:5, Medicorp), polyclonal rabbit anti-S100β (1:1000; Swant Switzerland) and polyclonal rabbit anti-PGP 9.5 antibody (1:800, Cedarlane; Burlington Ont.). To test for antibody specificity of anti-proNGF by immunohistochemistry, the control antigen was preincubated with the control antigen supplied by Alomone (3μg of control peptide to 0.8μg of antibody) for 3hrs over ice prior to incubation with naïve control tissue. After washing, the sections were incubated with secondary antibody diluted in PBS-T for two hours at room temperature. The following secondary antibodies were used: a) for those antibodies raised in mouse, a highly cross-adsorbed goat anti-mouse IgG conjugated to Alexa 596 (1:800, Molecular Probes, Eugene, OR); b) for those raised in rabbit or guinea-pig, a goat anti-rabbit conjugated to Alexa 488 (1:800, Molecular Probes, Eugene, OR). Sections were washed and mounted on gelatin-coated slides and coverslipped using Aquapolymount (Polysciences; Warrington, PA). In the case of bright field images using anti-proNGF antibodies, sections were prepared as described above except for a 10 min incubation with 0.1% H_2O_2 prior to blocking and following incubation with primary antibody, incubated for 2 hours in a biotinylated rabbit anti-goat secondary antibody (1:200, Vector). The sections were washed with PBS and incubated for 1 hour with the A and B reagents (4 μl of A + 4 μl of B per mL of PBS, ABC Vectastain Elite kit). The sections were then washed in PBS and incubated for 5 minutes in a solution of 3-3'-diaminobenzidine (Sigma, 5 mg for 10 ml of PBS-T). Hydrogen peroxide was then added to the solution to reach a final concentration of 0.01%. The reaction was terminated after 10 minutes by the addition of PBS. The sections were washed in PBS, mounted on gelatin-subbed slides and air dried. Slides were rehydrated and briefly exposed to a 1% solution

of toluidine blue, rinsed and dehydrated in ascending alcohols and xylene, then coverslipped with Entellan (EMD, Gibbstown, NJ).

Primary Antibody Characterization

CGRP: The anti-CGRP antibody raised in guinea pig was purchased from Bachem (T-5027, lot A00098-2). It was generated against a synthetic peptide from human α-CGRP with the following sequence: H-Ala-Cys-Asp-Thr-Ala-Thr-Cys-Val-Thr-His-Arg-Leu-Ala-Gly-Leu-Leu-Ser-Arg-Ser-Gly-Gly-Val-Val-Lys-Asn-Asn-Phe-Val-Pro-Thr-Asn-Val-Gly-Ser-Lys-Al a-Phe-NH2. The antibody has 100% reactivity with human and rat α-CGRP, human CGRP (8-37), chicken CGRP, and human β-CGRP. It has 0.04% crossreactivity with human amylin and 0% crossreactivity with rat amylin and with human and salmon calcitonin as determined by radioimmunoassay (manufacturer's technical information). Although Western blot information was not available, the immunostaining has been localized in the skin to IB4 negative C-fibers, and fibers innervating blood vessels in rats (Fundin et al., 1997; Rice et al., 1997) and in monkeys (Paré et al., 2007).

DBH: The anti-dopamine β-hydroxylase monoclonal antibody was received as a gift from MediMabs (clone DBH 41; gift from Dr. Claudio Cuello). It was generated against rat purified DBH. The specificity was tested by Western blot, ELISA and immunocytochemistry and it was found that does not cross-react with mouse, human, rabbit, bovine, guinea pig or cat tissues (Mazzoni et al., 1991).

S100β: A rabbit polyclonal antibody purchased from Swant (Code Number 37A). It was generated against purified bovine brain S100β and shows <0.5% cross-reactivity with S100α and reacts with S100β from all species (ie bovine, rat, chicken and human) (data obtained from product insert). This antibody has been used as a marker for Schwann cells (Yu et al., 2009).

P75: The monoclonal antibody against the low-affinity neurotrophin receptor (MC192, Medicorp; Montreal, Qc) was generated from solubilized rat PC12 cell membranes and was found to be selective towards rat p75 to the exclusion of gerbil, hamster, guinea pig or mouse p75 (Taniuchi and Johnson, 1985). Its

distribution in rat skin was described at both light microscopic and electron microscopic levels (Ribeiro-da-Silva et al., 1991)
TrkA: Monoclonal anti-Trka (R&D Systems MAB1056 Clone: 315104 Lot #WPO0108021) raised against recombinant rat TrkA extracellular domain (a.a. 33-418). This antibody recognized rrTrkA by ELISA and Western Blot with no cross-reactivity towards recombinant human TrkA, TrkB, TrkC, recombinant mouse TrkB and TrkC (product insert).

PGP 9.5: The rabbit anti-PGP 9.5 antibody (Ultraclone code RA95101) was generated by repeated injection of purified whole human PGP 9.5 in Freund's adjuvant into rabbits. The antibody crossreacts with PGP 9.5 protein in all mammalian species (manufacturer's technical information). By Western blot it recognizes a band at 38 kDa from human and rat skin, and preadsorption with purified PGP 9.5 completely abolished this recognition (Doran et al., 1983; Thompson et al., 1983). Immunohistochemical staining with this antibody in either rat or human skin was absent following preadsorption with purified human PGP 9.5 protein (Doran et al., 1983; Thompson et al., 1983).

proNGF: The rabbit anti-proNGF antibody (Alomone #ANT-005 Lot#AN-03) was generated by injection of a synthetic peptide corresponding to a.a. 84-104 of the precursor form of rat NGF. It cross-reacts with rat, mouse and human proNGF (product insert).

Western Blot
Samples were kept at -20^{o}C until manually homogenized with liquid nitrogen and added to RIPA buffer (1% NP-40, 1% sodium deoxycholate, 0.1% sodium dodecyl sulfate, 150 mM NaCl, 25 mL Tris–HCl, pH 7.6) containing protease inhibitors (Complete, Roche Molecular Biochemicals, Indianapolis, IN). Samples were agitated overnight at 4^{o}C, followed by 45 minute centrifugation at 13,200rpm to separate supernatant. The supernatant was pipetted and protein quantified using Bio-Rad DC Protein Assay (Bio-Rad, Mississauga Ont). Samples were then prepared as either reduced (in the case of TrkA and proNGF)

or not (in the case of p75) using 10% β-mercaptoethanol (Bio-Rad, Mississauga Ont) SDS-based protein loading buffer. Samples were then boiled for 5min prior to loading in a 4% stacking and 12% separating acrylamide gel for SDS-PAGE at 100V. Samples were transferred to nitrocellulose membranes for 90 minutes at 110mA and blocked for 1 hour. Primary antibodies such as mouse anti-TrkA (1:500, MAB1056, R&D Systems, Minneapolis, MN), rabbit anti-proNGF (1:500, ANT-005, Alomone Labs, Isreal), or mouse anti-p75 (1:200, MC192, Medicorp Inc., Montreal, Qc) were incubated overnight in blocking buffer at 4^{o}C. The following day, membranes were washed with tris-buffered saline with 0.1% Tween-20 (TBS-T) and incubated for 2 hours at room temperature with secondary antibodies raised against either mouse (Product no.: 715-035-151) or rabbit (Product no.: 711-035-152) IgG, conjugated to horseradish peroxidase (1:5000, Jackson ImmunoResearch, West Grove PA), and incubated for 1 minute with ECL substrate (Western Lighting, Perkin Elmer, Montreal, Qc). Following x-ray film exposure, membranes were incubated for 1 hour with stripping buffer, blocked and incubated with mouse anti β-actin primary antibody (1:400, A5441, Sigma) in blocking buffer for 1 hour washed with TBS-T and incubated with anti-mouse IgG-HRP (1:5000). Immunoreactive bands were quantified by simultaneously obtaining equally sized bands and quantification was based on optical density and normalized against the loading control (β-actin) using MCID Image Analysis software (MCID4 Image Analysis System; Imaging Research Inc.; St Catherine's ON, Canada).

Images for the Figures

Pictures for the figures of this publication were taken as Z-stacks of confocal optical sections using a Zeiss LSM 510 confocal microscope equipped with argon and helium neon lasers applying a 40X water-immersion objective. Images were originally saved in the Zeiss format, then exported directly into the TIFF format and adjusted for brightness and contrast only, using Adobe Photoshop CS4. Bright field images were taken using a Zeiss Axioplan 2 imaging microscope equipped with a 40× Plan-Fluotar oil-immersion objective. Images were acquired with a high-resolution color digital camera using the Zeiss AxioVision software.

Representative images of Western Blots were taken using an Epson scanner, saved as TIFF format and realigned using Adobe Photoshop CS4.

4.4. Results:

proNGF Distribution

To study the normal distribution of proNGF immunoreactivity, we used bright field microscopy (Fig. 1A). proNGF immunoreactivity was detected in well defined but sparse patches as a brown DAB precipitate in the epidermis and dermis. In the epidermis, proNGF immunoreactivity was restricted to small patches of labeled keratinocytes along the dermo-epidermal junction (Figure 1A; arrowhead). Mast cells were identified based on metachromatic staining of heparin in granules using toluidine blue. In sections from control animals, mast cells were not abundant in the upper dermis and were only faintly immunoreactive for proNGF (not shown). proNGF was also found in the endothelium of capillaries and venules, identified based on the flattened appearance of the cells outlining the vessel lumen, and in perivascular cells (Figure 1A). One week post-CCI, the mast cell number qualitatively increased in the upper dermis and these cells were proNGF immunoreactive (Figure 1B; arrows). Two weeks following nerve lesion, mast cell infiltration in the upper dermis decreased, however proNGF immunoreactivity increased in other non-neuronal structures, including the vascular endothelium, fibroblasts and, particularly, keratinocytes (Figure 1C). The results at 4 weeks post-lesion were similar to those at 2 weeks, although labeling of keratinocytes was much less (Figure 1D**).** Preincubation of antibody with control peptide abolished all specific staining (Figure 1E).

Western blots were done in order to more accurately quantify this change in expression levels of proNGF protein itself rather than indirectly through levels of intensity of bright-field images (Figure 1F). The sampled protein was taken from the same area of the glabrous skin in which immunohistochemistry was conducted. Care was taken during sample extraction and preparation to ensure no contaminating protein from cartilage or deep tissues such as striated muscle. Data from the Western blots demonstrate an increase in target tissue levels of proNGF

at one week post-injury, with a further increase at 2-4 weeks (Figure 1F). These results taken together indicate that the increase in proNGF at one week post-injury is predominantly from infiltrating mast cells whereas at two weeks post-injury this increase in target tissue levels of proNGF has switched to keratinocytes and blood vessels.

It has long been shown that p75 is expressed on the cell surface of Schwann cells and that this expression is upregulated following nerve injury (Ribeiro-da-Silva et al., 1991). To confirm and expand this observation, S100 was used as a marker for Schwann cells at the light microscopy level in a co-staining for p75 to show the distribution of the receptor on Schwann cells following nerve injury. In sham operated animals, S100 immunoreactivity was present with varying intensities depending on location (Figure 2A, in green). Thicker cutaneous nerves, further from the dermo-epidermal junction, were most intensely labeled, likely because they are rich in A-fibers surrounded by myelinating Schwann cells, in which S100 content is known to be high. We also observed some S100 immmunostaining, usually not very intense, along the dermo-epidermal junction which might represent non-myelinating Schwann cells associated with C-fibers, which are known to contain less S100 protein than myelinating Schwann cells (Gonzalez-Martinez et al., 2003). P75 receptor immunoreactivity (in red) in sham-operated controls was low and often surrounded S100-IR structures, likely representing immunostaining in perineurial cells; it was also occasionally seen within the S100-IR structures, possible representing p75 expression on sensory axons (Figure 2A). One week following nerve injury (Figure 2B), the relative intensity of p75 to S100 changed dramatically as p75 immunoreactivity was significantly more intense than that of S100, correlating with the significant increase in protein content (see Figure 6). At two to four weeks post injury (Figures 2C-D), S100 and p75 immunoreactivities were both intense and heavily colocalized. The co-localization of the two immunoreactivities occurred at all time points studied post-injury. A triple labeling showing p75, S100 and proNGF immunoreactivities (Figures 2E-F) in sham-operated and at 2 weeks post-injury allowed us to show

the distribution of each of these immunoreactive structures with respect to the other either before or after injury. It was found that in sham operated controls that p75 and S100 immunoreactivity are found within the same nerve fiber bundles, where the S100 was more intense than that of p75. However, after injury, proNGF immunoreactivity increased in vascular endothelial-like structures and keratinocytes, whereas strong p75 immunoreactivity was seen in Schwann cells. Importantly, however, a co-localization between p75 on Schwann cells and proNGF was not observed.

Changes in NGF-Responsive Fiber Innervation

Due to the known cell surface expression of the high-affinity TrkA receptor and of p75 on both post-ganglionic sympathetic efferents and sensory peptidergic afferents, we sought to determine what relationship existed between proNGF producing cell types and these fibers in sham operated controls and after nerve injury (Figure 3). We observed that the post-ganglionic sympathetic efferent population, as detected by DβH immunoreactivity, seemed to innervate proNGF-IR structures (Figure 3A). In sham operated controls, the DβH-IR fibers appeared to wrap around the proNGF-IR cells in the wall of presumptive blood vessels. At one and two weeks post-injury, the association of DβH-IR fibers with proNGF producing cells remained similar to sham (Figures 3B-C). However, at four weeks post-injury, a time point when our lab has previously reported a significant presence of sympathetic efferents in the upper dermis away from blood vessels (Grelik et al., 2005b; Yen et al., 2006), we observed that DβH-IR fibers still innervated proNGF producing structures; however, the sections of the fibers closer to the epidermis were not associated with proNGF (Figure 3D). In sham-operated animals, the peptidergic, CGRP-IR afferents were also seen to have segments close to proNGF producing structures, but the association of the two was not as obvious as for the sympathetic (Figure 3E). At one week post-injury, a time point at which CGRP-IR afferent loss was maximal; there was no association between the remaining CGRP-IR fibers and proNGF-IR structures (Figure 3F). At two weeks post-injury, however, there was an obvious association

between CGRP-IR fibers and proNGF producing cells (Figure 3G). Interestingly, at four weeks post-CCI, a time point at which peptidergic afferents returned to sham-operated levels (Peleshok and Ribeiro-da-Silva, 2011; Yen et al., 2006), the association was not as close as that observed at two weeks (Figure 3H).

P75 Association with Other Structures

We have also investigated the association of nerve fibers identified with the pan-neuronal marker, PGP-9.5, with p75 expression (Figure 4). In sham operated controls, PGP-9.5-IR nerve fibers were distributed throughout the epidermis and in the upper dermis and formed a dense plexus (Figure 4A). In the lower dermis, PGP9.5-IR fibers were found in small cutaneous nerves with a sheath of p75 immunoreactivity around them, likely representing staining of perineurial cells (Figure 4A). Interestingly, PGP9.5-IR fibers penetrating the epidermis were not associated with p75 immunoreactivity (Figure 4A). At 1 week post-nerve injury, there was scarce`````` PGP-9.5 immunoreactivity in the upper dermis, consistent with previous reports of a dramatic decrease in nerve fiber innervation at this time point (Peleshok and Ribeiro-da-Silva, 2011) (Figure 4B). However, p75 was strongly upregulated (Figure 4B) due to strong Schwann cell labeling (see Figure 2A). At later time points (Figures 4C-D), PGP9.5-IR fibers were progressively more abundant and were associated with p75 immunoreactivity. At one to four weeks post-injury, PGP-9.5-IR structures in the epidermis represented mostly Langerhans cells staining (Figures 4B-D), as nerve fibers were mostly depleted from the epidermis.

We also investigated the relationship of p75 with respect to proNGF immunoreactivity. We found that in the sham-operated controls (Figure 4E), proNGF-IR patches within the upper dermis loosely associated with p75-IR structures, however there was no colocalization as indicated by the absence of yellow color. At one week post-injury, the intensity of the p75 immunoreactivity greatly surpassed that of proNGF (Figure 4F), and at two and four weeks post injury, we were able to demonstrate sparse p75 immunoreactive fibers in the epidermis as well as in the upper dermis (Figures 4G-H).

Western Blot

The results of quantification of by Western blot of the relative increase in p75 expression following nerve injury are illustrated on Figure 5. Consistent with the immunohistochemical data, there was a very significant increase in p75 expression shortly after nerve injury which remained significant up to four weeks, with a maximum expression at 2 weeks post-lesion.

The quantification of the changes in TrkA expression within the glabrous skin of the rat hind paw was done using Western Blot (Figure 6). We observed that a significant decrease in TrkA protein content occurred at 1 and 2 weeks following nerve injury with a recovery at 4 weeks post-lesion. This is consistent with the observation that peptidergic afferents retract from the upper dermis and epidermis shortly after injury and recover by 4 weeks (Peleshok and Ribeiro-da-Silva, 2011; Yen et al., 2006).

`

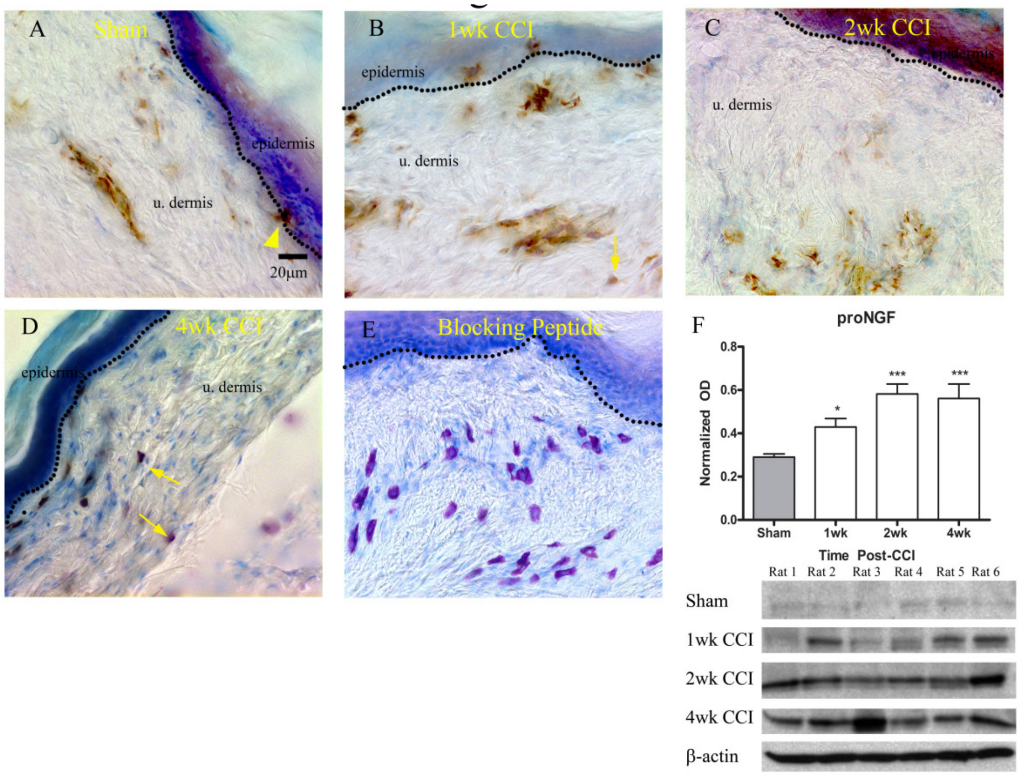

Figure 1 – Distribution of proNGF immunoreactivity in naïve glabrous skin and following application of CCI. A) In sham operated controls, proNGF (brown precipitate) was found in the upper dermis, particularly in wall of blood vessels, and in small patches of keratinocytes (arrowhead). B) One week post-injury proNGF was detected in mast cells (arrows), in blood vessels in the upper dermis as well as in keratinocytes. C) At 2 weeks post-injury, note the intense labelling of keratinocytes, the labelling of some unidentified structures in dermis and a lower number of mast cells identified based on toluidine blue counterstain. D) At 4 weeks post-injury, note mast cell labelling by toluidine blue counterstaining. E) Preincubation of antibody with control peptide abolished all specific staining. F) proNGF quantification was done by Western Blot analysis (n=6) from sham, and animals 1 – 4 week post-injury. OD was normalized against β-actin loading controls. ***$p<0.001$, **$p<0.01$, *$p<0.05$; mean + SEM; all comparisons made against sham operated controls

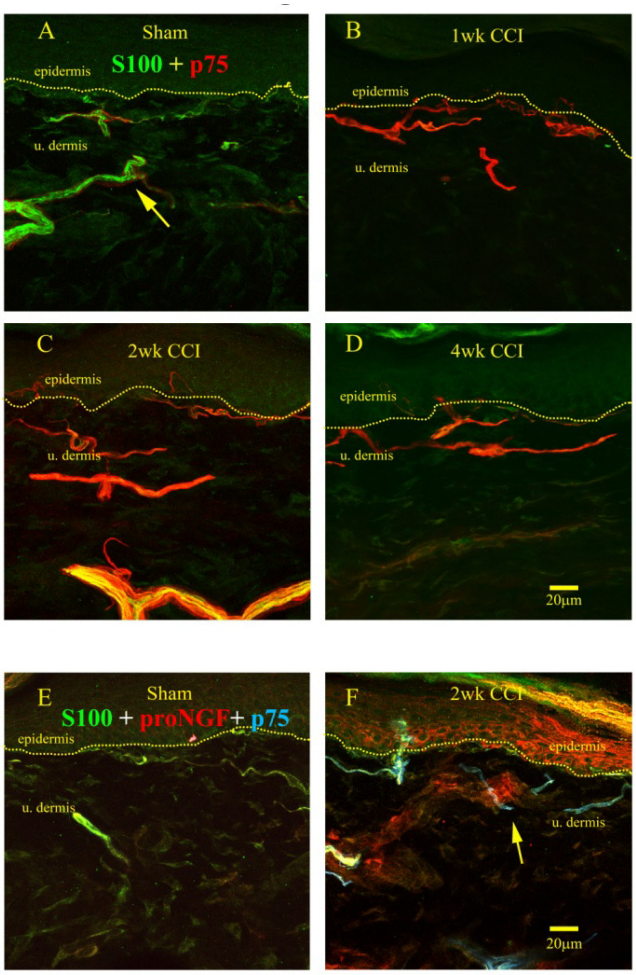

Figure 2: Changes in p75 expression on S100-IR Schwann cells. A) In sham-operated rats Schwann cells (green) were detected by means of S100 immunoreactivity in small nerves, with immunoreactivity of varying intensity from bright (arrow), lower in the dermis, to dim, along the dermo-epidermal junction. P75 immunoreactivity (red) was evident surrounding all S100-IR Schwann cells. B) One week following nerve injury, p75 immunostaining was dramatically upregulated in Schwann cells; the intense red colour masked the mixture of red and green stainings which could be detected by analysing separately the S100 and p75 stainings (not shown). C-D) Two and four weeks post-injury a decrease in p75 intensity was observed in that the yellow indicative of S100 co-labelling was able to be visualized. E) proNGF (red) S100 (green) and p75 (blue) triple labelling to demonstrate the relative distribution of Schwann cells with respect to proNGF; note a limited distribution of Schwann cells with proNGF and faint immunoreactivity for p75 in sham-operated controls. F) 2 weeks post-injury, the clear upregulation of p75 immunoreactivity associated with S100 (arrow) was observed, which wrapped around proNGF-IR blood vessels.

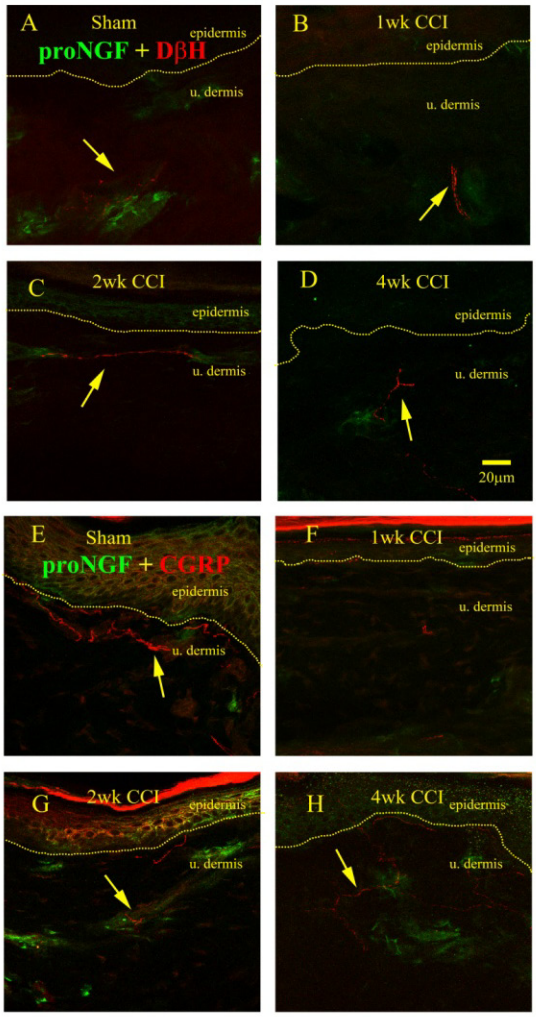

Figure 3: Sympathetic and peptidergic nerve fibre association with proNGF. A) DβH-IR sympathetic efferents (red) were closely associated with proNGF (green) in sham operated control animals. B-C) At 1 and 2 weeks post-injury, no detectable difference was observed in the pattern of sympathetic efferent distribution with respect to proNGF. D) At 4 weeks post-lesion sprouted sympathetic efferents retained their association with proNGF, and continued to sprout towards the dermo-epidermal junction. E) In sham-operated rats, peptidergic afferents were distributed along the dermo-epidermal junction in which the occasional proNGF group of immunoreactive cells was found. F) At 1 week following nerve injury, very few peptidergic afferents were observed. G) At 2 weeks post-injury, peptidergic afferents were found along the dermo-epidermal junction as well as along proNGF immunoreactive cells (arrow). H) At 4 weeks post-lesion, peptidergic afferents increased in numbers and were loosely associated with proNGF-IR cells (arrow).

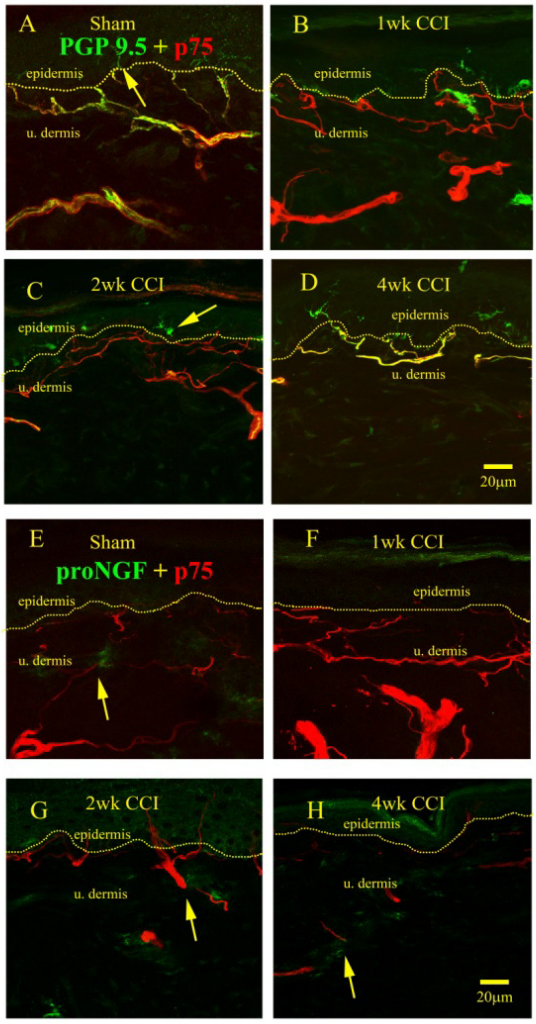

Figure 4: Distribution of p75 immunoreactivity following nerve injury and relationship to nerve fibres and proNGF. A) In sham-operated animals, p75 was distributed (red) around and with PGP 9.5-IR nerve fibres (green). p75 staining was found more clearly around large cutaneous PGP 9.5-IR nerve fibre bundles and smaller fibres along the dermo-epidermal junction. Where nerve fibres crossed the dermo-epidermal junction into the epidermis, the yellow color representing p75 associating with nerve fibres was lost (arrow). B) At 1 week post-injury, virtually all PGP-9.5-IR nerve fibres disappeared from the upper dermis and epidermis; immunostaining in p75-IR Schwann was very intense. C) At 2 weeks post-injury, a low number of PGP-9.5-IR fibres were detected and were associated with p75 Schwann cells (yellow), however most of the PGP-9.5-IR was restricted to Langerhans cells in epidermis (arrow) D) At 4 weeks post-injury, p75 immunoreactivity decreased co-incidentally with the increase in PGP-9.5 immunoreactivity in the upper dermis (yellow). E-H) proNGF and p75 association in sham-operated controls and in lesioned animals was loose in that most proNGF immunoreactivity was segregated from that for p75 and there was no obvious co-localization (arrows).

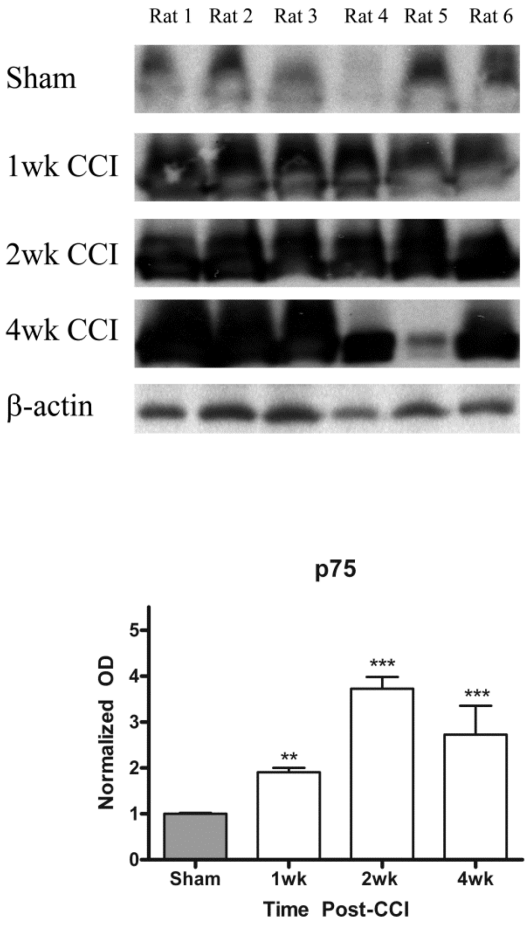

Figure 5 - Quantification of p75 protein content in glabrous skin. Glabrous skin was taken from same region sampled for immunocytochemistry. A single band corresponding to that of the PC12 supernatant used as positive control was observed. The increase in p75 protein was two-fold at 1 week post-injury. P75 levels increased to 4x of sham operated controls at 2 weeks post-injury and at 4 weeks decreased to 3x. OD was normalized against β-actin loading controls. N = 6; ***$p<0.001$, **$p<0.01$, *$p<0.05$; mean +SEM; comparisons made against sham operated control.

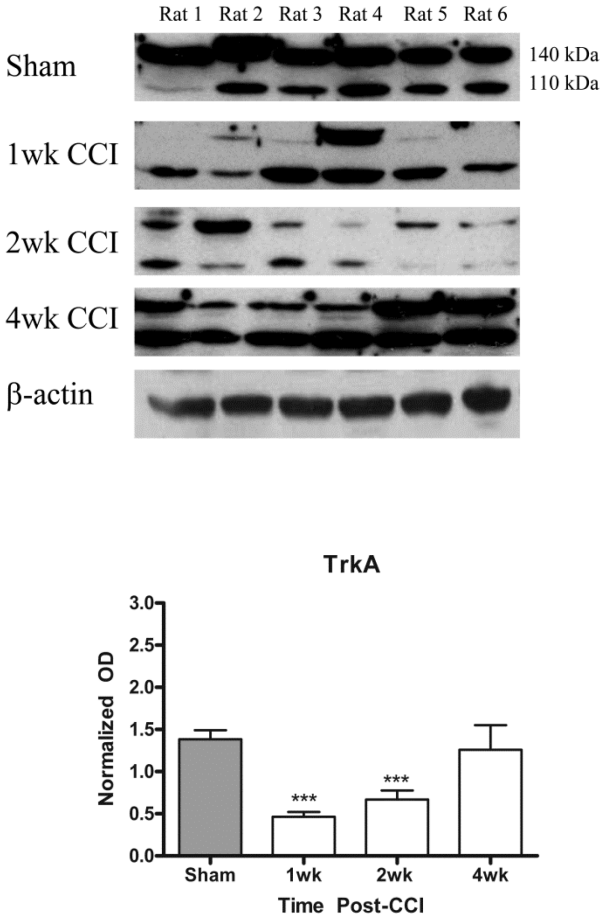

Figure 6 - Quantification of TrkA protein content in glabrous skin. TrkA protein was sampled from glabrous skin of same region used for immunocytochemistry. Two bands were recognized by the monoclonal anti-TrkA antibody, a 110kDa and 140kDa form corresponding to the immature, unglycosylated form and mature form respectively. TrkA levels decreased significantly at 1 week post-injury and remained significantly lower at 2 weeks post-injury until 4 weeks, at which point no difference was observed compared to sham-operated controls. OD is normalized against β-actin loading controls. ***$p<0.001$, **$p<0.01$, *$p<0.05$; mean + SEM; comparisons made against sham operated controls.

4.5. Discussion:

In this study, we performed for the first time a detailed description of the relationship of the NGF-responsive nerve fiber populations to the neurotrophin-producing cells following the application of a commonly used neuropathic pain model, the CCI of the sciatic nerve. Because NGF is known to occur in cells in its precursor form (Bruno and Cuello, 2006), proNGF, we used antibodies specific for this precursor form.

Previous research has focused on the changes in mature NGF uptake following nerve injury given that mNGF is expressed at very low levels in target tissues in sham or naïve animals (Wu et al., 2007). Methods such as *in situ* hybridization have shown that the mRNA for NGF is transcribed in Schwann cells (Bandtlow et al., 1987; Heumann et al., 1987a) and fibroblasts (Mearow et al., 1993) and that the protein exists in mast cells (Leon et al., 1994) and keratinocytes (English et al., 1994). Cultured mast cells have also been demonstrated to upregulate NGF when presented with the cytokines IL-1β and TNF-α (Hattori et al., 1993; Lindholm et al., 1988; Lindholm et al., 1987), and when degranulated release NGF into the culture media (Leon et al., 1994). Schwann cell production of NGF has been demonstrated using culturing methods in which morphology of Schwann cells in explanted optic nerve has been shown to correlate with NGF expression (Bandtlow et al., 1987). A line of evidence that has pervaded research literature is that a chemoattractant gradient of NGF created by its retention through cell surface expressed low-affinity NGF receptors, p75 (Johnson et al., 1988; Taniuchi et al., 1988). However, due to the restrictions of the available methodology, this has not yet been directly proven.

In the current study we provide some important new evidence, namely that a significant expression of proNGF by Schwann cells, identified by S100 immunoreactivity, was not evident. We also show an association of proNGF-producing cell types with NGF-responsive sensory and sympathetic fibers. Consistent with a number of prior observations, we were able to confirm the observed upregulation of p75 on non-neuronal cell types, namely Schwann cells, following nerve injury (Heumann et al., 1987b; Ribeiro-da-Silva et al., 1991;

Zhou et al., 1996). This upregulation was significant from early time points. Also, we have been able to correlate an immunocytochemical decrease in peptidergic innervation in the dermis and epidermis (the territories we sampled by Western blotting) with TrkA protein levels. Unfortunately, because of limitations of the availability of a reliable, commercially available anti-TrkA antibody for immunocytochemistry applications, we could not study the detailed anatomical distribution of TrkA immunoreactivity. TrkA levels in the skin can change due to a number of reasons, namely by a decrease in the level of expression in the cells or by a migration of the TrkA-expressing cells to other territories. Previous work from our lab and others demonstrate a retraction or 'dying back' of peptidergic and non-peptidergic nociceptive primary afferents from the epidermis and upper dermis (Ma and Bisby, 2000). This has been demonstrated by examining the distal regions of the common sciatic nerve following application of the CCI in which axons can be shown to degenerate, as well as by examining the upper dermis directly using retrograde tracers and pan-neuronal markers (Peleshok and Ribeiro-da-Silva, 2011; Taylor and Ribeiro-da-Silva, 2011). The results of these studies strongly suggest that that lack of peptidergic innervation is not due to a decrease in phenotypic markers such as receptor or peptide expression, but rather to fiber loss. It is also TrkA expression on the regenerating afferents which permits the regeneration to occur (Scott and Ramer, 2010). We have previously shown that peptidergic afferents return to innervation density of sham-operated controls by 4 weeks post-lesion, and that this recovery precedes that of any other fiber population (Peleshok and Ribeiro-da-Silva, 2011).

This report provides further evidence that Schwann cells persist within the denervated territory. We have previously shown at the light and electron microscopic levels that following a complete transaction of a peripheral nerve, there was a complete loss of sensory fibers from peripheral nerves and that the denervated Schwann cells upregulate p75 in the absence of axon-Schwann cell contact (Ribeiro-da-Silva et al., 1991). Our present data expands on that observation by using a model in which there is a partial nerve lesion and some axons remain uninjured (Basbaum et al., 1991; Coggeshall et al., 1993). Indeed,

in our material it was clear that from 2 weeks post-lesion Schwann cells upregulated p75 and surrounded nerve fibers labeled with the pan-neuronal marker PGP-9.5, which we used as a marker of the overall innervation, and represent undamaged or regeneration fibers.

A surprising result from this study is the lack of a dramatic upregulation of proNGF levels in Schwann cells. Indeed, it has been suggested in many studies that, following nerve injury, Schwann cells would be among the key producers of NGF and it would be mostly the NGF from this source that would contribute to the sprouting of peptidergic afferents within the periphery (Taniuchi et al., 1988). One of our central premises is that cells immunoreactive for proNGF are sources of NGF for responsive nerves. Furthermore, that proNGF is released from the cells into the extracellular space in an activity dependent manner, and transformed into the active form, mNGF (Bruno and Cuello, 2006) . One possibility might be that we are detecting only proNGF and not mNGF, and that the latter form would occur on Schwann cells. We can exclude that possibility because mNGF occurs in very low concentrations even after injury, as detected by Western blot using an antibody that recognizes both proNGF and mNGF (unpublished observations). Another possibility would be that the turnover of proNGF in Schwann cells is very high, meaning that the relative lack of immunoreactivity could be indicative of rapid rate of release rather than a lack of production. Schwann cells, like keratinocytes, have been suggested to express ion channels such as P2X receptors (Irnich et al., 2001) and sodium channels (Baker, 2002) and that upon activation depolarize the cell's membrane which could potentiate the release of neuroactive molecules such as proNGF into the intercellular space, but this does not explain why proNGF can be detected on keratinocytes and not in Schwann cells. However, based on the above, it is may also be possible that Schwann cells represent only a minor source of NGF.

We were also able to demonstrate a close association between proNGF producing cells and NGF responsive afferents from one to four weeks post-injury; these include sympathetic efferents and peptidergic afferents. There seemed to be a closer association between the sympathetic fibers and proNGF-IR cells than

between peptidergic afferents and proNGF-IR cells. Historically it has been shown that sympathetic efferents, rather than sensory afferents are exquisitely responsive to changes in levels of NGF in the environment and this was demonstrated by neurite outgrowth when NGF was added to culture media (Levi-Montalcini and Angeletti, 1963; Levi-Montalcini and Booker, 1960b). Our observations that there was a closer association between the sympathetic efferents and proNGF producing cell types than for the peptidergic afferents may be reflective of the relative degree of dependence or sensitivity of each fiber population to NGF. It is thus not surprising that those structures which were more immunoreactive for proNGF were blood vessels (Fig 1B, 2F, 3C), which are known to receive dense innervation by sympathetic efferents (Ruocco et al., 2002). The changes after lesion in proNGF production are consistent with the changes following the onset of Wallerian degeneration, as within one week following nerve injury we observed a large degree of mast-cell infiltration in the upper dermis (Fig 1B).

In summary, we were able to show that following application of the traditional CCI model of neuropathic pain, mast cells followed by keratinocytes and vascular endothelium upregulated proNGF, and that this upregulation was significant until at least four weeks post-injury, as confirmed by Western blotting. This is in contrast to the relative changes in TrkA protein levels and p75 within the same area. Following nerve injury, there was a dying back of peptidergic afferents and a correlative decrease in TrkA protein until four weeks post-injury, at which point it returned to levels of sham-operated animals, coinciding with the recovery of the peptidergic innervation. Our data suggests that the sprouting after lesion of NGF-responsive fibers is initiated by the increase in local proNGF (and thus mNGF) levels, and may be maintained with the involvement of other factors.

Chapter Five

General Discussion

5.1. Overview

The work presented in this thesis includes three experimental chapters. The work presented in Chapter 2 investigated the morphological changes of the peripheral nervous system following application of the traditional chromic gut-based CCI neuropathic pain model from 3 days to 1.5 years after the lesion. The objective of this study was to characterize the changes in the three principal sensory fibre groups comprising the sciatic nerve. We sought to build on the initial description made in our lab of changes in sensory fibres innervating the glabrous skin. However, this preliminary body of work was restricted to a description of the changes in only one population of sensory afferents, the peptidergic and of the post-ganglionic sympathetic efferents, using CGRP and DβH as markers for each respective population, and no behavioural correlates were studied (Yen et al., 2006). In addition, there were recent advances made in our lab using an antibody directed against the P2X3 receptor to be used as a marker of non-peptidergic C-fibres innervating glabrous skin (Taylor et al., 2009). This study, of which I am second author, provided the required technical background to allow for an accurate description of changes in the non-peptidergic C-fibres following nerve injury to be made. This is what we have carried out in Chapter 2 of this thesis. In this study, the development of evoked mechanical and thermal hypersensitivity post-CCI confirmed the success of the nerve injury model. From this, we can assume that the morphological changes following the application of the CCI are correlative with the subsequent behavioural changes following nerve injury. This study demonstrated that 3 days following the application of the CCI, at a time in which hypersensitivity to applied heat and mechanical stimuli were still developing, a dramatic loss of myelinated and peptidergic afferents, as well as non-peptidergic C-fibres, was observed. From the dramatic and highly significant loss of the three sensory fibre populations observed, remarkably different regeneration patterns ensued. The myelinated afferent density remained significantly lowered but a few fibres were observed from 2 to 4 months post-CCI. The peptidergic afferents, consistent with prior

studies (Yen et al., 2006), quickly returned to sham-operated control levels and sprouted shortly thereafter, a point at which they remained up to 1.5 years post-CCI. The non-peptidergic C-fibres remained significantly decreased and only sprouted at a point from 4 months to 1.5 years post-injury. This differential degree of sensitivity inherent to myelinated afferents towards nerve injury, which is not found of unmyelinated afferents, could imply a mechanism specific to each fibre population. In order to demonstrate whether these morphological changes affecting the sensory component of the sciatic nerve following a partial nerve lesion were consistent through other constriction injuries, we compared the data to that obtained following the application of another commonly used constriction injury model, the polyethylene cuff model.

Following application of the cuff, we observed similar progression and maintenance of thermal sensitivity compared to that following application of the CCI. Whereas the cuff generated a more sustained mechanical allodynia and hyperalgesia through to the 4 month time point, the CCI did not and mechanical allodynia and hyperalgesia resolved a little after 1 month to 1.5 months post-injury respectively. The morphological changes also differed between the two models; sprouting of peptidergic fibres did not occur at any time up to 4 months post-injury following application of the cuff, the non-peptidergic C-fibre depletion was delayed in comparable severity following application of the cuff and, unlike the peptidergic afferents, the non-peptidergic C-fibres did return to sham operated controls at 4 months following cuff application. Based on the results of the Chapter 2 where non-peptidergic C-fibres only sprouted between 4 months and 1.5 years post-injury, it may be possible that further sprouting into the upper dermis of this population may occur. The myelinated afferents remained significantly low compared to sham-operated controls following application of both models, however the myelinated fibres following application of the CCI were more affected than the myelinated fibres following application of the polyethylene cuff. These results demonstrate that the two nerve injury models are not to be used interchangeably and represent two different constriction injury models with different reinnervation patterns by sensory afferents. Reinnervation

of sensory fibres and sprouting of sympathetic efferents are both sensitive to target tissue produced NGF. Since mNGF is quickly taken up by their responsive nerve fibres, its precursor form was used to elucidate its distribution through the epidermis and upper dermis prior to and after application of the CCI.

We found that proNGF was produced in keratinocytes, endothelium, epithelium and mast cells. Following nerve injury, the production of proNGF in mast cells and around vascular-like structures was significantly increased and remained significantly higher than in sham operated controls through 4 weeks post-injury. Those fibres responsive to NGF do so via TrkA expression and we found levels of TrkA which were significantly lowered through up to 4 weeks post-injury, a time point at which recovery was observed. The protein quantification provided in chapter 4 confirmed the immunohistochemical data describing loss and sprouting of these afferents (see chapters 2 and 3) in conjunction with the progressive sprouting of sympathetic efferents. We can suppose that the changes in TrkA protein can be associated with sympathetic sprouting since the increase from 2 to 4 weeks post-injury coincides with a highly significant increase in sympathetic sprouting observed in previous reports from our lab (Yen et al., 2006). The expression of p75 was significantly increased from 1 through to 4 weeks post-injury and the majority of this expression seemed to be on the surface of Schwann cells. Schwann cells expressing p75 become rapidly denervated following nerve injury, consistent with previous reports to this effect (Ribeiro-da-Silva et al., 1991). The distribution of peptidergic afferents were loosely associated with proNGF producing structures, in contrast to the sympathetic efferents which were tightly associated until they began to sprout at 4 weeks post-injury.

5.1.1. Sympathetic Sprouting

In this body of work, we have demonstrated that peptidergic sensory afferents display a dynamic innervation pattern following application of either of two constriction-based nerve injury models (Chapters 2 and 3). I was also able to demonstrate that following application of either of these two nerve injury models, differential sprouting of NGF-responsive sympathetic efferents occurred and these

data was not included in Chapter 3 as it requires further confirmation. However, the preliminary data are shown in Appendix, Figure 1A, B and C. To visualize the changes in the sympathetic efferent population following application of both the polyethylene cuff and the CCI by immunohistochemistry, an antibody against DβH was used as a marker for this nerve fibre population. I observed a reduction in fibre distance indicating an approach of sympathetic efferents to the dermo-epidermal junction following application of the CCI (Appendix Figure 1A) which is consistent with previously published results (Yen et al., 2006). The distance of sham-operated control animals was found to be an average of 110μm from the dermo-epidermal junction and decreases to 50-40μm from 2 weeks through 4 months post-CCI (Appendix Figure 1C). Following application of the polyethylene cuff, this sprouting of sympathetic efferents was not observed. In fact, a significant retraction of sympathetic efferents was observed at 1 week post-injury where distances increased to 176μm and remained significantly increased to 2 weeks post-cuff (Appendix Figure 1C). The distances of the tip of the DβH-IR nerve fibre began to decrease from 2 weeks through 16 weeks post-injury, a point at which there was no difference compared to sham-operated controls (Appendix Figure 1C). Statistical analysis was conducted using a 2-way ANOVA with Bonferroni post-hoc test and comparisons made to sham-operated controls. These results reaffirm the conclusion that the cuff and CCI models of neuropathic injury are independent nerve injury models and should not be used as interchangeable models of constriction injury. If we assume that it is in large part excess production of NGF which contributes to sprouting of sympathetic efferents into the upper dermis following application of the CCI (Davis et al., 1994; Ramer and Bisby, 1999; Ramer and Bisby, 1997c) it would then be a reasonable correlate to this argument that there may be an insufficient level of NGF produced in the target tissue to induce sympathetic efferents to sprout in the cuff model. Further experiments are necessary to substantiate this observation as this would indicate that the cuff model of neuropathic pain is also one which does not include a sympathetic component. Such experiments would be the administration of guanethidine by intraplantar injection 2 weeks following application of the cuff

injury, a time in which mechanical allodynia and hyperalgesia as well as thermal sensitivity are maximal (Chapter 3 Figures 2, 3 and 4). The time point of 2 weeks following the application of the polyethylene cuff also coincides with a time at which the sympathetic efferents are still significantly retracted from the dermo-epidermal junction (Appendix 1C). If it is true that the cuff model one in which there is a lack of sympathetic involvement, intra-plantar administration of guanethidine, which acts to deplete the local stores of norepinephrine from sympathetic terminals, should have no effect on any of the evoked pain measures. This would be in contrast to those models in which there is a clearly established sympathetic involvement (e.g. the CCI model) and guanethidine administration leads to a reduction in evoked pain behaviours (Lee et al., 1998). This model would be a valuable tool to reproduce those human neuropathic conditions in which a sympathetic involvement is not observed. There is currently no available neuropathic pain model in which a clear lack of sympathetic sprouting is observed making this one unique. It is this significance which motivates us to fully validate our findings prior to publication. To support the suggestion that one of the possible contributing factors to the lack of sympathetic sprouting (including a lack of peptidergic afferent sprouting) following the application of the cuff is an insufficient level of NGF, Western blot analysis of the innervated territory should be done to quantify the level of it. If it is the case that NGF levels are elevated to a point comparable to that seen following application of the CCI, a model in which there is a clearly established sympathetic and peptidergic sprouting, an argument would be made that other factors within the target tissue are present which repulse these fibres from the upper dermis.

The application of a nerve injury involves the irritation and constriction of the nerve itself which then causes axon damage and a myriad of phenotypic changes discussed in the General Introduction. In addition to the changes in receptor and ion channel expression on the sensory afferents, an inflammatory response develops and can be measured in areas as distal to the nerve injury as the dermis of the glabrous skin. Inflammation, as a consequence of the nerve injury, may differ between nerve injury models, and it is these differences which may

underlie the changes in innervation patterns. For example, a previous publication from our lab used a model of complete Freund's adjuvant (CFA) induced chronic inflammation leading to the development of arthritis restricted to the joints of the hind paw (Almarestani et al., 2008). Using this inflammatory model of chronic pain, a robust sprouting of sympathetic efferents into the upper dermis was observed together with a delayed and transient peptidergic sprouting. In addition, it has been well documented that an increase in local NGF production occurs following induction of chronic inflammation such as that following local CFA injection (Pezet et al., 2001). A comparative examination using purely inflammatory models such as the CFA injection, as well as nerve injury models such as the CCI and cuff application would be useful to determine the relative degree of inflammation occurring in each model. We would use markers such as TNF-α and IL-1β levels (proteins which induce increase in NGF levels) as well as measure levels of NGF itself, perform macrophage and mast cell counts and correlate all this with the presence (or absence) of sympathetic and peptidergic sprouting in the upper dermis.

The results from chapter 4 involved an investigation of the distribution of proNGF in the upper dermis and epidermis following nerve injury, and its association with responsive nerve fibres. The results from chapter 4, taken together with those obtained in chapter 3 on the comparative examination of the application of the cuff compared to the CCI, point to a possibility that the level of NGF production is reduced following application of the polyethylene cuff. If it is the case that elevated levels of target derived NGF are responsible for sprouting of sympathetic and peptidergic afferents, we can infer that the lack of sprouting and reduction of sympathetic efferents may be indicative of a relative lack of NGF. A limited amount of literature has recently become available suggesting a role of artemin in the support of post-natal sympathetic neurons. Artemin has been shown to be expressed by vascular smooth muscle and promotes the development of the sympathetic nervous system towards the normal innervation of blood vessels (Honma et al., 2002). As a rat ages, sympathetic neurons lose their dependence on NGF for survival (Andres et al, 2001; Gorin and Johnson, 1980).

Cultured adult superior cervical sympathetic neurons respond to artemin as efficiently as it does to NGF in enhancing survival, and when added with NGF to cultured adult superior cervical sympathetic neurons, in promoting neurite elongation (Andres et al, 2001). Since there currently is no available literature suggesting an *in vivo* link between target tissue derived artemin and its ability to promote sympathetic sprouting, it would be interesting to administer function-blocking antibodies against artemin. The anti-artemin antibody administration could be done either in combination with anti-NGF antibodies or alone, following the application of a model of neuropathic pain such as the CCI, which has a clear sympathetic involvement, to determine to what extent artemin could have a role in the promotion of sympathetic sprouting.

It has also been suggested that development of spontaneous activity of peripheral nerves mediates the sprouting observed in the DRG by sympathetic fibres (Xie et al., 2010; Zhang et al., 2004). Spontaneous activity of sensory neurons can be initiated by exposure to a proinflammatory soup which includes NGF (Scholz and Woolf, 2007). It has been reported that the attenuation of spontaneous activity of C-fibres and A-fibres following nerve injury can be accomplished through application of lidocaine (Abram et al, 1994; Liu et al, 2001). An adequate explanation as to the mechanism underlying this phenomenon is lacking and has not been properly discussed in the literature. A possible explanation could be a dual effect of lidocaine on two separately responsive cell populations but which co-incidentally culminates in the effect of reducing spontaneous activity as well as reducing sympathetic sprouting. This could be due to the recent observation that those cells that produce and release proNGF also express sodium channels. Therefore, the release of NGF would promote two things, the growth of sympathetic afferents and development of spontaneous activity. The application of systemic lidocaine could have the effect of reducing the activity-dependant release of proNGF by cells in close proximity to sensory afferent cell bodies; this attenuation of proNGF release from non-neuronal cells could then in turn abrogate the NGF-mediated sprouting of sympathetic efferents around DRG cell bodies. Lidocaine reduces sodium

channel-mediated ectopic activity of sensory afferents. Therefore, the effects of lidocaine on sympathetic sprouting may not be directly linked to the spontaneous activity of the sensory afferents, but rather on the non-neuronal cell types which synthesize and subsequently secrete proNGF in an activity-dependent manner.

Studying the role of the skin as it pertains to nerve injury may prove fruitful in identifying the integument as playing an important role not just as an organ that can translate external cues to the innervating sensory afferents, but as existing in a dynamic relationship that can modulate the responsiveness of the innervating afferents and in turn can be affected by injury to the neurons. Work on the dynamic nature of keratinocytes and the unique relationship that exists between them and the skin innervation may provide insights onto how nerve lesions can affect the responsiveness of keratinocytes to changes in environmental stimuli such as heat, cold and mechanical stimulation. As well, it has been well established that inflammation is associated with increases in the levels of locally available pro-inflammatory mediators such as IL-6 and NGF, with consequences such as decreased threshold of activation of nociceptive sensory afferents including C-fibres responsive to these mediators (Benn et al., 2001; Djouhri et al., 2001).

Innervation changes observed in this body of work, in addition to those results obtained by previous members of our lab, point to interesting differences in chronic pain models either with or without a direct nerve injury. In one case, the development of chronic pain due to chronic inflammation is associated with increased peripheral NGF levels followed by sympathetic and peptidergic sprouting. Secondly, the CCI model also has sympathetic sprouting, increased levels of NGF and peptidergic sprouting in addition to a direct nerve injury. Thirdly, the cuff injury in which a lack of peptidergic and sympathetic sprouting but a diminution in overall fibre density is observed, with the interesting exception of the non-peptidergic C-fibres. These differences raise interesting questions about the possible mechanisms underlying the development of the pathologies of each chronic pain model and the relative contribution of nerve

injury and inflammation to the morphological changes affecting NGF-responsive nerves.

5.1.2. NGF and Pain:

It has been demonstrated that proNGF can be released by cultured keratinocytes (Dallos et al., 2006) which further substantiates the hypothesis that proNGF can be converted in the extracellular space into its mature form following release from dermal and epidermal cells. As there is a cascade for proNGF conversion to mNGF and subsequent degradation in the extracellular space (Bruno and Cuello, 2006; Lee et al., 2001), it is then theoretically possible to modulate this cascade to block the degradation of mNGF or the conversion of proNGF to mNGF. The original description made by Bruno and Cuello was carried out initially in the CNS, however those enzymes implicated in this cascade have been localized to both non-neuronal tissue such as synovium (for the possible treatment of arthritis) and fibroblasts and keratinocytes. This cascade was described in the General Introduction and so will be described only briefly. Plasminogen can be converted to its active form plasmin by either tPa or uPa, converting proNGF to mNGF. The activity of either tPa or uPa can be inhibited by plasminogen activator inhibitor type-1 (PAI-1) and PAI-1 has been found in mast cells (Cho et al., 2000). It has also been demonstrated that NGF has the ability to increase levels of plasminogen by three fold (Gutierrez-Fernandez et al., 2007). I have carried out some preliminary work establishing the presence of plasminogen and its peripheral inhibitor, tPa, in the ankle joint of the rat for modulation of NGF in animal models of chronic inflammation leading to arthritis (Appendix Figure 2A and B). This work was then continued further by other members of our lab, and provided strong evidence that the inhibition of MMP-9 by a MMP-2/9 inhibitor was sufficient to block the degradation of mNGF and promote its accumulation thus resulting in sprouting of sympathetic efferents (Longo et al., 2011). The accumulation of mNGF through this method was not sufficient to promote sprouting of peptidergic afferents which is in line with current data obtained within this thesis that there may be an adequate level of

NGF which is sufficient to promote the sympathetic efferent growth within the dermis and this may be different from that required of peptidergic afferents.

NGF has been validated as a pharmacological target for almost 20 years (Garber, 2011; McMahon et al., 1995) and this has led to various methods of blocking its effect as a pain mediator. Recent work stemming from the finalized description of the extracellular maturation cascade of proNGF to mNGF in the CNS (Bruno and Cuello, 2006) opens the attractive possibility that not only is this maturation cascade present in the periphery but, importantly, that it can be modulated. This is current work ongoing in our lab. The strong involvement of NGF as a sensitizing agent in chronic pain associated with arthritis has opened the possibility that the modulation of its maturation might address the issue of NGF still being required for normal, acute inflammatory reactions and for bone homeostasis. This may be a crucial point, because of the known issues with NGF sequestering antibodies in clinical trials of osteoarthritis patients. Indeed, there were cases of bone necrosis and emergency joint replacement surgery which led to the suppression of the trials (Wood, 2010). One possible approach is to inhibit tPa, through the form of an externally applied patch or conjugation to a large, innocuous protein to keep it peripherally restricted. The objective of developing a small molecule antagonist towards tPa would be to slow or modulate the conversion of proNGF to mNGF by plasminogen, in the hope that this may aid in decreasing the amount of peripherally available NGF. By the administration of a compound able to modulate the activity of upstream processing enzymes of NGF, it opens the possibility of dosing, whereby plasma titers of NGF could be taken from patients being treated until an amount of available NGF is achieved, where the potential of adverse events encountered by complete sequestration of NGF would be prevented.

5.1.2.1. Further Experiments:

Given that these results elucidate that two models of neuropathic pain previously thought of as being interchangeable are in fact quite different, our data point to the lack of grading or qualification of neuropathic pain models. The results of a general comparative examination could be published as a handbook

for pain researchers evaluating each of the commonly used pain models. Perhaps grading neuropathic pain models not only on their evoked pain severity, longevity or regenerative/sprouting capabilities but also including relative inflammation would also be important. Markers of inflammation (such as IL-6 and TNF-α production) could be quantified in all neuropathic pain models. These would be quantified in excised sciatic nerve at the point of injury as well as in the glabrous skin in order to ascertain the distal effects of the applied injury. Other markers of inflammation would include the more basic method of counting the number of infiltrating mast cells in the upper dermis of the glabrous skin of either models of pure inflammation (such as the CFA) or neuropathic pain models. Studies of neuropathic pain models could include discharge frequency from injured Aβ, Aδ and C-fibres, spontaneous activity of each of the three fibre populations, degree of mast, macrophage cell infiltration, and degree of fibre loss/regeneration, sympathetic involvement and responsiveness to sympathectomy. Other endpoints could include standardized responsiveness to pharmacological agents such as indomethacin, morphine, gabapentin or lidocaine. The behavioural endpoints would measure duration of mechanical allodynia/hyperalgesia, Hargreaves heat thresholds, cold allodynia and other spontaneous measurements of pain such as facial grimace or directed grooming. This endeavour is obviously not something that can be conducted in any one individual lab, rather would be an initiative developed or mandated by the basic science arm of the IASP which could also provide much of the data through stringent meta-analysis of existing literature granted that stringent inclusion criterion be met.

5.1.3. A-Fibres and Mechanical Sensitivity:

Throughout the course of this thesis reference to changes in "peptidergic afferents" has been made. Although most peptidergic afferents are C-fibres, approximately 20% of A-fibres express the TrkA receptor and the neuropeptide CGRP (Averill et al., 1995). What we have been able to demonstrate in this body of work is that, following nerve injury, there is a greater than 90% reduction in the myelinated afferents innervating the upper dermis as elucidated using NF200 as a marker. We can deduce that the remaining afferents which sprout comprise the C-

fibre population. Since it is known that there is not a clear separation between the populations, CGRP immunoreactive peptidergic C-fibres have not been referred to as being peptidergic C-fibres throughout this body of work. To stress the importance of this, it is important to point out that in Chapter 2 we mention that at 16 weeks post-CCI, when the occasional A-fibre could be detected in the upper dermis, some of these afferents also express CGRP, therefore likely being small diameter myelinated afferents (Appendix Figure 3).

Research on this thesis has demonstrated that the application of either the CCI or cuff models resulted in either an almost complete ablation of myelinated afferents in the case of the CCI where at 8-16 weeks a minor recovery was observed or in the case of the polyethylene cuff where a significant, but not complete, loss occurred. These observed differences point to the possible existence of two mechanisms underlying the generation of mechanical allodynia.

It has been debated whether there is a major contribution of Aβ-fibres to the development of the abnormal pain sensations following nerve injury. Abnormal pain following nerve injury can be attributed to A-fibres which represent non-nociceptive low threshold mechanoreceptors (LTM) in that the lack of them is permissive for the noxious stimuli via nociceptive input through central disinhibition (Djouhri and Lawson, 2004; Van Hees et al., 1981), although this is a negative rather than a positive role. Other centrally-mediated mechanisms include the reversal of the chloride gradient in inhibitory interneurons receiving GABAergic input from activated A-fibres resulting in excitation rather than inhibition (Coull et al., 2005). One of the key supporting pieces of evidence underlying the importance of A-fibres in mechanical allodynia is that, following ablation of C-fibres, the application of a nerve injury did not produce a complete reduction of evoked pain related behaviours indicating a role of A-fibres in the transduction of noxious information in nerve-injured animals (Ossipov et al., 1999). However, a very simplistic observation is that those fibres which are not present cannot possibly be activated. Following application of the CCI, there is simply no significant innervation by A-fibres, as we revealed in Chapter 2. Therefore the second hypothesis of mechanical allodynia would apply to this

scenario, namely that a reduction of high-threshold mechanoreceptive C-fibres or an 'unmasking' of C-fibres activated by light touch occurs. It is these alterations which must contribute to the observation that normally non-noxious stimuli is now sufficient to generate action potentials which are then interpreted as painful (Andrew, 2010; Craig, 2010). In the case of the application of the polyethylene cuff, both A-fibres and C-fibres density is significantly reduced, but in comparison to those changes following application of the CCI, there are relatively more A-fibres that remain in the upper dermis following lesion. However, even in the cuff model, more small diameter fibres persist than A-fibres. These results suggest that, depending on the neuropathic pain model used, there may be either the sole involvement of the sensitization of C-fibres to innocuous stimulation or a mixed contribution by C-fibre and A-fibres in stimulus-evoked mechanical allodynia. These observations raise the point that further studies should be made into the relative differences generating the overall similarities in evoked pain related behaviours in the myriad of neuropathic pain models available to pain researchers. Hopefully, once an understanding of the underlying differences between each of the models is elucidated and the link made between these differences and the relevance to the human conditions made, then the possibility arises of better model development. If animal models can be more representative of the human pathology, advances can be made towards more efficient use of preclinical testing of appropriate pharmacological agents.

5.2. Original Contributions to Science

Delayed reinnervation by non-peptidergic nociceptive afferents of the glabrous skin of the rat hindpaw in a neuropathic pain model (published in 2011 in the Journal of Comparative Neurology).

This study detailed for the first time the almost complete loss at 3 days after the application of the CCI model of neuropathic pain of myelinated afferents in the skin and that such loss was sustained through 4 months post-injury. Prior to this, detailed information of the loss and regeneration of myelinated afferents was restricted to electron microscopy counts of fibres in the sciatic nerve immediately distal to the site of injury, but had not extended to more distal sites such as

glabrous skin. Following application of the CCI, the loss of peptidergic afferents was observed as early as 3 days, and the sprouting which is known to occur at a period from 4 to 8 weeks was maintained through 1.5 years post-injury, indicating that this is a permanent morphological change affecting the peptidergic afferents innervating the upper dermis. The ability to accurately quantify the innervation changes in the upper dermis by the non-peptidergic C-fibres was developed in our lab, in a previous publication in which I participated. Applying this approach, I was able to quantify changes in non-peptidergic C-fibres from 3 days through 1.5 years post-injury. It was also found that the initial loss of non-peptidergic C-fibres persisted for some time and it was not until a point between 4 months and 1.5 years post-injury that non-peptidergic C-fibres sprouted.

Comparative study of two chronic constriction injury neuropathic pain models (Submitted to Journal of Comparative Neurology).

This study expanded on the results obtained from the initial description of the morphological changes following application of the CCI by comparing them to changes occurring following application of the polyethylene cuff model. We were able to reveal for the first time that in the cuff, compared to the CCI model, there was less myelinated fibre loss and a gradual loss with lack of recovery in the peptidergic afferent population. The non-peptidergic C-fibres had a delayed loss in the cuff model and, like that observed following application of the CCI, returned to levels similar to that of sham-operated controls. The descriptions made here of the morphology of the sensory afferents innervating the glabrous skin had not been made following application of the polyethylene cuff and these observations had not been conducted in a head-to-head comparative examination to the closely related CCI model of neuropathic pain. The initial description of the behavioural correlates following application of the polyethylene cuff had included the observation that mechanical thresholds were lowered through 145 days post-injury. Studies of thermal sensitivity in the cuff model had been restricted to only 21 days post-injury, and consequentially, the observation that

the resolution of this sensitivity occurs at the same time as that following application of the CCI had not been previously reported.

Changes in neurotrophic factors in the rat thick skin following chronic constriction injury of the sciatic nerve

(Molecular Pain, under revision).

This study takes advantage of the existence of a good quality anti-proNGF antibody to describe for the first time the distribution of proNGF in the rat skin. To this end, we confirmed that proNGF is produced by mast cells in the upper dermis and keratinocytes of the epidermis, as well as other dermal cell types which were unable to be identified based on the use of toluidine blue contrast stain, although some cells were obviously endothelial cells in the vessel wall. We were also able to demonstrate for the first time the relationship between sympathetic efferents and peptidergic afferents with the proNGF producing cells before and after application of nerve injury. We also demonstrated that following application of nerve injury, a co-localization between proNGF and Schwann cells was not observed, contrary to previous assumptions.

Appendices

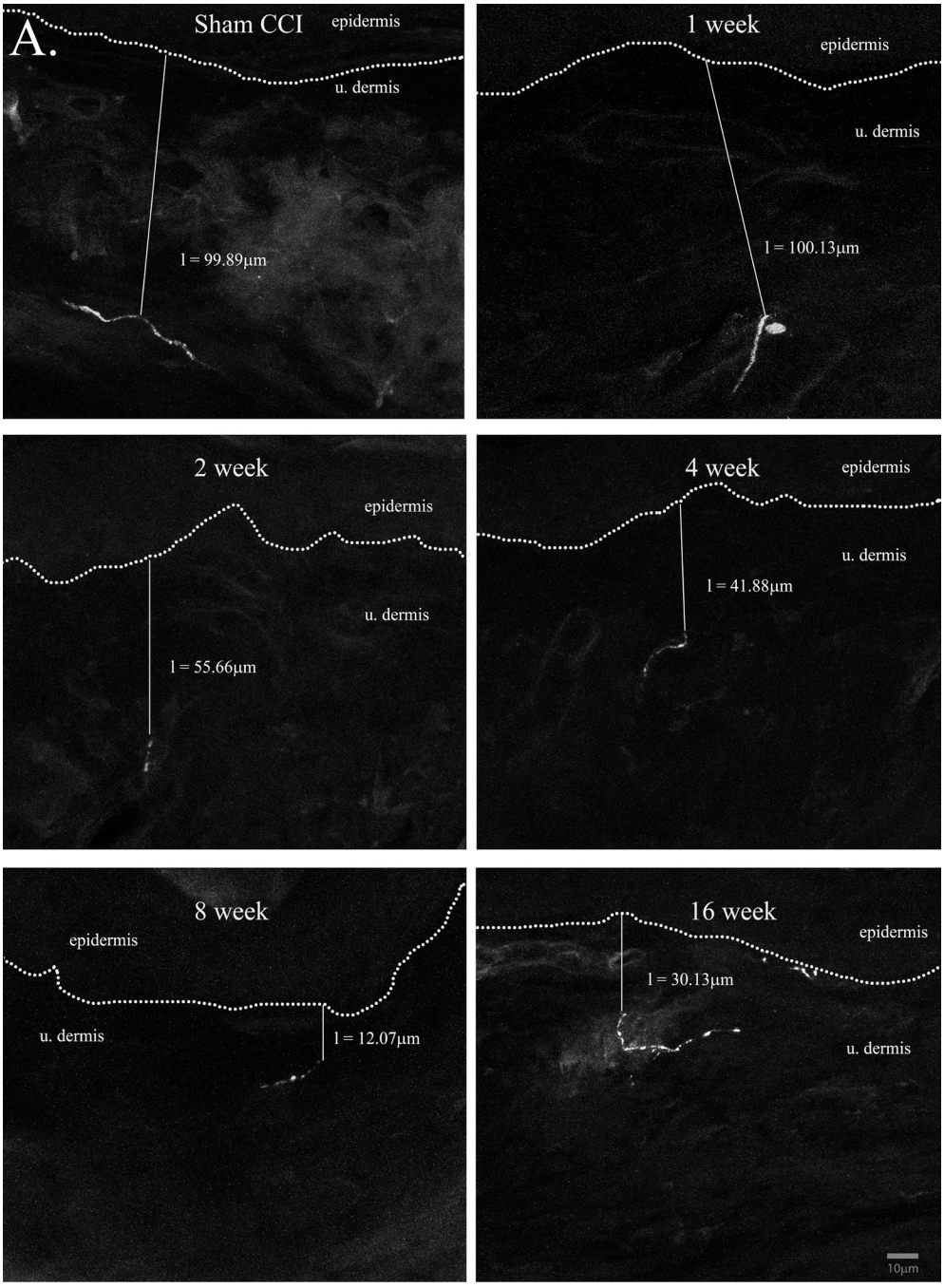

Figure 1A: Effects of chromic gut based chronic constriction injury on sympathetic fibres. Representative images taken using 40X objective. Location of DβH immunoreactive **sympathetic** efferents in the dermis of glabrous skin from sham and animals from 1 – 16 weeks post-injury.

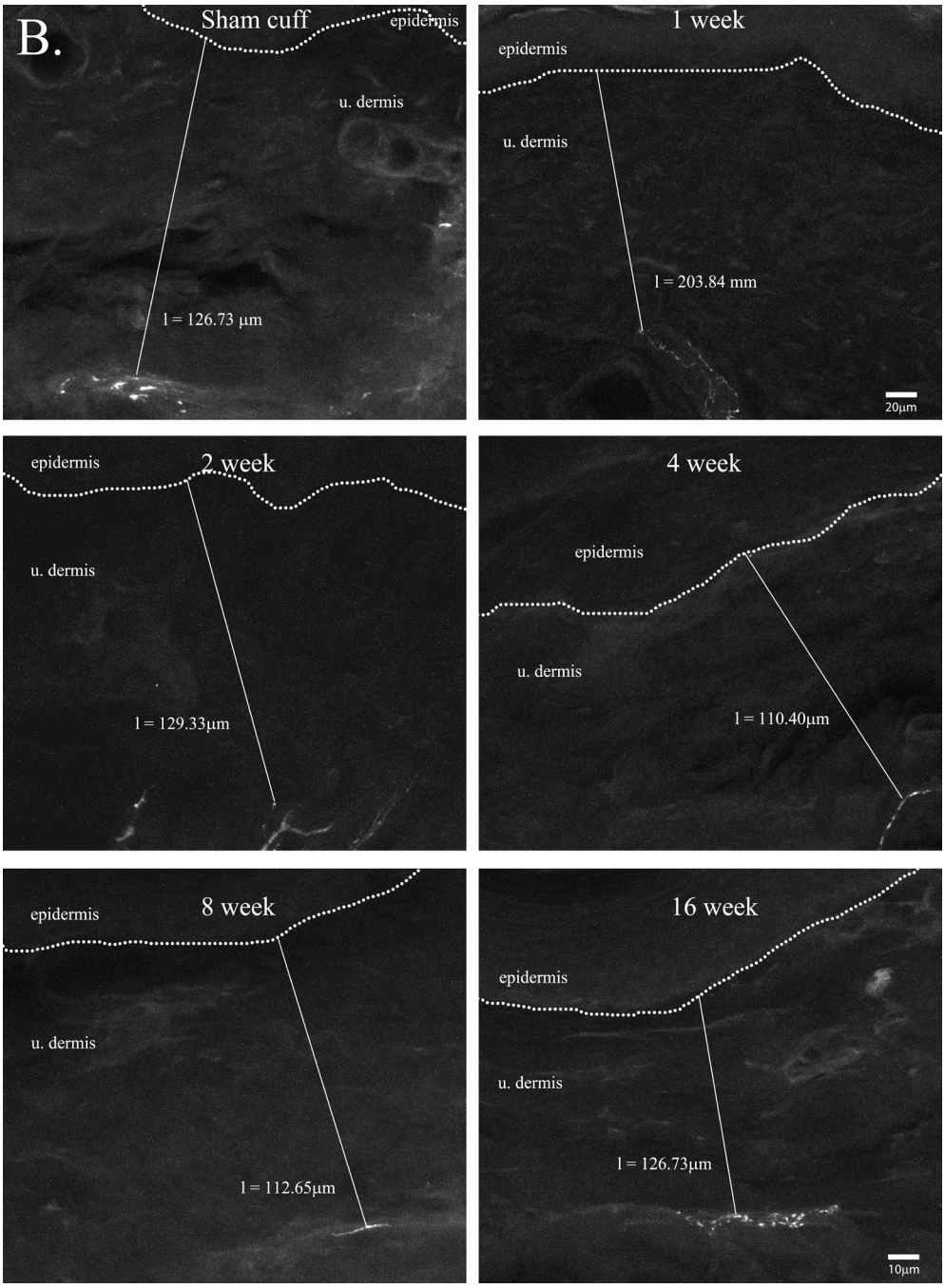

Figure 1B: Effects of polyethylene cuff constriction injury on sympathetic fibres. Location of DβH immunoreactive sympathetic efferents in the dermis of glabrous skin from sham and animals from 1 – 16 weeks post-injury (note – image taken at 1 week post-cuff was obtained with a 20X objective).

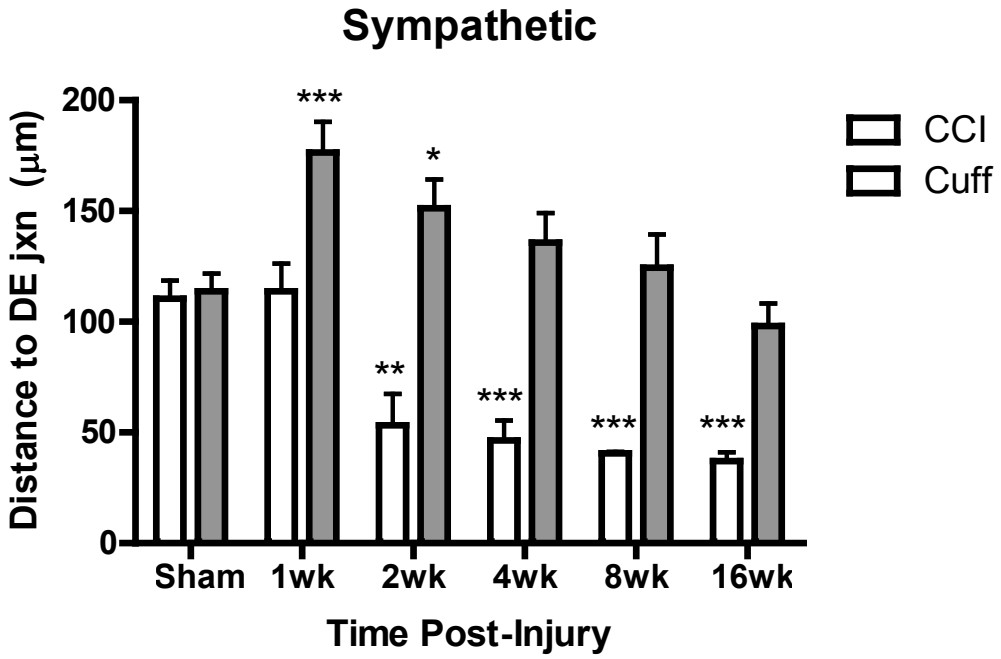

Figure 1C: Effects of constriction nerve injury on sympathetic fibre distance. Average distance of DβH immunoreactive fibres from dermo-epidermal junction. All distances compared to that of sham-operated controls. ***p<0.001 **p<0.01 *p<0.05; n=6; mean +SEM; comparisons made against sham operated controls.

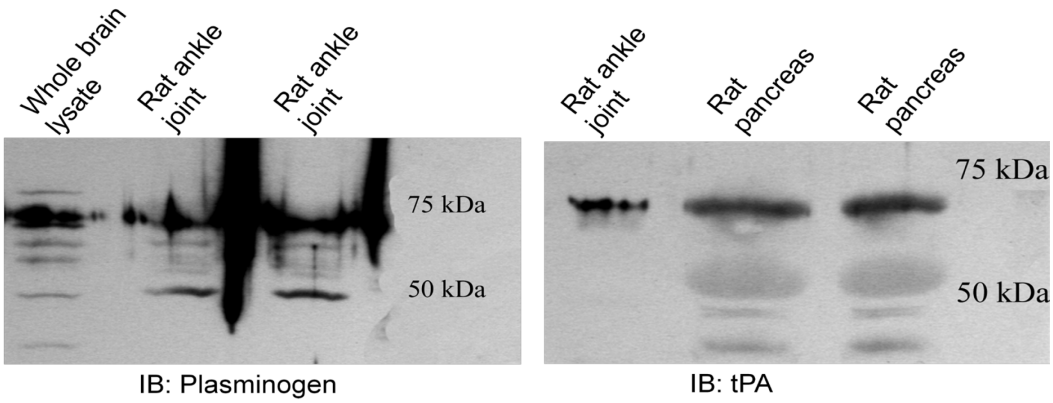

Figure 2: Western blot of naive rat ankle homogenate. A) Immunoblot of plasminogen (Santa Cruz; H-90 sc-25546; 1:500) from homogenized rat ankle joint demonstrates the presence of plasminogen (precursor to plasmin). Bands from 50 to 75kDa with positive control, whole brain lysate. B) Immunoblot of tPa (Santa Cruz; H-90 sc-15346; 1:500), activating enzyme of plasmin (from plasminogen) demonstrates it is present in rat ankle joint. Single band at 67kDa with positive control, rat pancreas homogenate.

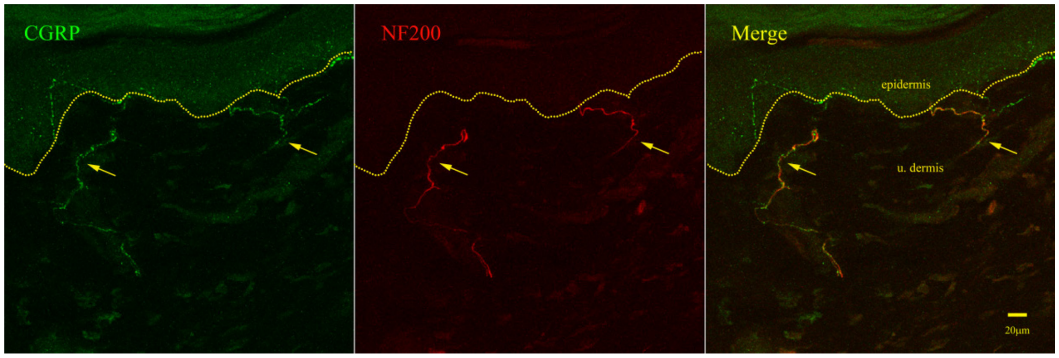

Figure 3: Merged images (yellow) of CGRP immunoreactive regenerated afferents 8 weeks post-CCI (green) with NF200 immunoreactive afferents (red). All afferents co-localizing CGRP and NF200 are represented with arrows. Pictures were taken as Z-stacks of confocal optical sections using a Zeiss LSM 510 confocal microscope equipped with argon and helium neon lasers applying a 40X water-immersion.

References

Abram SE, Yaksh TL. 1994. Systemic lidocaine blocks nerve injury-induced hyperalgesia and nociceptor-driven spinal sensitization in the rat. Anesthesiology 80(2):383-391

Airaksinen MS, Saarma M. 2002. The GDNF family: Signalling, biological functions and therapeutic value. Nat Rev Neurosci 3(5):383-394.

Albers KM, Woodbury CJ, Ritter AM, Davis BM, Koerber HR. 2006. Glial cell-line-derived neurotrophic factor expression in skin alters the mechanical sensitivity of cutaneous nociceptors. J Neurosci 26(11):2981-2990.

Albers KM, Wright DE, Davis BM. 1994. Overexpression of nerve growth factor in epidermis of transgenic mice causes hypertrophy of the peripheral nervous system. J Neurosci 14:1422-1432.

Ali Z, Raja SN, Wesselmann U, Fuchs PN, Meyer RA, Campbell JN. 2000. Intradermal injection of norepinephrine evokes pain in patients with sympathetically maintained pain. Pain 88(2):161-168.

Almarestani L, Longo G, Ribeiro-da-Silva A. 2008. Autonomic fiber sprouting in the skin in chronic inflammation. Mol Pain 4(1):56.

Aloe L, Levi-Montalcini R. 1977. Mast cells increase in tissues of neonatal rats injected with the nerve growth factor. Brain Res 133(2):358-366.

Aloe L, Tuveri MA, Angelucci F. 1995. Nerve Growth Factor, Mast Cells and Arthritis. Biomedical Reviews 4:7-14.

Alvarez FJ, Taylor-Blake B, Fyffe REW, de Blas AL, Light AR. 1996. Distribution of immunoreactivity for the á 2 and á 3 subunits of the GABA A receptor the mammalian spinal cord. J Comp Neurol 365(3):392-412.

Alvarez FJ, Villalba RM, Zerda R, Schneider SP. 2004. Vesicular glutamate transporters in the spinal cord, with special reference to sensory primary afferent synapses. J Comp Neurol 472(3):257-280.

Anderton BH, Breinburg D, Downes MJ, Green PJ, Tomlinson BE, Ulrich J, Wood JN, Kahn J. 1982. Monoclonal antibodies show that neurofibrillary tangles and neurofilaments share antigenic determinants. Nature 298(5869):84-86.

Andres R, Forgie A, Wyatt S, Chen Q, de Sauvage FJ, Davies AM. 2001. Multiple effects of artemin on sympathetic neurone generation, survival and growth. Development 128(19)3685-3695

Andrew D. 2010. Quantitative characterization of low-threshold mechanoreceptor inputs to lamina I spinoparabrachial neurons in the rat. J Physiol 588(Pt 1):117-124.

Averill S, McMahon SB, Clary DO, Reichardt LF, Priestley JV. 1995. Immunocytochemical localization of trkA receptors in chemically identified subgroups of adult rat sensory neurons. Eur J Neurosci 7:1484-1494.

Averill S, Michael GJ, Shortland PJ, Leavesley RC, King VR, Bradbury EJ, McMahon SB, Priestley JV. 2004. NGF and GDNF ameliorate the increase in ATF3 expression which occurs in dorsal root ganglion cells in response to peripheral nerve injury. Eur J Neurosci 19(6):1437-1445.

Bailey AL, Ribeiro-da-Silva A. 2006. Transient loss of terminals from non-peptidergic nociceptive fibers in the substantia gelatinosa of spinal cord following chronic constriction injury of the sciatic nerve. Neuroscience 138:675-690.

Baker MD. 2002. Electrophysiology of mammalian Schwann cells. Prog Biophys Mol Biol 78(2-3):83-103.

Bandtlow CE, Heumann R, Schwab ME, Thoenen H. 1987. Cellular localization of nerve growth factor synthesis by in situ hybridization. EMBO J 6:891-899.

Bao L, Wang HF, Cai HJ, Tong YG, Jin SX, Lu YJ, Grant G, H”kfelt T, Zhang X. 2002. Peripheral axotomy induces only very limited

sprouting of coarse myelinated afferents into inner lamina II of rat spinal cord. Eur J Neurosci 16(2):175-185.

Barker PA. 2007. High affinity not in the vicinity? Neuron 53(1):1-4.

Basbaum AI, Bushnell MC. 2009. Science of pain. Oxford; San Diego: Elsevier/Academic Press.

Basbaum AI, Gautron M, Jazat F, Mayes M, Guilbaud G. 1991. The spectrum of fiber loss in a model of neuropathic pain in the rat: An electron microscopic study. Pain 47:359-367.

Bechtel MJ, Reinartz J, Rox JM, Inndorf S, Schaefer BM, Kramer MD. 1996. Upregulation of cell-surface-associated plasminogen activation in cultured keratinocytes by interleukin-1 beta and tumor necrosis factor-alpha. Exp Cell Res 223(2):395-404.

Benn SC, Costigan M, Tate S, Fitzgerald M, Woolf CJ. 2001. Developmental expression of the TTX-resistant voltage-gated sodium channels Nav1.8 (SNS) and Nav1.9 (SNS2) in primary sensory neurons. J Neurosci 21(16):6077-6085.

Bennett DLH. 1998. A distinct subgroup of small DRG cells express GDNF receptor components and GDNF is protective for these neurons following nerve injury. J Neurosci 18:3059-3072.

Bennett DLH, Boucher TJ, Michael GJ, Popat RJ, Malcangio M, Averill SA, Poulsen KT, Priestley JV, Shelton DL, McMahon SB. 2006. Artemin has potent neurotrophic actions on injured C-fibres. J Peripher Nerv Syst 11(4):330-345.

Bennett DLH, Koltzenburg M, Priestley JV, Shelton DL, McMahon SB. 1998a. Endogenous nerve growth factor regulates the sensitivity of nociceptors in the adult rat. Eur J Neurosci 10(4):1282-1291.

Bennett DLH, Michael GJ, Ramachandran N, Munson JB, Averill S, Yan Q, McMahon SB, Priestley JV. 1998b. A distinct subgroup of small DRG cells express GDNF receptor components and GDNF is

protective for these neurons after nerve injury. J Neurosci 18(8):3059-3072.

Bennett GJ. 1991. The role of the sympathetic nervous system in painful peripheral neuropathy. Pain 45:221-223.

Bennett GJ. 2010. Pathophysiology and animal models of cancer-related painful peripheral neuropathy. Oncologist 15 Suppl 2:9-12.

Bennett GJ, Watson CP. 2009. Herpes zoster and postherpetic neuralgia: past, present and future. Pain Res Manag 14(4):275-282.

Bennett GJ, Xie YK. 1988. A peripheral mononeuropathy in rat that produces disorders of pain sensation like those seen in man. Pain 33:87-107.

Berger A, Dukes EM, Oster G. 2004. Clinical characteristics and economic costs of patients with painful neuropathic disorders. J Pain 5(3):143-149.

Bergsteinsdottir K, Kingston A, Mirsky R, Jessen KR. 1991. Rat Schwann cells produce interleukin-1. J Neuroimmunol 34(1):15-23.

Birder LA, Perl ER. 1994. Cutaneous Sensory Receptors. J Clin Neurophysiol 11(6):534-552.

Birder LA, Perl ER. 1999. Expression of α2-adrenergic receptors in rat primary afferent neurones after peripheral nerve injury or inflammation. J Physiol 515(2):533-542.

Black JA, Kocsis JD, Waxman SG. 1990. Ion channel organization of the myelinated fiber. Trends Neurosci 13(2):48-54.

Bland-Ward PA, Humphrey PPA. 1997. Acute nociception mediated by hindpaw P2X receptor activation in the rat. Br J Pharmacol 122(2):365-371.

Blumenkrantz N, Asboe-Hansen G. 1975. A selective stain for mast cells. The Histochemical Journal 7(3):277-282.

Bogen O, Dreger M, Gillen C, Schröder W, Hucho F. 2005. Identification of versican as an isolectin B4-binding glycoprotein from mammalian spinal cord tissue. FEBS J 272(5):1090-1102.

Bogen O, Joseph EK, Chen X, Levine JD. 2008. GDNF hyperalgesia is mediated by PLCgamma, MAPK/ERK, PI3K, CDK5 and Src family kinase signaling and dependent on the IB4-binding protein versican. Eur J Neurosci 28(1):12-19.

Boucher TJ, Okuse K, Bennett DLH, Munson JB, Wood JN, McMahon SB. 2000. Potent Analgesic Effects of GDNF in Neuropathic Pain States. Science 290(5489):124-127.

Bradbury EJ, Burnstock G, McMahon SB. 1998. The expression of P2X3 purinoceptors in sensory neurons: effects of axotomy and glial-derived neurotrophic factor. Mol Cell Neurosci 12:256-268.

Bruno MA, Cuello AC. 2006. Activity-dependent release of precursor nerve growth factor, conversion to mature nerve growth factor, and its degradation by a protease cascade. Proceedings of the National Academy of Sciences 103(17):6735-6740.

Burgess PR, Perl ER. 1967. Myelinated afferent fibres responding specifically to noxious stimulation of the skin. J Physiol (Lond) 190(3):541-562.

Burnstock G. 1990. Local mechanisms of blood flow control by perivascular nerves and endothelium. J Hypertens Suppl 8(7):S95-106.

Burnstock G. 1999. Purinergic cotransmission. Brain Res Bull 50(5-6):355-357.

Burnstock G. 2000. P2X receptors in sensory neurones. Br J Anaesth 84(4):476-488.

Burnstock G. 2004. Cotransmission. Curr Opin Pharm 4(1):47-52.

Campbell JN, Meyer RA, LaMotte RH. 1979. Sensitization of myelinated nociceptive afferents that innervate monkey hand. J Neurophysiol 42(6):1669-1679.

Campbell JN, Raja SN, Meyer RA, Mackinnon SE. 1988. Myelinated afferents signal the hyperalgesia associated with nerve injury. Pain 32(1):89-94.

Capsoni S, Covaceuszach S, Marinelli S, Ceci M, Bernardo A, Minghetti L, Ugolini G, Pavone F, Cattaneo A. 2011. Taking pain out of NGF: a "painless" NGF mutant, linked to hereditary sensory autonomic neuropathy type V, with full neurotrophic activity. PLoS One 6(2):e17321.

Carlton SM, Coggeshall RE. 1999. Inflammation-induced changes in peripheral glutamate receptor populations. Brain Res 820(1-2):63-70.

Carlton SM, Dougherty PM, Pover CM, Coggeshall RE. 1991. Neuroma formation and numbers of axons in a rat model of experimental peripheral neuropathy. Neurosci Lett 131:88-92.

Caterina MJ, Schumacher MA, Tominaga M, Rosen TA, Levine JD, Julius D. 1997. The capsaicin receptor: a heat-activated ion channel in the pain pathway. Nature 389(6653):816-824.

Catterall WA, Goldin AL, Waxman SG. 2005. International Union of Pharmacology. XLVII. Nomenclature and Structure-Function Relationships of Voltage-Gated Sodium Channels. Pharmacol Rev 57(4):397-409.

Chao MV. 1994. The p75 neurotrophin receptor. JNeurobiol 25:1373-1385.

Chao MV. 2003. Neurotrophins and their receptors: a convergence point for many signalling pathways. Nature Rev Neurosci 4:299-309.

Chao MV, Hempstead BL. 1995. p75 and Trk: A two-receptor system. Trends Neurosci 18:321-326.

Chaplan SR, Bach FW, Pogrel JW, Chung JM, Yaksh TL. 1994. Quantitative assessment of tactile allodynia in the rat paw. J Neurosci Methods 53(1):55-63.

Chen Y, Li G-W, Wang C, Gu Y, Huang L-YM. 2005. Mechanisms underlying enhanced P2X receptor-mediated responses in the neuropathic pain state. Pain 119(1-3):38-48.

Cho HJ, Kim DS, Lee NH, Kim JK, Lee KM, Han KS, Kang YN, Kim KJ. 1997. Changes in the à 2 -adrenergic receptor subtypes gene expression in rat dorsal root ganglion in an experimental model of neuropathic pain. Neuroreport 8(14):3119-3122.

Cho SH, Tam SW, Demissie-Sanders S, Filler SA, Oh CK. 2000. Production of Plasminogen Activator Inhibitor-1 by Human Mast Cells and Its Possible Role in Asthma. J Immunol 165(6):3154-3161.

Chung K, Kim HJ, Na HS, Park MJ, Chung JM. 1993. Abnormalities of sympathetic innervation in the area of an injured peripheral nerve in a rat model of neuropathic pain. Neurosci Lett 162(1-2):85-88.

Clewes O, Fahey MS, Tyler SJ, Watson JJ, Seok H, Catania C, Cho K, Dawbarn D, Allen SJ. 2008. Human ProNGF: biological effects and binding profiles at TrkA, P75NTR and sortilin. J Neurochem 107(4):1124-1135.

Coderre TJ, Bennett GJ. 2010. A hypothesis for the cause of complex regional pain syndrome-type I (reflex sympathetic dystrophy): pain due to deep-tissue microvascular pathology. Pain Med 11(8):1224-1238.

Coggeshall RE, Dougherty PM, Pover CM, Carlton SM. 1993. Is large myelinated fiber loss associated with hyperalgesia in a model of experimental peripheral neuropathy in the rat. Pain 52:233-242.

Cohen S. 1960. Purification and metabolic effects of a nerve growth promoting protein from the mouse salivary gland and its neurocytotoxic antiserum. Proc Natl Acad Sci U S A 46:302-311.

Cohen S, Levi-Montalcini R. 1956. A nerve growth stimulating factor isolated from snake venom. Proc Natl Acad Sci U S A 42:571-574.

Cohen S, Levi-Montalcini R, Hamburger V. 1954. A nerve growth stimulating factor isolated from sarcomas 37 and 180. Proc Natl Acad Sci U S A 40:1014-1018.

Coons AH, Creech HJ, Jones N, Berliner E. 1942. The Demonstration of Pneumococcal Antigen in Tissues by the Use of Fluorescent Antibody. The Journal of Immunology 45(3):159-170.

Coons AH, Kaplan MH. 1950. Localization of antigen in tissue cells; improvements in a method for the detection of antigen by means of fluorescent antibody. The Journal of experimental medicine 91(1):1-13.

Coull JA, Beggs S, Boudreau D, Boivin D, Tsuda M, Inoue K, Gravel C, Salter MW, De Koninck Y. 2005. BDNF from microglia causes the shift in neuronal anion gradient underlying neuropathic pain. Nature 438(7070):1017-1021.

Coull JA, Boudreau D, Bachand K, Prescott SA, Nault F, Sik A, De Koninck P, De Koninck Y. 2003. Trans-synaptic shift in anion gradient in spinal lamina I neurons as a mechanism of neuropathic pain. Nature 424(6951):938 -942.

Craig AD. 2003. Pain mechanisms: labeled lines versus convergence in central processing. Annu Rev Neurosci 26:1-30.

Craig AD. 2010. Why a soft touch can hurt. J Physiol. 588(Pt 1):13

Cuello AC, Galfre G, Milstein C. 1979. Detection of substance P in the central nervous system by a monoclonal antibody. Proc Natl Acad Sci U S A 76:3532-3536.

Cummins TR, Sheets PL, Waxman SG. 2007. The roles of sodium channels in nociception: Implications for mechanisms of pain. Pain 131(3):243-257.

Dallos A, Kiss M, Polyanka H, Dobozy A, Kemeny L, Husz S. 2006. Effects of the neuropeptides substance P, calcitonin gene-related peptide, vasoactive intestinal polypeptide and galanin on the production of nerve growth factor and inflammatory cytokines in cultured human keratinocytes. Neuropeptides 40(4):251-263.

Davis BM, Albers KM, Seroogy KB, Katz DM. 1994. Overexpression of nerve growth factor in transgenic mice induces novel sympathetic projections to primary sensory neurons. J Comp Neurol 349(3):464-474.

Davis BM, Fundin BT, Albers KM, Goodness TP, Cronk KM, Rice FL. 1997. Overexpression of nerve growth factor in skin causes preferential increases among innervation to specific sensory targets. J Comp Neurol 387(4):489-506.

Davis BM, Lewin GR, Mendell LM, Jones ME, Albers KM. 1993. Altered expression of nerve growth factor in the skin of transgenic mice leads to changes in response to mechanical stimuli. Neuroscience 56(4):789-792.

Dellarole A, Grilli M. 2008. Adult dorsal root ganglia sensory neurons express the early neuronal fate marker doublecortin. J Comp Neurol 511(3):318-328.

Derby A, Engleman VW, Frierdich GE, Neises G, Rapp SR, Roufa DG. 1993. Nerve growth factor facilitates regeneration across nerve gaps: Morphological and behavioral studies in rat sciatic nerve. Exp Neurol 119:176-191.

Devers A, Galer BS. 2000. Topical Lidocaine Patch Relieves a Variety of Neuropathic Pain Conditions: An Open-Label Study. The Clinical Journal of Pain 16(3):205-208.

Devor M, Wall PD. 1976. Type of sensory nerve fibre sprouting to form a neuroma. Nature 262(5570):705-708.

Di Castro A, Drew LJ, Wood JN, Cesare P. 2006. Modulation of sensory neuron mechanotransduction by PKC- and nerve growth factor-dependent pathways. Proc Natl Acad Sci U S A 103(12):4699-4704.

Dib-Hajj SD, Cummins TR, Black JA, Waxman SG. 2010. Sodium channels in normal and pathological pain. Annu Rev Neurosci 33:325-347.

Dickson A, Avelino A, Cruz F, Ribeiro-da-Silva A. 2006. Peptidergic sensory and parasympathetic fibre sprouting in the mucosa of the rat urinary bladder in a chronic model of cyclophosphamide-induced cystitis. Neuroscience 139(2):671-685.

Djouhri L, Dawbarn D, Robertson A, Newton R, Lawson SN. 2001. Time course and nerve growth factor dependence of inflammation-induced alterations in electrophysiological membrane properties in nociceptive primary afferent neurons. J Neurosci 21(22)8722-8733

Djouhri L, Fang X, Okuse K, Wood JN, Berry CM, Lawson SN. 2003. The TTX-resistant sodium channel Nav1.8 (SNS/PN3): expression and correlation with membrane properties in rat nociceptive primary afferent neurons. JPhysiol 550(Pt 3):739-752.

Djouhri L, Lawson SN. 2004. Abeta-fiber nociceptive primary afferent neurons: a review of incidence and properties in relation to other afferent A-fiber neurons in mammals. Brain Reseach Reviews 46(2):131-145.

Dong XW, Goregoaker D, Engler H, Zhou X, Mark L, Crona J, et al. 2007. Small interfering RNA-mediated selective knockdown of Na(V)1.8 tetrodotoxin-resistant sodium channel reverses mechanical allodynia in neuropathic rats. Neuroscience 146(2)812-821

Donnerer J. 2003. Regeneration of primary sensory neurons. Pharmacology 67(4):169-181.

Donnerer J, Schuligoi R, Stein C. 1992. Increased content and transport of substance P and calcitonin gene-related peptide in sensory nerves innervating inflamed tissue: Evidence for a regulatory function of nerve growth factor in vivo Neuroscience 49:693-698.

Doran JF, Jackson P, Kynoch PAM, Thompson RJ. 1983. Isolation of PGP 9.5, a New Human Neurone-Specific Protein Detected by High-Resolution Two-Dimensional Electrophoresis. J Neurochem 40(6):1542-1547.

Dray A, Perkins M. 1993. Bradykinin and inflammatory pain. Trends Neurosci 16(3):99-104.

Drew LJ, Rugiero F, Cesare P, Gale JE, Abrahamsen B, Bowden S, Heinzmann S, Robinson M, Brust A, Colless B, Lewis RJ, Wood JN. 2007. High-threshold mechanosensitive ion channels blocked by a novel conopeptide mediate pressure-evoked pain. PLoS One 2(6):e515.

Durbec P, Marcos-Gutierrez CV, Kilkenny C, Grigoriou M, Wartiowaara K, Suvanto P, Smith D, Ponder B, Costantini F, Saarma M, Sariola H, Pachnis V. 1996. GDNF signalling through the Ret receptor tyrosine kinase. Nature 381(6585):789-793.

Dworkin RH, Backonja M, Rowbotham MC, Allen RR, Argoff CR, Bennett GJ, Bushnell MC, Farrar JT, Galer BS, Haythornthwaite JA, Hewitt DJ, Loeser JD, Max MB, Saltarelli M, Schmader KE, Stein C, Thompson D, Turk DC, Wallace MS, Watkins LR, Weinstein SM. 2003. Advances in neuropathic pain: diagnosis, mechanisms, and treatment recommendations. Arch Neurol 60(11):1524-1534.

Eckert Iii WA, Julius D, Basbaum AI. 2006. Differential contribution of TRPV1 to thermal responses and tissue injury-induced sensitization

of dorsal horn neurons in laminae I and V in the mouse. Pain 126(1-3):184-197.

Eisenberg E, River Y, Shifrin A, Krivoy N. 2007. Antiepileptic Drugs in the Treatment of Neuropathic Pain. Drugs 67(9):1265-1289.

English KB, Harper S, Stayner N, Wang ZM, Davies AM. 1994. Localization of nerve growth factor (NGF) and low-affinity NGF receptors in touch domes and quantification of NGF mRNA in keratinocytes of adult rats. J Comp Neurol 344:470-480.

Fahnestock M, Yu G, Michalski B, Mathew S, Colquhoun A, Ross GM, Coughlin MD. 2004. The nerve growth factor precursor proNGF exhibits neurotrophic activity but is less active than mature nerve growth factor. J Neurochem 89(3):581-592.

Fang X, Djouhri L, Black JA, Dib-Hajj SD, Waxman SG, Lawson SN. 2002. The presence and role of the tetrodotoxin-resistant sodium channel Na(v)1.9 (NaN) in nociceptive primary afferent neurons. J Neurosci 22(17):7425-7433.

Fang X, Djouhri L, McMullan S, Berry C, Waxman SG, Okuse K, Lawson SN. 2006. Intense Isolectin-B4 Binding in Rat Dorsal Root Ganglion Neurons Distinguishes C-Fiber Nociceptors with Broad Action Potentials and High Nav1.9 Expression. The Journal of Neuroscience 26(27):7281-7292.

Feng D, Kim T, Ozkan E, Light M, Torkin R, Teng KK, Hempstead BL, Garcia KC. 2010. Molecular and structural insight into proNGF engagement of p75NTR and sortilin. J Mol Biol 396(4):967-984.

Flatters SJ, Bennett GJ. 2004. Ethosuximide reverses paclitaxel- and vincristine-induced painful peripheral neuropathy. Pain 109(1-2):150-161.

Fundin BT, Arvidsson J, Aldskogius H, Johansson O, Rice SN, Rice FL. 1997. Comprehensive immunofluorescence and lectin binding

analysis of intervibrissal fur innervation in the mystacial pad of the rat. J Comp Neurol 385(2):185-206.

Gammaitoni AR, Alvarez NA, Galer BS. 2003. Safety and Tolerability of the Lidocaine Patch 5%, a Targeted Peripheral Analgesic: A Review of the Literature. The Journal of Clinical Pharmacology 43(2):111-117.

Garber K. 2011. Fate of novel painkiller mAbs hangs in balance. Nat Biotechnol 29(3):173-174.

Gartner LP, Hiatt JL. 2001. Color Textbook of Histology. Philadelphia: Saunders.

Geffen LB, Livett BG, Rush RA. 1969. Immunohistochemical localizatio of protein components of catecholamine storage vesicles. J Physiol 204(3):593-605.

Gerevich Z, Illes P. 2004. P2Y receptors and pain transmission. Purinergic Signal 1(1):3-10.

Gibb JW, Spector S, Udenfriend S. 1967. Production of antibodies to dopamine-beta-hydroxylase of bovine adrenal medulla. Mol Pharmacol 3(5):473-478.

Gibbins IL, Morris JL. 1997. Autonomic pathways to cutaneous effectors. In: Burnstock G, editor. Autonomic Innervation of Skin. Amsterdam: Harwood Academic Publishers. p 1-56.

Goedert M, Otten U, Hunt SP, Bond A, Chapman D, Schlumpf M, Lichtensteiger W. 1984. Biochemical and anatomical effects of antibodies against nerve growth factor on developing rat sensory ganglia. Proc Natl Acad Sci U S A 81:1580-1584.

Goedert M, Stoeckel K, Otten U. 1981. Biological importance of the retrograde axonal transport of nerve growth factor in sensory neurons. Proc Natl Acad Sci U S A 78(9):5895-5898.

Gold MS, Weinreich D, Kim CS, Wang R, Treanor J, Porreca F, Lai J. 2003. Redistribution of Na(V)1.8 in uninjured axons enables neuropathic pain. J Neurosci 23(1):158-166.

Gonzalez-Martinez T, Perez-Pinera P, Diaz-Esnal B, Vega JA. 2003. S-100 proteins in the human peripheral nervous system. Microsc Res Tech 60(6):633-638.

Gorin PD, Johnson EM, Jr. 1980. Effects of long term nerve growth factor deprivation on the nervous system of rat: an experimental autoimmune approach. Brain Res 198:27-42.

Grelik C, Allard S, Ribeiro-da-Silva A. 2005a. Changes in nociceptive sensory innervation in the epidermis of the rat lower lip skin in a model of neuropathic pain. Neurosci Lett 389(3):140-145.

Grelik C, Bennett GJ, Ribeiro-da-Silva A. 2005b. Autonomic fiber sprouting and changes in nociceptive sensory innervation in the rat lower lip skin following chronic constriction injury. Eur J Neurosci 21(9):2475-2487.

Guilbaud G, Gautron M, Jazat F, Ratinahirana H, Hassig R, Hauw JJ. 1993. Time course of degeneration and regeneration of myelinated nerve fibres following chronic loose ligatures of the rat sciatic nerve: can nerve lesions be linked to the abnormal pain-related behaviours? Pain 53(2):147-158.

Guo A, Vulchanova L, Wang J, Li X, Elde R. 1999. Immunocytochemical localization of the vanilloid receptor 1 (VR1): relationship to neuropeptides, the P2X 3 purinoceptor and IB4 binding sites. Eur J Neurosci 11(3):946-958.

Gutierrez-Fernandez A, Parmer RJ, Miles LA. 2007. Plasminogen gene expression is regulated by nerve growth factor. Journal of Thrombosis and Haemostasis 5(8):1715-1725.

Hammarberg H, Piehl F, Cullheim S, Fjell J, H”kfelt T, Fried K. 1996. GDNF mRNA in Schwann cells and DRG satellite cells after chronic sciatic nerve injury. Neuroreport 7(4):857-860.

Han YP, Downey S, Garner WL. 2005. Interleukin-1alpha-induced proteolytic activation of metalloproteinase-9 by human skin. Surgery 138(5):932-939.

Hargreaves K, Dubner R, Brown F, Flores C, Joris J. 1988. A new and sensitive method for measuring thermal nociception in cutaneous hyperalgesia. Pain 32(1):77-88.

Harper AA, Lawson SN. 1985. Conduction velocity is related to morphological cell type in rat dorsal root ganglion neurones. J Physiol 359:31-46.

Harrington AW, Leiner B, Blechschmitt C, Arevalo JC, Lee R, Mörl K, Meyer M, Hempstead BL, Yoon SO, Giehl KM. 2004. Secreted proNGF is a pathophysiological death-inducing ligand after adult CNS injury. Proc Natl Acad Sci U S A 101(16):6226-6230.

Hattori A, Tanaka E, Murase K, Ishida N, Chatani Y, Tsujimoto M, Hayashi K, Kohno M. 1993. Tumor necrosis factor stimulates the synthesis and secretion of biologically active nerve growth factor in non-neuronal cells. J Biol Chem 268(4):2577-2582.

Hefti FF, Rosenthal A, Walicke PA, Wyatt S, Vergara G, Shelton DL, Davies AM. 2006. Novel class of pain drugs based on antagonism of NGF. Trends Pharmacol Sci 27(2):85-91.

Hempstead BL, Martin-Zanca D, Kaplan DR, Parada LF, Chao MV. 1991. High-affinity NGF binding requires coexpression of the trk proto-oncogene and the low-affinity NGF receptor. Nature 350:678-683.

Herzberg U, Eliav E, Dorsey JM, Gracely RH, Kopin IJ. 1997. NGF involvement in pain induced by chronic constriction injury of the rat sciatic nerve. Neuroreport 8(7):1613-1618.

Heumann R, Korsching S, Bandtlow C, Thoenen H. 1987a. Changes of nerve growth factor synthesis in nonneuronal cells in response to sciatic nerve transection. J Cell Biol 104:1623-1631.

Heumann R, Korsching S, Scott J, Thoenen H. 1984. Relationship between levels of nerve growth factor (NGF) and its messenger RNA in sympathetic ganglia and peripheral target tissues. EMBO J 3:3183-3189.

Heumann R, Lindholm D, Bandtlow C, Meyer M, Radeke MJ, Misko TP, Shooter E, Thoenen H. 1987b. Differential regulation of mRNA encoding nerve growth factor and its receptor in rat sciatic nerve during development, degeneration, and regeneration: role of macrophages. Proc Natl Acad Sci U S A 84:8735-8739.

Hoheisel U, Unger T, Mense S. 2007. Sensitization of rat dorsal horn neurons by NGF-induced subthreshold potentials and low-frequency activation. A study employing intracellular recordings in vivo. Brain Res 1169:34-43.

Holland DR, Cousens LS, Meng W, Matthews BW. 1994. Nerve growth factor in different crystal forms displays structural flexibility and reveals zinc binding sites. J Mol Biol 239(3):385-400.

Honore P, Kage K, Mikusa J, Watt AT, Johnston JF, Wyatt JR, Faltynek CR, Jarvis MF, Lynch K. 2002. Analgesic profile of intrathecal P2X3 antisense oligonucleotide treatment in chronic inflammatory and neuropathic pain states in rats. Pain 99(1-2):11-19.

Honma Y, Araki T, Gianino S, Bruce A, Heuckeroth R, Johnson E. 2002. Artemin is a vascular-derived neurotrophic factor for developing sympathetic neurons. Neuron 35(2):267-282

Hudmon A, Choi JS, Tyrrell L, Black JA, Rush AM, Waxman SG, Dib-Hajj SD. 2008. Phosphorylation of sodium channel Na(v)1.8 by p38 mitogen-activated protein kinase increases current density in dorsal root ganglion neurons. J Neurosci 28(12):3190-3201.

Hudson LJ, Bevan S, Wotherspoon G, Gentry C, Fox A, Winter J. 2001. VR1 protein expression increases in undamaged DRG neurons after partial nerve injury. Eur J Neurosci 13(11):2105-2114.

Hughes DI, Scott DT, Riddell JS, Todd AJ. 2007. Upregulation of substance P in low-threshold myelinated afferents is not required for tactile allodynia in the chronic constriction injury and spinal nerve ligation models. J Neurosci 27:2035-2044.

Hughes DI, Scott DT, Todd AJ, Riddell JS. 2003. Lack of evidence for sprouting of Abeta afferents into the superficial laminas of the spinal cord dorsal horn after nerve section. J Neurosci 23(29):9491-9499.

Ibrahim MM, Porreca F, Lai J, Albrecht PJ, Rice FL, Khodorova A, Davar G, Makriyannis A, Vanderah TW, Mata HP, Malan TP, Jr. 2005. CB2 cannabinoid receptor activation produces antinociception by stimulating peripheral release of endogenous opioids. Proc Natl Acad Sci U S A 102(8):3093-3098.

Ichikawa H, Sugimoto T. 2004. The co-expression of P2X3 receptor with VR1 and VRL-1 in the rat trigeminal ganglion. Brain Res 998(1):130-135.

Inoue K, Denda M, Tozaki H, Fujishita K, Koizumi S. 2005. Characterization of multiple P2X receptors in cultured normal human epidermal keratinocytes. The Journal of investigative dermatology 124(4):756-763.

Inoue K, Koizumi S, Fuziwara S, Denda S, Denda M. 2002. Functional vanilloid receptors in cultured normal human epidermal keratinocytes. Biochem Biophys Res Commun 291(1):124-129.

Irnich D, Burgstahler R, Bostock H, Grafe P. 2001. ATP affects both axons and Schwann cells of unmyelinated C fibres. Pain 92(3):343-350.

Ivanisevic L, Zheng W, Woo SB, Neet KE, Saragovi HU. 2007. TrkA Receptor “Hot Spots” for Binding of NT-3 as a Heterologous Ligand. J Biol Chem 282(23):16754-16763.

Jarvis MF. 2003. Contributions of P2X3 homomeric and heteromeric channels to acute and chronic pain. Expert Opinion on Therapeutic Targets 7(4):513-522.

Jarvis MF, Burgard EC, McGaraughty S, Honore P, Lynch K, Brennan TJ, Subieta A, Van Biesen T, Cartmell J, Bianchi B, Niforatos W, Kage K, Yu H, Mikusa J, Wismer CT, Zhu CZ, Chu K, Lee CH, Stewart AO, Polakowski J, Cox BF, Kowaluk E, Williams M, Sullivan J, Faltynek C. 2002. A-317491, a novel potent and selective non-nucleotide antagonist of P2X3 and P2X2/3 receptors, reduces chronic inflammatory and neuropathic pain in the rat. Proc Natl Acad Sci U S A 99(26):17179-17184.

Jensen TS, Madsen CS, Finnerup NB. 2009. Pharmacology and treatment of neuropathic pains. Curr Opin Neurol 22(5):467-474 410.1097/WCO.1090b1013e3283311e3283313.

Ji R-R, Samad TA, Jin S-X, Schmoll R, Woolf CJ. 2002. p38 MAPK Activation by NGF in Primary Sensory Neurons after Inflammation Increases TRPV1 Levels and Maintains Heat Hyperalgesia. Neuron 36(1):57-68.

Johnson Jr EM, Taniuchi M, DiStefano PS. 1988. Expression and possible function of nerve growth factor receptors on Schwann cells. Trends Neurosci 11(7):299-304.

Julius D, Basbaum AI. 2001. Molecular mechanisms of nociception. Nature 413(6852):203-210.

Kandel ER, Schwartz JH, Jessell TM. 2000. Principles of Neural Science.

Kaplan DR, Stephens RM. 1994. Neurotrophin signal transduction by the Trk receptor. J Neurobiol 25(11):1404-1417.

Keller AF, Beggs S, Salter MW, De Koninck Y. 2007. Transformation of the output of spinal lamina I neurons after nerve injury and microglia stimulation underlying neuropathic pain. Mol Pain 3:27.

Kim K, Yoon Y, Chung J. 1997. Comparison of three rodent neuropathic pain models. Exp Brain Res 113:200 - 206.

Kim S, Na H, Sheen K, Chung J. 1993. Effects of sympathectomy on a rat model of peripheral neuropathy. Pain 55:85 - 92.

Kiss M, Dallos A, Kormos B, Santha P, Dobozy A, Husz S, Kemeny L. 2010. Sortilin Is Expressed in Cultured Human Keratinocytes and Is Regulated by Cutaneous Neuropeptides. J Invest Dermatol 130(11):2553-2560.

Koneff HH. 1886. Beitrage zur Kenntnis der Nervenzellen in den peripheren Ganglien. Mittheilungen der Naturforschenden Gesellschaft in Bern 44-45:13-44.

Kruger L, Perl ER, Sedivec MJ. 1981. Fine structure of myelinated mechanical nociceptor endings in cat hairy skin. J Comp Neurol 198(1):137-154.

Kupers RC, Nuytten D, De Castro-Costa M, Gybels JM. 1992. A time course analysis of the changes in spontaneous and evoked behaviour in a rat model of neuropathic pain. Pain 50(1):101-111.

Kuruvilla R, Zweifel LS, Glebova NO, Lonze BE, Valdez G, Ye H, Ginty DD. 2004. A Neurotrophin Signaling Cascade Coordinates Sympathetic Neuron Development through Differential Control of TrkA Trafficking and Retrograde Signaling. Cell 118(2):243-255.

Lavand'homme PM, Eisenach JC. 2003. Perioperative administration of the alpha2-adrenoceptor agonist clonidine at the site of nerve injury reduces the development of mechanical hypersensitivity and modulates local cytokine expression. Pain 105(1-2):247-254.

Lawson S. 2002. Phenotype and function of somatic primary afferent nociceptive neurones with C-, Adelta- or Aalpha/beta-fibres. Exp Physiol 87(2):239-244.

Lawson SN, Harper AA, Harper EI, Garson JA, Anderton BH. 1984. A monoclonal antibody against neurofilament protein specifically

labels a subpopulation of rat sensory neurones. J Comp Neurol 228:263-272.

Lawson SN, Waddell PJ. 1991. Soma neurofilament immunoreactivity is related to cell size and fibre conduction velocity in rat primary sensory neurons. J Physiol 435(1):41-63.

Leclere PG, Norman E, Groutsi F, Coffin R, Mayer U, Pizzey J, Tonge D. 2007. Impaired Axonal Regeneration by Isolectin B4-Binding Dorsal Root Ganglion Neurons In Vitro. J Neurosci 27(5):1190-1199.

Lee BH, Yoon YW, Chung KS, Chung JM. 1998. Comparison of sympathetic sprouting in sensory ganglia in three animal models of neuropathic pain. Exp Brain Res 120(4):432-438.

Lee R, Kermani P, Teng KK, Hempstead BL. 2001. Regulation of cell survival by secreted proneurotrophins. Science 294:1945-1948.

Lee YJ, Zachrisson O, Tonge DA, McNaughton PA. 2002. Upregulation of bradykinin B2 receptor expression by neurotrophic factors and nerve injury in mouse sensory neurons. Mol Cell Neurosci 19(2):186-200.

Leffler A, Monter B, Koltzenburg M. 2006. The role of the capsaicin receptor TRPV1 and acid-sensing ion channels (ASICS) in proton sensitivity of subpopulations of primary nociceptive neurons in rats and mice. Neuroscience 139(2):699-709.

Leon A, Buriani A, Dal Toso R, Fabris M, Romanello S, Aloe L, Levi-Montalcini R. 1994. Mast cells synthesize, store, and release nerve growth factor. Proc Natl Acad Sci U S A 91(9):3739-3743.

Levi-Montalcini R. 1976. The nerve growth factor: its role in growth, differentiation and function of the sympathetic adrenergic neuron. Prog Brain Res 45:235-258.

Levi-Montalcini R, Angeletti PU. 1963. Essential role of the nerve growth factor in the survival and maintenance of dissociated sensory and sympathetic embryonic nerve cells in vitro. Dev Biol 7:653-659.

Levi-Montalcini R, Booker B. 1960a. Destruction of the sympathetic ganglia in mammals by an antiserum to a nerve-growth protein. Proc Natl Acad Sci U S A 46:384-391.

Levi-Montalcini R, Booker B. 1960b. Excessive growth of the sympathetic ganglia evoked by a protein isolated from mouse salivary glands. Proc Natl Acad Sci U S A 46:373-384.

Light AR, Perl ER. 1979a. Reexamination of the dorsal root projection to the spinal dorsal horn including observations on the differential termination of coarse and thin fibers. J Comp Neurol 186:117-132.

Light AR, Perl ER. 1979b. Spinal termination of functionally identified primary afferent neurons with slowly conducting myelinated fibers. J Comp Neurol 186:133-150.

Lin YW, Cheng CM, Leduc PR, Chen CC. 2009. Understanding sensory nerve mechanotransduction through localized elastomeric matrix control. PLoS One 4(1):e4293.

Lindholm D, Heumann R, Hengerer B, Thoenen H. 1988. Interleukin 1 increases stability and transcription of mRNA encoding nerve growth factor in cultured rat fibroblasts. J Biol Chem 263:16348-16351.

Lindholm D, Heumann R, Meyer M, Thoenen H. 1987. Interleukin-1 regulates synthesis of nerve growth factor in non-neuronal cells of rat sciatic nerve. Nature 330:658-659.

Liu X, Zhou JL, Chung K, Chung JM. 2001. Ion channels associated with the ectopic discharges generated after segmental spinal nerve injury in the rat. Brain Res 900(1):119-127

Ljungberg C, Novikov L, Kellerth JO, Ebendal T, Wiberg M. 1999. The neurotrophins NGF and NT-3 reduce sensory neuronal loss in adult rat after peripheral nerve lesion. Neurosci Lett 262(1):29-32.

Longo G, Osikowicz M, Cuello AC, Ribeiro-da-Silva A. Blocking nerve growth factor degradation in the rat hind paw skin leads to

hypersensitivity to noxious stimuli and to sympathetic fibre sprouting; 2011; Florence.

Lorenzo L-E, Ramien M, Louis MS, Koninck YD, Ribeiro-Da-Silva A. 2008. Postnatal changes in the Rexed lamination and markers of nociceptive afferents in the superficial dorsal horn of the rat. J Comp Neurol 508(4):592-604.

Lumsden AG, Davies AM. 1983. Earliest sensory nerve fibres are guided to peripheral targets by attractants other than nerve growth factor. Nature 306(5945):786-788.

Ma W, Bisby MA. 2000. Calcitonin gene-related peptide, substance P and protein gene product 9.5 immunoreactive axonal fibers in the rat footpad skin following partial sciatic nerve injuries. J Neurocytol 29(4):249-262.

Ma W, Zhang Y, Bantel C, Eisenach JC. 2005. Medium and large injured dorsal root ganglion cells increase TRPV-1, accompanied by increased alpha2C-adrenoceptor co-expression and functional inhibition by clonidine. Pain 113(3):386-394.

Ma WY, Ribeiro-da-Silva A, Noel G, Julien JP, Cuello AC. 1995. Ectopic substance P and calcitonin gene-related peptide immunoreactive fibres in the spinal cord of transgenic mice over-expressing nerve growth factor. Eur J Neurosci 7(10):2021-2035.

Malin SA, Molliver DC, Koerber HR, Cornuet P, Frye R, Albers KM, Davis BM. 2006. Glial cell line-derived neurotrophic factor family members sensitize nociceptors in vitro and produce thermal hyperalgesia in vivo. J Neurosci 26(33):8588-8599.

Maruo K, Yamamoto H, Yamamoto S, Nagata T, Fujikawa H, Kanno T, Yaguchi T, Maruo S, Yoshiya S, Nishizaki T. 2006. Modulation of P2X receptors via adrenergic pathways in rat dorsal root ganglion neurons after sciatic nerve injury. Pain 120(1-2):106-112.

Masoudi R, Ioannou MS, Coughlin MD, Pagadala P, Neet KE, Clewes O, Allen SJ, Dawbarn D, Fahnestock M. 2009. Biological Activity of Nerve Growth Factor Precursor Is Dependent upon Relative Levels of Its Receptors. J Biol Chem 284(27):18424-18433.

Massa SM, Xie Y, Yang T, Harrington AW, Kim ML, Yoon SO, Kraemer R, Moore LA, Hempstead BL, Longo FM. 2006. Small, Nonpeptide p75NTR Ligands Induce Survival Signaling and Inhibit proNGF-Induced Death. J Neurosci 26(20):5288-5300.

Maxwell RA. 1982. Guanethidine after twenty years: a pharmacologist's perspective. Br J Clin Pharmacol 13(1):35-44.

Mazzoni I, Jaffe E, Cuello A. 1991. Production and immunocytochemical application of a highly sensitive and specific monoclonal antibody against rat dopamine-beta-hydroxylase. Histochemistry 96:45 - 50.

McDonald NQ, Lapatto R, Murray-Rust J, Gunning J, Wlodawer A, Blundel TL. 1991. New protein fold revealed by a 2.3-A resolution crystal structure of nerve growth factor. Nature 354:411-414.

McKemy DD, Neuhausser WM, Julius D. 2002. Identification of a cold receptor reveals a general role for TRP channels in thermosensation. Nature 416(6876):52-58.

McLachlan E, Janig W, Devor M, Michaelis M. 1993. Peripheral nerve injury triggers noradrenergic sprouting within dorsal root ganglia. Nature 363:543 - 546.

McMahon SB, Armanini MP, Ling LH, Phillips HS. 1994. Expression and coexpression of Trk receptors in subpopulations of adult primary sensory neurons projecting to identified peripheral targets. Neuron 12:1161-1171.

McMahon SB, Bennett DLH, Priestley JV, Shelton DL. 1995. The biological effects of endogenous nerve growth factor on adult sensory neurons revealed by a trkA-IgG fusion molecule. Nat Med 1:774-780.

McMahon SB, Bennett DLH, Wall PD, Melzack R. 1999. Trophic factors and pain. Textbook of Pain. Edinburgh: Churchill Livingstone. p 105-128.

McMahon SB, Priestley JV. 1995. Peripheral neuropathies and neurotrophic factors: Animal models and clinical perspectives. Curr Opin Neurobiol 5(5):616-624.

Mearow KM, Kril Y, Diamond J. 1993. Increased NGF mRNA expression in denervated rat skin. Neuroreport 4(4):351-354.

Meisner JG, Waldron JB, Sawynok J. 2007. [alpha]1-Adrenergic Receptors Augment P2X3 Receptor-Mediated Nociceptive Responses in the Uninjured State. J Pain 8(7):556-562.

Mellick LB, Mellick GA. 1995. Successful treatment of reflex sympathetic dystrophy with gabapentin. The American journal of emergency medicine 13(1):96.

Merskey H, Bogduk N. 1994. Classification of chronic pain: descriptions of chronic pain syndromes and definitions of pain terms. Seattle: IASP Press. 209-214 p.

Meyer-Rosberg K, Kvarnstrom A, Kinnman E, Gordh T, Nordfors LO, Kristofferson A. 2001. Peripheral neuropathic pain--a multidimensional burden for patients. Eur J Pain 5(4):379-389.

Molliver DC, Wright DE, Leitner ML, Parsadanian AS, Doster K, Wen D, Yan Q, Snider WD. 1997. IB4-binding DRG neurons switch from NGF to GDNF dependence in early postnatal life. Neuron 19(4):849-861.

Moore KA, Kohno T, Karchewski LA, Scholz J, Baba H, Woolf CJ. 2002. Partial peripheral nerve injury promotes a selective loss of GABAergic inhibition in the superficial dorsal horn of the spinal cord. J Neurosci 22(15):6724-6731.

Mosconi T, Kruger L. 1996. Fixed-diameter polyethylene cuffs applied to the rat sciatic nerve induce a painful neuropathy: Ultrastructural morphometric analysis of axonal alterations. Pain 64(1):37-57.

Moulin DE, Clark AJ, Speechley M, Morley-Forster PK. 2002. Chronic pain in Canada--prevalence, treatment, impact and the role of opioid analgesia. Pain Res Manag 7(4):179-184.

Munger BL, Bennett GJ, Kajander KC. 1992. An experimental painful peripheral neuropathy due to nerve constriction. I. Axonal pathology in the sciatic nerve. Exp Neurol 118:204-214.

Munglani R, Bond A, Smith GD, Harrison SM, Elliot PJ, Birch PJ, Hunt, Sp. 1995. Changes in neuronal markers in a mononeuropathic rat model relationship between neuropeptide Y, pre-emptive drug treatment and long-term mechanical hyperalgesia. Pain 63(1):21-31.

Nagano M, Sakai A, Takahashi N, Umino M, Yoshioka K, Suzuki H. 2003. Decreased expression of glial cell line-derived neurotrophic factor signaling in rat models of neuropathic pain. BrJPharmacol 140(7):1252-1260.

Naska S, Lin DC, Miller FD, Kaplan DR. 2010. p75NTR is an obligate signaling receptor required for cues that cause sympathetic neuron growth cone collapse. Mol Cell Neurosci 45(2):108-120.

Neumann S, Doubell TP, Leslie T, Woolf CJ. 1996. Inflammatory pain hypersensitivity mediated by phenotypic switch in myelinated primary sensory neurons. Nature 384(6607):360-364.

Newmark P. 1986. Nobel prizes. Growth factors bring rewards. Nature 323(6089):572.

Nicol GD, Vasko MR. 2007. Unraveling the Story of NGF-mediated Sensitization of Nociceptive Sensory Neurons: ON or OFF the Trks? Mol Interventions 7(1):26-41.

Nirenberg MJ, Chan J, Liu YJ, Edwards RH, Pickel VM. 1996. Ultrastructural localization of the vesicular monoamine transporter-2 in midbrain dopaminergic neurons: Potential sites for somatodendritic storage and release of dopamine. J Neurosci 16(13):4135-4145.

Nykjaer A, Lee R, Teng KK, Jansen P, Madsen P, Nielsen MS, Jacobsen C, Kliemannel M, Schwarz E, Willnow TE, Hempstead BL, Petersen CM. 2004. Sortilin is essential for proNGF-induced neuronal cell death. Nature 427(6977):843-848.

Oaklander AL. 2001. The density of remaining nerve endings in human skin with and without postherpetic neuralgia after shingles. Pain 92(1-2):139-145.

Oaklander AL, Siegel SM. 2005. Cutaneous innervation: form and function. J Am Acad Dermatol 53(6):1027-1037.

Obata K, Yamanaka H, Dai Y, Tachibana T, Fukuoka T, Tokunaga A, Yoshikawa H, Noguchi K. 2003. Differential activation of extracellular signal-regulated protein kinase in primary afferent neurons regulates brain-derived neurotrophic factor expression after peripheral inflammation and nerve injury. J Neurosci 23(10):4117-4126.

Olausson H, Lamarre Y, Backlund H, Morin C, Wallin BG, Starck G, Ekholm S, Strigo I, Worsley K, Vallbo AB, Bushnell MC. 2002. Unmyelinated tactile afferents signal touch and project to insular cortex. Nat Neurosci 5(9):900-904.

Oliveira AL, Hydling F, Olsson E, Shi T, Edwards RH, Fujiyama F, Kaneko T, Hokfelt T, Cullheim S, Meister B. 2003. Cellular localization of three vesicular glutamate transporter mRNAs and proteins in rat spinal cord and dorsal root ganglia. Synapse 50(2):117-129.

Ossipov MH, Bian D, Malan TP, Jr., Lai J, Porreca F. 1999. Lack of involvement of capsaicin-sensitive primary afferents in nerve-ligation injury induced tactile allodynia in rats. Pain 79(2-3):127-133.

Paré M, Albrecht PJ, Noto CJ, Bodkin NL, Pittenger GL, Schreyer DJ, Tigno XT, Hansen BC, Rice FL. 2007. Differential hypertrophy and atrophy among all types of cutaneous innervation in the glabrous skin of the monkey hand during aging and naturally occurring type 2 diabetes. J Comp Neurol 501(4):543-567.

Park SK, Chung K, Chung JM. 2000. Effects of purinergic and adrenergic antagonists in a rat model of painful peripheral neuropathy. Pain 87(2):171-179.

Patapoutian A, Reichardt LF. 2001. Trk receptors: mediators of neurotrophin action. Curr Opin Neurobiol 11(3):272-280.

Peier AM, Reeve AJ, Andersson DA, Moqrich A, Earley TJ, Hergarden AC, Story GM, Colley S, Hogenesch JB, McIntyre P, Bevan S, Patapoutian A. 2002. A heat-sensitive TRP channel expressed in keratinocytes. Science 296(5575):2046-2049.

Peleshok JC, Ribeiro-da-Silva A. 2011. Delayed reinnervation by nonpeptidergic nociceptive afferents of the glabrous skin of the rat hindpaw in a neuropathic pain model. J Comp Neurol 519(1):49-63.

Perkins MN, Campbell E, Dray A. 1993. Antinociceptive activity of the bradykinin B1 and B2 receptor antagonists, des-Arg9, [Leu8]-BK and HOE 140, in two models of persistent hyperalgesia in the rat. Pain 53(2):191-197.

Perret D, Luo ZD. 2009. Targeting voltage-gated calcium channels for neuropathic pain management. Neurotherapeutics 6(4):679-692.

Perrot S, Attal N, Ardid D, Guilbaud G. 1993. Are mechanical and cold allodynia in mononeuropathic and arthritic rats relieved by systemic treatment with calcitonin or guanethidine? Pain 52(1):41-47.

Perry VH, Brown MC, Gordon S. 1987. The macrophage response to central and peripheral nerve injury. A possible role for macrophages in regeneration. J Exp Med 165(4):1218-1223.

Pezet S, Marchand F, D'Mello R, Grist J, Clark AK, Malcangio M, Dickenson AH, Williams RJ, McMahon SB. 2008. Phosphatidylinositol 3-Kinase Is a Key Mediator of Central Sensitization in Painful Inflammatory Conditions. J Neurosci 28(16):4261-4270.

Pezet S, McMahon SB. 2006. NEUROTROPHINS: Mediators and Modulators of Pain. Annu Rev Neurosci 29(1):507-538.

Pezet S, Onteniente B, Jullien J, Junier M, Grannec G, Rudkin B. 2001. Differential regulation of NGF receptors in primary sensory neurons by adjuvant-induced arthritis in the rat. Pain 90:113 - 125.

Pitcher GM, Henry JL. 2004. Nociceptive response to innocuous mechanical stimulation is mediated via myelinated afferents and NK-1 receptor activation in a rat model of neuropathic pain. Exp Neurol 186(2):173-197.

Pitcher GM, Ritchie J, Henry JL. 1999. Nerve constriction in the rat: model of neuropathic, surgical and central pain. Pain 83(1):37-46.

Plenderleith MB, Snow PJ. 1993. The plant lectin Bandeiraea simplicifolia I-B4 identifies a subpopulation of small diameter primary sensory neurones which innervate the skin in the rat. Neurosci Lett 159(1-2):17-20.

Priestley JV, Michael GJ, Averill S, Liu M, Willmott N. 2002. Regulation of nociceptive neurons by nerve growth factor and glial cell derived neurotrophic factor. Can J Physiol Pharmacol 80 495-505.

Puig S, Sorkin LS. 1996. Formalin-evoked activity in identified primary afferent fibers: Systemic lidocaine suppresses phase-2 activity. Pain 64(2):345-355.

Radtke C, Vogt PM, Devor M, Kocsis JD. 2010. Keratinocytes acting on injured afferents induce extreme neuronal hyperexcitability and chronic pain. Pain 148(1):94-102.

Ramage-Morin PL. 2008. Chronic pain in Canadian seniors. Health reports / Statistics Canada, Canadian Centre for Health Information = Rapports sur la sante / Statistique Canada, Centre canadien d'information sur la sante 19(1):37-52.

Ramage-Morin PL, Gilmour H. 2010. Chronic pain at ages 12 to 44. Health reports / Statistics Canada, Canadian Centre for Health Information = Rapports sur la sante / Statistique Canada, Centre canadien d'information sur la sante 21(4):53-61.

Ramer M, Bisby M. 1997a. Rapid Sprouting Of Sympathetic Axons In Dorsal Root Ganglia Of Rats With a Chronic Constriction Injury. Pain 70:237 - 244.

Ramer M, Bisby M. 1997b. Reduced sympathetic sprouting occurs in dorsal root ganglia after axotomy in mice lacking low-affinity neurotrophin receptor. Neurosci Lett 228(1):9-12.

Ramer M, Bisby M. 1999. Adrenergic innervation of rat sensory ganglia following proximal or distal painful sciatic neuropathy: distinct mechanisms revealed by anti-NGF treatment. Eur J Neurosci 11:837 - 846.

Ramer M, Thompson S, McMahon S. 1999. Causes and consequences of sympathetic basket formation in dorsal root ganglia. Pain 82, Suppl 6:S111 - S120.

Ramer MS, Bisby MA. 1997c. Rapid sprouting of sympathetic axons in dorsal root ganglia of rats with a chronic constriction injury. Pain 70(2-3):237-244.

Ramer MS, French GD, Bisby MA. 1997. Wallerian degeneration is required for both neuropathic pain and sympathetic sprouting into the DRG. Pain 72(1-2):71-78.

Ramer MS, Kawaja MD, Henderson JT, Roder JC, Bisby MA. 1998a. Glial overexpression of NGF enhances neuropathic pain and adrenergic sprouting into DRG following chronic sciatic constriction in mice. Neurosci Lett 251(1):53-56.

Ramer MS, Murphy PG, Richardson PM, Bisby MA. 1998b. Spinal nerve lesion-induced mechanoallodynia and adrenergic sprouting in sensory ganglia are attenuated in interleukin-6 knockout mice. Pain 78(2):115-121.

Ramien M, Ruocco I, Cuello AC, St.Louis M, Ribeiro-da-Silva A. 2004. Parasympathetic nerve fibers invade the upper dermis following sensory denervation of the rat lower lip skin. J Comp Neurol 469(1):83-95.

Randall LO, Selitto JJ. 1957. A method for measurement of analgesic activity on inflamed tissue. Arch Int Pharmacodyn Ther 111(4):409-419.

Reichardt LF. 2006. Neurotrophin-regulated signalling pathways. Philos Trans R Soc Lond B Biol Sci 361(1473):1545-1564.

Rempel DM, Diao E. 2004. Entrapment neuropathies: pathophysiology and pathogenesis. Journal of electromyography and kinesiology : official journal of the International Society of Electrophysiological Kinesiology 14(1):71-75.

Rexed B. 1952. The cytoarchitectonic organization of the spinal cord in the cat. J Comp Neurol 96:415-495.

Rexed B. 1954. A cytoarchitectonic atlas of the spinal cord in the cat. J Comp Neurol 100:297-397.

Ribeiro-da-Silva A. 1995. Ultrastructural features of the colocalization of calcitonin gene related peptide with substance P or somatostatin in the dorsal horn of the spinal cord. Can J Physiol Pharmacol 73(7):940-944.

Ribeiro-da-Silva A, Cuello AC, Henry JL. 2000. NGF over-expression during development leads to permanent alterations in innervation in the spinal cord and in behavioural responses to sensory stimuli. Neuropeptides 34(5):281-291.

Ribeiro-da-Silva A, De Koninck Y. 2009. Morphological and Neurochemical Organization of the Spinal Dorsal Horn. In: Basbaum AI, Bushnell MC, editors. Science of Pain. San Diego: Elsevier. p 279-310.

Ribeiro-da-Silva A, Kenigsberg RL, Cuello AC. 1991. Light and electron microscopic distribution of nerve growth factor receptor-like immunoreactivity in the skin of the rat lower lip. Neuroscience 43:631-646.

Rice FL, Fundin BT, Arvidsson J, Aldskogius H, Johansson O. 1997. Comprehensive immunofluorescence and lectin binding analysis of vibrissal follicle sinus complex innervation in the mystacial pad of the rat. J Comp Neurol 385(2):149-184.

Riedl MS, Schnell SA, Overland AC, Chabot-Dore AJ, Taylor AM, Ribeiro-da-Silva A, Elde RP, Wilcox GL, Stone LS. 2009. Coexpression of alpha 2A-adrenergic and delta-opioid receptors in substance P-containing terminals in rat dorsal horn. J Comp Neurol 513(4):385-398.

Ro LS, Chen ST, Tang LM, Jacobs JM. 1999. Effect of NGF and anti-NGF on neuropathic pain in rats following chronic constriction injury of the sciatic nerve. Pain 79(2-3):265-274.

Ruocco I, Cuello AC, Parent A, Ribeiro-da-Silva A. 2002. Skin blood vessels are simultaneously innervated by sensory, sympathetic, and parasympathetic fibers. J Comp Neurol 448(4):323-336.

Ruocco I, Cuello AC, Ribeiro-da-Silva A. 2000. Peripheral nerve injury leads to the establishment of a novel pattern of sympathetic fibre innervation in the rat skin. J Comp Neurol 422(2):287-296.

Ruscheweyh R, Forsthuber L, Schoffnegger D, Sandkühler J. 2007. Modification of classical neurochemical markers in identified primary afferent neurons with Abeta-, Adelta-, and C-fibers after chronic constriction injury in mice. J Comp Neurol 502(2):325-336.

Sakai A, Asada M, Seno N, Suzuki H. 2008. Involvement of neural cell adhesion molecule signaling in glial cell line-derived neurotrophic factor-induced analgesia in a rat model of neuropathic pain. Pain 137(2):378-388.

Sandkuhler J. 2009. Models and Mechanisms of Hyperalgesia and Allodynia. Physiol Rev 89(2):707-758.

Sandrock JAW, Matthew WD. 1987. Substrate-bound nerve growth factor promotes neurite growth in peripheral nerve. Brain Res 425(2):360-363.

Santha P, Jancso G. 2003. Transganglionic transport of choleragenoid by capsaicin-sensitive C-fibre afferents to the substantia gelatinosa of the spinal dorsal horn after peripheral nerve section. Neuroscience 116(3):621-627.

Schicho R, Skofitsch G, Donnerer J. 1999. Regenerative effect of human recombinant NGF on capsaicin-lesioned sensory neurons in the adult rat. Brain Res 815(1):60-69.

Scholz J, Woolf CJ. 2007. The neuropathic pain triad: neurons, immune cells and glia. Nat Neurosci 10(11):1361-1368.

Scott AL, Ramer MS. 2010. Schwann cell p75NTR prevents spontaneous sensory reinnervation of the adult spinal cord. Brain 133(Pt 2):421-432.

Seidah NG, Benjannet S, Pareek S, Savaria D, Hamelin J, Goulet B, Laliberte J, Lazure C, Chretien M, Murphy RA. 1996. Cellular processing of the nerve growth factor precursor by the mammalian pro-protein convertases. Biochem J 314 (Pt 3):951-960.

Shir Y, Seltzer Z. 1991. Effects of sympathectomy in a model of causalgiform pain produced by partial sciatic nerve injury in rats. Pain 45(3):309-320.

Silverman JD, Kruger L. 1990. Selective neuronal glycoconjugate expression in sensory and autonomic ganglia: Relation of lectin reactivity to peptide and enzyme markers. J Neurocytol 19:789-801.

Snutch TP. 2005. Targeting chronic and neuropathic pain: the N-type calcium channel comes of age. NeuroRx 2(4):662-670.

Song XJ, Zhang JM, Hu SJ, LaMotte RH. 2003. Somata of nerve-injured sensory neurons exhibit enhanced responses to inflammatory mediators. Pain 104(3):701-709

Spitsbergen JM, Stewart JS, Tuttle JB. 1995. Altered regulation of nerve growth factor secretion by cultured VSMCs from hypertensive rats. Am J Physiol 269(2 Pt 2):H621-628.

Stamboulian S, Choi JS, Ahn HS, Chang YW, Tyrrell L, Black JA, Waxman SG, Dib-Hajj SD. 2010. ERK1/2 mitogen-activated protein kinase phosphorylates sodium channel Na(v)1.7 and alters its gating properties. J Neurosci 30(5):1637-1647.

Streit WJ, Schulte BA, Balentine JD, Spicer SS. 1986. Evidence for glycoconjugate in nociceptive primary sensory neurons and its origin from the Golgi complex. Brain Res 377:1-17.

Stucky CL, Koltzenburg M, Schneider M, Engle MG, Albers KM, Davis BM. 1999. Overexpression of nerve growth factor in skin selectively affects the survival and functional properties of nociceptors. J Neurosci 19(19):8509-8516.

Sutter A, Riopelle LF, Harris-Harrik RM, Shooter EM. 1979. Nerve growth factor receptors: characterization of two distinct classes of binding sites on chick embryo sensory gnglia cells. J Biol Chem 254:5972-5982.

Sweet WH. 1981. Animal models of chronic pain: Their possible validation from human experience with posterior rhizotomy and congenital analgesia (Part I of the Second John J. Bonica Lecture). Pain 10(3):275-295.

Tandrup T. 1995. Are the neurons in the dorsal root ganglion pseudounipolar? A comparison of the number of neurons and number of myelinated and unmyelinated fibres in the dorsal root. J Comp Neurol 357:341-347.

Taniuchi M, Clark HB, Johnson EM, Jr. 1986. Induction of nerve growth factor receptor in Schwann cells after axotomy. Proc Natl Acad Sci U S A 83:4094-4098.

Taniuchi M, Clark HB, Schweitzer JB, Johnson EM, Jr. 1988. Expression of nerve growth factor receptors by Schwann cells of axotomized peripheral nerves: ultrastructural location, suppression by axonal contact, and binding properties. J Neurosci 8:664-681.

Taniuchi M, Johnson EM, Jr. 1985. Characterization of the binding properties and retrograde axonal transport of a monoclonal antibody directed against the nerve growth factor receptor. J Cell Biol 101:1100-1106.

Taylor AM, Peleshok JC, Ribeiro-da-Silva A. 2009. Distribution of P2X(3)-immunoreactive fibers in hairy and glabrous skin of the rat. J Comp Neurol 514:555-566.

Taylor AM, Ribeiro-da-Silva A. 2011. GDNF levels in the lower lip skin in a rat model of trigeminal neuropathic pain: Implications for nonpeptidergic fiber reinnervation and parasympathetic sprouting. Pain.

Taylor CP. 2009. Mechanisms of analgesia by gabapentin and pregabalin - Calcium channel [alpha]2-[delta] [Cav[alpha]2-[delta]] ligands. Pain 142(1-2):13-16.

Taylor CP, Angelotti T, Fauman E. 2007. Pharmacology and mechanism of action of pregabalin: the calcium channel alpha2-delta (alpha2-delta) subunit as a target for antiepileptic drug discovery. Epilepsy Res 73(2):137-150.

Thacker MA, Clark AK, Marchand F, McMahon SB. 2007. Pathophysiology of peripheral neuropathic pain: immune cells and molecules. Anesth Analg 105(3):838-847.

Thakor DK, Lin A, Matsuka Y, Meyer EM, Ruangsri S, Nishimura I, et al. 2009. Increased peripheral nerve excitability and local NaV1.8 mRNA up-regulation in painful neuropathy. Mol Pain 5:14

Thomas PK. 1971. The morphological basis for alterations in nerve conduction in peripheral neuropathy. Proc R Soc Med 64(3):295-298.

Thompson RJ, Doran JF, Jackson P, Dhillon AP, Rode J. 1983. PGP 9.5--a new marker for vertebrate neurons and neuroendocrine cells. Brain Res 278(1-2):224-228.

Thomson CE, Mitchell LS, Griffiths IR, Morrison S. 1991. Retarded Wallerian degeneration following peripheral nerve transection in C57BL/6/Ola mice is associated with delayed down-regulation of the P 0 gene. Brain Res 538:157-160.

Todd AJ. 2003. The expression of vesicular glutamate transporters VGLUT1 and VGLUT2 in neurochemically defined axonal populations in the rat spinal cord with emphasis on the dorsal horn. Eur J Neurosci 17:13-27.

Todd AJ. 2010. Neuronal circuitry for pain processing in the dorsal horn. Nat Rev Neurosci 11(12):823-836.

Torrance N, Smith BH, Bennett MI, Lee AJ. 2006. The epidemiology of chronic pain of predominantly neuropathic origin. Results from a general population survey. J Pain 7(4):281-289.

Toth C, Lander J, Wiebe S. 2009. The prevalence and impact of chronic pain with neuropathic pain symptoms in the general population. Pain Med 10(5):918-929.

Tsuda M, Koizumi S, Kita A, Shigemoto Y, Ueno S, Inoue K. 2000. Mechanical Allodynia Caused by Intraplantar Injection of P2X Receptor Agonist in Rats: Involvement of Heteromeric P2X2/3 Receptor Signaling in Capsaicin-Insensitive Primary Afferent Neurons. The Journal of Neuroscience 20(15):RC90.

Ugolini G, Marinelli S, Covaceuszach S, Cattaneo A, Pavone F. 2007. The function neutralizing anti-TrkA antibody MNAC13 reduces inflammatory and neuropathic pain. Proceedings of the National Academy of Sciences 104(8):2985-2990.

Vaegter CB, Jansen P, Fjorback AW, Glerup S, Skeldal S, Kjolby M, Richner M, Erdmann B, Nyengaard JR, Tessarollo L, Lewin GR, Willnow TE, Chao MV, Nykjaer A. 2011. Sortilin associates with Trk receptors to enhance anterograde transport and neurotrophin signaling. Nat Neurosci 14(1):54-61.

Van Hees J, Gybels J. 1981. C nociceptor activity in human nerve during painful and non painful skin stimulation. J Neurology, Neurosurgery and Psychiatry 44(7):600-607

Vellani V, Zachrisson O, McNaughton PA. 2004. Functional bradykinin B1 receptors are expressed in nociceptive neurones and are upregulated by the neurotrophin GDNF. J Physiol 560(Pt 2):391-401.

Verdu B, Decosterd I, Buclin T, Stiefel F, Berney A. 2008. Antidepressants for the Treatment of Chronic Pain. Drugs 68(18):2611-2632

Verge VMK, Richardson PM, Benoit R, Riopelle RJ. 1989a. Histochemical characterization of sensory neurons with high-affinity receptors for nerve growth factor. J Neurocytol 18:583-591.

Verge VMK, Riopelle RJ, Richardson PM. 1989b. Nerve growth factor receptors on normal and injured sensory neurons. J Neurosci 9:914-922.

Vulchanova L, Riedl MS, Shuster SJ, Buell G, Surprenant A, North RA, Elde R. 1997. Immunohistochemical study of the P2X2 and P2X3 receptor subunits in rat and monkey sensory neurons and their central terminals. Neuropharmacology 36(9):1229-1242.

Vulchanova L, Riedl MS, Shuster SJ, Stone LS, Hargreaves KM, Buell G, Surprenant A, North RA, Elde R. 1998. P2X 3 is expressed by DRG neurons that terminate in inner lamina II. Eur J Neurosci 10(11):3470-3478.

Wehrman T, He X, Raab B, Dukipatti A, Blau H, Garcia KC. 2007. Structural and mechanistic insights into nerve growth factor interactions with the TrkA and p75 receptors. Neuron 53(1):25-38.

Weihe E, Eiden LE. 2000. Chemical neuroanatomy of the vesicular amine transporters. The FASEB Journal 14(15):2435-2449.

Weihe E, Schäfer M, Erickson J, Eiden L. 1994. Localization of vesicular monoamine transporter isoforms (VMAT1 and VMAT2) to endocrine cells and neurons in rat. J Mol Neurosci 5(3):149-164.

Wiesmann C, Ultsch MH, Bass SH, de Vos AM. 1999. Crystal structure of nerve growth factor in complex with the ligand-binding domain of the TrkA receptor. Nature 401(6749):184-188.

Wilkinson KD, Lee KM, Deshpande S, Duerksen-Hughes P, Boss JM, Pohl J. 1989. The neuron-specific protein PGP 9.5 is a ubiquitin carboxyl-terminal hydrolase. Science 246(4930):670-673.

Wood JN. 2010. Nerve growth factor and pain. The New England journal of medicine 363(16):1572-1573

Wood JN, Anderton, BH. 1981. Monoclonal antibodies to mammalian neurofilaments. Biosci Rep 1(3):263-268.

Woolf CJ, Doubell TP. 1994. The pathophysiology of chronic pain -- increased sensitivity to low threshold A[beta]-fibre inputs. Curr Opin Neurobiol 4(4):525-534.

Woolf CJ, Mannion RJ. 1999. Neuropathic pain: aetiology, symptoms, mechanisms, and management. Lancet 353(9168):1959-1964.

Woolf CJ, Salter MW. 2000. Neuronal plasticity: Increasing the gain in pain. Science 288(5472):1765-1768.

Woolf CJ, Shortland P, Coggeshall RE. 1992. Peripheral nerve injury triggers central sprouting of myelinated afferents. Nature 355:75-78.

Wu C, Boustany L, Liang H, Brennan TJ. 2007. Nerve growth factor expression after plantar incision in the rat. Anesthesiology 107(1):128-135.

Xie W, Strong JA, Zhang JM. 2010. Increased excitability and spontaneous activity of rat sensory neurons following in vitro stimulation of sympathetic fiber sprouts in the isolated dorsal root ganglion. Pain 151(2):447-459.

Xie WR, Deng H, Li H, Bowen TL, Strong JA, Zhang JM. 2006. Robust increase of cutaneous sensitivity, cytokine production and sympathetic sprouting in rats with localized inflammatory irritation of the spinal ganglia. Neuroscience 142(3):809-822.

Yen LD, Bennett GJ, Ribeiro-da-Silva A. 2006. Sympathetic sprouting and changes in nociceptive sensory innervation in the glabrous skin of the rat hind paw following partial peripheral nerve injury. J Comp Neurol 495(6):679-690.

Yu WM, Chen ZL, North AJ, Strickland S. 2009. Laminin is required for Schwann cell morphogenesis. J Cell Sci 122(Pt 7):929-936.

Zhang J, De Koninck Y. 2006. Spatial and temporal relationship between monocyte chemoattractant protein-1 expression and spinal glial activation following peripheral nerve injury. J Neurochem 97(3):772-783.

Zhang JM, Li H, Munir MA. 2004. Decreasing sympathetic sprouting in pathologic sensory ganglia: a new mechanism for treating neuropathic pain using lidocaine. Pain 109(1-2):143-149.

Zhang X, Huang J, McNaughton PA. 2005. NGF rapidly increases membrane expression of TRPV1 heat-gated ion channels. EMBO J 24(24):4211-4223.

Zhao P, Barr TP, Hou Q, Dib-Hajj SD, Black JA, Albrecht PJ, Petersen K, Eisenberg E, Wymer JP, Rice FL, Waxman SG. 2008. Voltage-gated sodium channel expression in rat and human epidermal keratinocytes: Evidence for a role in pain. Pain 139(1):90-105.

Zheng FY, Xiao WH, Bennett GJ. 2011. The response of spinal microglia to chemotherapy-evoked painful peripheral neuropathies is distinct from that evoked by traumatic nerve injuries. Neuroscience 176:447-454.

Zhou L, Yan C, Gieling RG, Kida Y, Garner W, Li W, Han YP. 2009. Tumor necrosis factor-alpha induced expression of matrix metalloproteinase-9 through p21-activated kinase-1. BMC Immunol 10:15.

Zhou XF, Rush RA, McLachlan EM. 1996. Differential expression of the p75 nerve growth factor receptor in glia and neurons of the rat dorsal root ganglia after peripheral nerve transection. J Neurosci 16(9):2901-2911.

Zhu W, Oxford GS. 2007. Phosphoinositide-3-kinase and mitogen activated protein kinase signaling pathways mediate acute NGF sensitization of TRPV1. Mol Cell Neurosci 34(4):689-700.

Zhuang ZY, Xu H, Clapham DE, Ji RR. 2004. Phosphatidylinositol 3-kinase activates ERK in primary sensory neurons and mediates inflammatory heat hyperalgesia through TRPV1 sensitization. J Neurosci 24:8300-8309.

Zhuo M. 2000. Silent glutamatergic synapses and long-term facilitation in spinal dorsal horn neurons. In: J. Sandkuhler BBGFG, editor. Prog Brain Res: Elsevier. p 101-113.